SYNTHESIS OF FUNCTIONALIZED [2.2]PARACYCLOPHANE PRECURSORS FOR FUNCTIONAL POLY(PARA-XYLYLENE) THIN FILM DEPOSITION

SYNTHESIS OF FUNCTIONALIZED [2.2]PARACYCLOPHANE PRECURSORS FOR FUNCTIONAL POLY(PARA-XYLYLENE) THIN FILM DEPOSITION

By

SAEID RAHIMI RAZIN, B.Sc., M.Sc.

A Thesis

Submitted to the School of Graduate Studies

in Partial Fulfilment of the Requirements

for the Degree

Master of Science

McMaster University

MASTER OF SCIENCE (2015) McMaster University

(CHEMISTRY) Hamilton, Ontario

TITLE: SYNTHESIS OF FUNCTIONALIZED [2.2]PARACYCLOPHANE PRECURSORS FOR FUNCTIONAL POLY(PARA-XYLYLENE) THIN FILM DEPOSITION

AUTHOR: Saeid Rahimi Razin, B.Sc., M.Sc. (Amirkabir University)

SUPERVISOR: Doctor Jose M. Moran-Mirabal

NUMBER OF PAGES: x, 109.

Abstract

Functionalized poly(para-xylylene) (PPX) coatings can be useful for biomaterials applications due to their biocompatibility and useful chemistry for the immobilization of biomolecules. However, their application is not widespread due to the difficulty in synthesizing the corresponding precursors. Here, a two-step method for amine functionalization of [2.2]paracyclophane (PCP) via direct nitration and reduction is developed. Nitration at super acidic conditions and temperatures as low as -78 °C, improved the stability of PCP toward strong acids and successfully minimized side reactions such as oxidation and polymerization. This procedure resulted in quantitative yields of 4-nitro-PCP, which was successively reduced by Raney nickel catalysis with sodium borohydride. Compared to the many other reduction systems, this method is simple, inexpensive and applicable in large scales. Additionally, carboxylation of PCP using the Freidel-Crafts acylation was attempted and so far, we have been able to show the synthesis of intermediate acylated products.

Through the chemical vapour deposition polymerization of amino-PCP amine-functionalized poly(para-xylylene) (PPX-A) thin films were coated on Si wafer substrates. The substrates coated with PPX-A showed a higher surface energy compared with those of coated with un-substituted or chlorine substituted PPX films. Furthermore, results of the surface characterization demonstrated that the CVD process was able to transfer the functionalities of the precursors to deposited polymer films without alteration. However, the stability of primary amine groups in air and aqueous solutions is a matter of concern. Aging of amino-PCP and corresponding PPX-A films showed a decrease in the amount of

primary amines which was accompanied by the appearance and increase of oxygen, indicating that the decrease of available amine groups is associated with oxidation. Nevertheless, both aminated precursor and polymer films remained intact under argon. The method presented here has great potential for widespread application of PPX-A as a convenient biomaterial for microarrays and cell culture.

Keywords: [2.2]Paracyclophane, Poly(para-xylylene), CVD polymerization, Amine-functionalization, Stability of primary amines

Acknowledgement

My experience as a graduate student at McMaster University has been a rather fulfilling one. It gave me the opportunity to challenge myself both intellectually and psychologically. I have so many people to thank for helping me make it through. First and foremost, I would like to thank my research supervisor Dr. Jose M. Moran-Mirabal, to whom this work is beholden. I came into his research group, at the department of Chemistry and Chemical Biology, after spending almost six years in engineering school. His patience helped me to adapt with the different research environment than that I had internationally experienced in the past. Furthermore, I became able to refine my research skills and advance my project through his thoughtful guidance.

I would be remiss, if I did not thank my supervisory committee member, Dr. James McNulty, who by many measures is a remarkable individual. The constructive comments that he made during the meetings have significant impacts on the progress of my research project. A number of other people were instrumental in my project. None was as important as Carlos A. Zepeda-Velazquez, a former PhD student of Dr. McNulty, who helped me very much in the beginning with his valuable experiences in synthetic organic chhemistry. I would also like to thank Dr. Kirk Green, Dr. Steven A. Kornic and Dr. Danielle Covelli for their assistances with MS, FTIR and XPS measurements. And last, my labmates specially Yujie Zhu and Ayodele Fatona who not only helped me at many points in my study but held the energy and motivation in the lab to carry out the research.

Table of Contents

List of Tables

List of Illustrations, Figures and Schemes

Chapter one: Introduction to functionalized Parylene coatings

1-1- Organic thin coatings: Parylene

There is great demand for thin-film polymer coatings for advanced applications from integrated optoelectronic devices[1] and circuit boards[2] to biomaterials[3] and optical or microelectro-mechanical systems.[4, 5] Traditionally polymers of poly(para-xylylene) (commercially trademarked as Parylene) are used as protective insulating thermoplastic coatings for electronic devices.[6] This is due to the uniform conformal coating properties of Parylene resulting from the specific nature of its polymerization, called chemical vapor deposition (CVD). The high mobility of the gaseous monomer (para-xylylene) (PX) in this process enables them to polymerize in the plane of the surface and create uniform surfaces with very low sticking coefficient ($<1 \times 10^{-3}$) at room temperature.[3] Therefore, Parylene is usually deemed a good candidate where an insulating conformal coating is needed.

In addition to high degree of uniformity (pinhole-free) that CVD polymerization endows to its polymers, no catalysts, solvent or initiator and consequently no by-produts are involved in this method. Therefore, polymers of poly(para-xylylene) (PPX) are chemically inert (unless intentionally modified with functional groups), resistant to swelling in aqueous solutions, and amenable to lithographic patterning on a variety of substrates.[7] Owing to these unique properties and their high biostability compared to traditional conformal coatings such as epoxies, silicones, acrylics, and urethanes, PPX-related polymers have drawn significant attention as structural materials for microfluidic

devices,[8] and as biomaterials.[9, 10] . This also means that Parylene-encapsulated medical devices implanted in the body can remain stable for many years, making them attractive for applications involving biological interfaces.

1-2- CVD polymerization of Parylene

In the past decades, vacuum deposited polymers have gained attention for their unique properties, such as inherent cleanliness and minimal generation of hazardous waste.[11] These advantages derive from the nature of vapour deposition polymerization, which does not require solvent and catalyst. The precursor used for depositing Parylene is a dimer of PX, called [2,2]para-cyclophane (PCP, **Scheme 1**). Synthesis of Parylene through vacuum polymerization of PX was first reported by Szwarc in 1947;[12] however, Parylene found a wider commercial use with the introduction of the Gorham method for CVD polymerization of PXs.[13] He found that PCP could be cleaved efficiently at temperatures as low as 600°C with 100% conversion into monomers.[14] This temperature is adequate for pyrolysis of many variants of PCPs and using higher temperatures is reported to produce reactive species that lead to undesired side reactions, crosslinking, and oligomerization.[15] As a whole, the method involves sublimation and vacuum pyrolysis of the PCP precursor at temperatures above 600 °C to yield the reactive monomers. Cooling to room temperature polymerizes the monomers adsorbed onto the surface and a high molecular weight Parylene film is formed on the surface. Because the pressure is still below the vapor pressure of monomer gas it has a finite residence time on the chamber walls. A

small fraction is consumed by either initiation or propagation; the remainder reenters the gas.

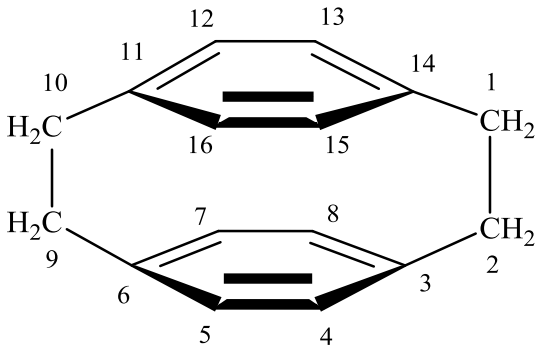

Scheme 1. Chemical structure of [2.2]paracyclophane, the simplest member of the paracyclophane family

The deposition of PX in a CVD chamber is controlled both by chemical and physical phenomena. Therefore, both aspects should be considered simultaneously to elucidate the mechanism of polymerization and develop a model for CVD process that allows us to predict and tune the final properties of the polymer films. The chemistry of polymerization, most notably the initiation reaction, had been investigated for many years until Errede and Szwarc illustrated a commonly-accepted pathway in 1958.[16] Initiation of the CVD polymerization of p-xylylene was unknown until thermodynamic studies[16 17] showed that a small number (λ) of PX molecules spontaneously convert into a single di-radical, as shown in **Scheme 2.** Since λ is greater than 1, polymerization does not occur in

the gas phase, where the concentration of monomers is low. The monomer is present in sufficient concentrations for initiation only after adsorption on the chamber walls.

Initiation

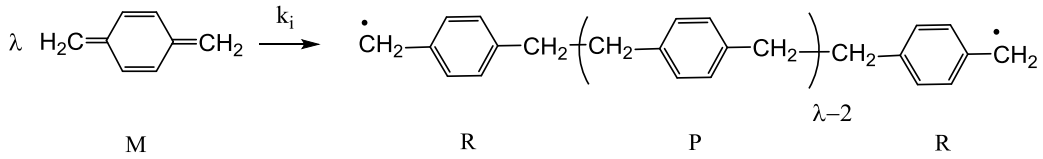

Propagation

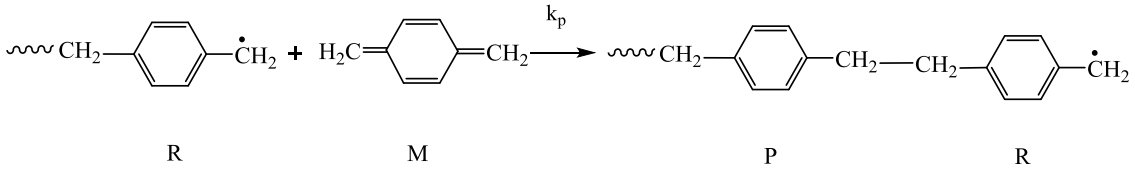

Scheme 2. Initiation and propagation reactions of para-xylylene polymerization (adapted from ref. *18*)

The minimum number of monomers (λ) to initiate the polymerization is found to be three for PX;[18] however, it could be different for other substituted PXs. For instance, Gaynor[15] reported that the results of polymerization of dichloro-PX best fits the experimental data when λ is assumed to be four and consequently the initiation reaction has a fourth-order kinetic rate with respect to the monomer. Therefore, in each initiation reaction λ monomer molecules (M) are consumed to produce two free-radical propagation centers (R) and (λ-2) polymer repeating units (P). The main step of polymerization, propagation, occurs by the addition of monomer (M) to free radical polymer chain end

propagation centers (R). Each single reaction, consumes one monomer molecule and produces one polymer repeat unit (P). The net change in the number of propagation centers (R) is zero (**Scheme 2**). Thus, the rates of consumption and production of these moieties in the initiation and propagation reactions can be described as follows:

$$\text{Initiation} \quad \begin{cases} -\left(\frac{\partial M}{\partial t}\right) = \lambda k_i M^{\lambda} \\ \left(\frac{\partial R}{\partial t}\right) = 2k_i M^{\lambda} \\ \left(\frac{\partial P}{\partial t}\right) = (\lambda - 2)k_i M^{\lambda} \end{cases} \qquad \text{(Eq. 1-1)}$$

$$\text{Propagation} \quad \begin{cases} -\left(\frac{\partial M}{\partial t}\right) = \left(\frac{\partial P}{\partial t}\right) = k_p RM \\ \left(\frac{\partial R}{\partial t}\right) = 0 \end{cases} \qquad \text{(Eq. 1-2)}$$

The last step in the chemistry of deposition is termination of polymerization. According to Errede and Szwarc,[16] propagation is assumed to continue as long as monomer is present in the vicinity of propagating chains. Growth of the chains is ceased when they are "buried" (isolated from the influx of fresh monomer) in the bulk of deposited polymer. Consequently, there is no need to consider the effect of any chemical event that stops the chain growth. Based on these findings, the polymer is assumed to be "living" and no termination reaction is assumed in this polymerization.[18] In order to determine concentration of monomer in the film we need to have a clear understanding of the physics of deposition as well. For this purpose, neglecting the volume change on polymerization,

Henry's law has been employed to relate the pressure of monomer gas to concentration of monomers at the growth surface:[18]

$$M_0 = \frac{\rho}{K_H}\frac{P}{P_{sat}} \qquad \text{(Eq. 1-3)}$$

Eventually, the first quantitative model for CVD polymerization of PX was introduced by Beach in 1978.[18] Almost every other model, published later, has used the basic precepts of this model. The approach is based on a mass balance in which the amount of monomer entering a volume element equals the amount of monomer that re-evaporates plus the amount that is consumed by reaction or is removed by convection. The model is a one-dimensional problem in which the only spatial dimension is the direction of film growth, perpendicular to the film plane. Beach has developed a steady-state diffusion/reaction model that assumes:

i) Through the equilibrium between the monomer gas and monomers adsorbed on the surface, surface concentration of monomers molecules on the surface is related to the partial pressure of the monomer gas by Henry's Law.

ii) The rate of initiation is very low compared to the rate of propagation.

iii) Convection effects in the film are negligible.

iv) All the temperature dependent parameters in reaction, diffusion and vaporization follow Arrhenius behavior.

With the simplifications introduced by Beach[18] for steady-state growth of the film, the properties of the polymer films (*i.e.* number average molecular weight and growth rate of the film thickness) can be related solely to process parameters:

$$\gamma = \left(\frac{2}{\lambda\rho^3}\right)^{1/4} \left(k_i k_p D^2\right)^{1/4} \left(\frac{\rho}{K_H P_0}\right)^{((\lambda+3)/4)} P^{((\lambda+3)/4)} \qquad \text{(Eq. 1-4)}$$

$$\bar{M}_n = \omega(2\rho\lambda)^{1/2} \left(k_p/k_i\right)^{1/2} \left(K_H P_0/\rho\right)^{((\lambda-1)/2)} P^{-((\lambda-1)/2)} \qquad \text{(Eq. 1-5)}$$

where γ is the growth rate, λ is the number of molecules required to create the di-radical initiator, ρ is the film density, k_i and k_p are the initiation and propagation rate constants, D is the diffusion rate of the monomer in the film, K_H is Henry's constant, P_0 is the vapor pressure of the monomer, P is the partial pressure of the monomer and ω is the molecular weight of the monomer. Gaynor[15] extended this model into two dimensions and applied it to the copolymerization of chloro-p-xylylene and p-xylylene. Additionally, Ganguli[19] showed that depending on the rate of polymerization, the CVD polymerization process can take a significant amount of time to reach steady state. Thanks to the new analytical solution methods, they were able to find a solution for the change of monomer concentration during the transient phase of polymerization. However, numerical solution methods show that the transient phase does not last long, and within a few seconds of starting the process, the growth rate of the film's thickness and the monomer concentration at the growth interface

are independent of time. Therefore, the steady state assumption of Beach holds for almost entire the process but a very short transient period at the beginning.

1-3- Functionalized coatings

Very soon after the discovery and development of PPX, researchers found that functionalized PPX films exhibit improved performance when used for coating applications. Beside PPX, a few other derivatives of Parylene are either well developed or have been reported in the literature. **Scheme 3** presents some of these derivatives with their chemical structures and commercial names. Among these derivatives, chlorine-functionalized PPX (PPX-C) is the most widely used variant of Parylene because it has improved dielectric and moisture barrier properties compared to un-substituted PPXs.[8] More importantly, there is an increasing demand for reactive polymer coatings, especially in the rapidly growing area of biomaterials research. In this regard, Parylene coatings containing reactive groups present interesting interfaces for biomedical applications, where the surface functionality of Parylene could be used to further derivatize the coating after polymerization. This could open new routes to biomaterials engineering by tuning the surface properties based on the precursor(s) used for polymerization. For instance, reactive Parylenes could be functionalized with biomolecules,[20] such as proteins or biopolymers, that improve the biocompatibility of Parylene coatings for their use in human body implants.[21]

Poly(p-xylylene), PPX

Parylene N

Poly(chloro-p-xylylene), PPX-C

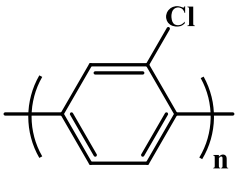

Parylene C

Poly(di-chloro-p-xylylene), PPX-D

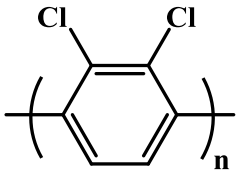

Parylene D

Poly(4-amino-p-xylylene-co-p-xylylene), PPX-A

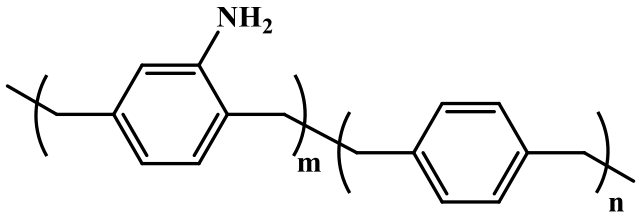

Parylene A

Scheme 3. Some of the common derivatives of Poly(para-xylylene) and their structures

The introduction of amine and carboxyl group functionalities are particularly interesting because they can provide reactive linking sites for covalent immobilization of biologically active molecules to the substrate surfaces.[22-27] A number of reports in the literature have demonstrated the versatility of amine-functionalized coatings in cell colonization[28] or adhesion promotion applications.[29] This is associated with positive charges of primary amine groups at physiological pH and their tendency to attract living cells via the negatively charged biomolecules present on the cell's membrane.[26, 30] However, the majority of the reports are devoted to the utilization of such chemically reactive groups as platforms in biochemistry for the covalent coupling of biomolecules. As

of yet, carbodiimide chemistry is the most widely used approach for the amidation reaction to link surface-tethered amine groups to mobile carboxyl groups. Using this method, in addition to nucleic acids and proteins, a number of other bioactive molecules (e.g. hyaluronic acid, heparin and other polysachharides) have been successfully immobilized on amine-functionalized surfaces.[26]

The carbodiimide coupling strategy can also be used to link carboxyl-functionalized coatings to mobile amine groups, like those present in proteins. Similar to amine functionalization, carboxyl groups can be inserted on the surface of substrates by techniques such as plasma treatment and plasma polymerization,[22, 31] or by exposure of the polymer surfaces to strong oxidants.[32, 33] The latter is applicable to any oxidation-sensitive polymer, but can degrade the polymer to produce carboxylic acids and other groups in the bulk of the polymer. A downside of plasma methods is that they usually leave behind free radicals trapped in bulk of the polymer, which can then cause crosslinking or further reactions with oxygen and water present in air or in solution. An alternate method to introduce carboxyl functionality is to use an interlayer that already contains carboxyl groups. The reactivity of the acid groups has been exploited for example in the adsorption of charged lipid bilayers on plasma polymerized maleic anhydride films.[23, 34] More generally, carboxylated coatings, like aminated surfaces, could be useful platforms for interfacial immobilization, via carbodiimide chemistry, of biomolecules that contain amine groups. Covalent attachment of collagen, anticoagulants such as human thrombomodulin and enzymes onto carboxyl-functionalized biomaterials have been successfully reported.[26] Despite its successful synthesis,[35] little attention has been paid to carboxylated Parylene

and no direct application has been reported, despite the fact that no substantial difference is expected between the reactivity of carboxyl groups on Parylene and that of other polymers.

1-4- Substitution of [2.2]para-cyclophanes: amine and carboxyl derivatives

Since CVD polymerization is carried out under high vacuum and its maximum temperature throughout the entire procedure is tolerable by many functional groups, functionalization of Parylene films can be achieved by polymerization of the corresponding substituted precursors. As discussed earlier, the simplest precursor used for the CVD of Parylene films is [2,2]para-cyclophane (PCP, **Scheme 1**), a dimer of the well-known family of aromatic materials called cyclophanes. Its chemistry has been extensively investigated since the seminal studies of Donald J. Cram in the early 1950s.[36] Among the functional Parylenes reported, amine- and carboxyl-bearing films can be useful in biomedical applications because biologically-active molecules can be covalently attached to these groups through carbodiimide chemistry or the use of linker molecules such as glutaraldehyde or succinimde.[25] Yet, their application by CVD is restricted due to the challenges posed by the synthesis of the corresponding amino- and carboxyl-substituted PCPs.

It can be envisioned that the simplest solution to obtain the amino-PCP, might be the direct nitration of PCP, followed by subsequent reduction of the nitro substituent(s). Since nitrated aromatic compounds in general are of industrial importance as organic

intermediates, a variety of synthetic routes have been reported so far. These include the use of nitrating acids, nitrate or nitrite salts, and solid acids. The method using a mixture of concentrated or fuming nitric acid with sulfuric acid has been the most widely cited.[37] Nevertheless, to nitrate the more reactive aromatic compounds and as well as to control the regioselectivity of substitution, different approaches with nitrate/nitrite salts have been developed.[38-40] For instance, regioselective nitration of the phenyl groups of meso-tetraphenylporphyrin (TPP) has been conducted using sodium nitrite ($NaNO_2$) and trifluorocetic acid (TFA).[41] In a different approach, with the goal of reducing the amount of sulfuric acid required for the nitration reaction, researchers have developed solid acids by simply soaking small amounts of solid supports such as silica gel in sulfuric acid followed by oven drying.[42] This is predominantly to reduce the amount of water produced as a byproduct when using excess sulfuric acid in industrial applications, which over the course of the reaction can dilute the acid and slow the reaction, with the added benefit of the concomitant reduction of risks of handling dangerous acids and process costs.

On the other hand, conversion of aromatic nitro compounds to corresponding aniline structures through the reduction of nitro substituent is one of the most significant transformations in synthetic organic chemistry. As a consequence, many reducing reagents have been introduced so far for this purpose. The most common method involving the iron catalysis in the presence of hydrochloric or acetic acid.[43] Some other conventional and important reducing agents reported in the literature are Sn/HCl, $SnCl_2$/HCl, Zn/HCl, $LiAlH_4$, $NaBH_4$, $TiCl_3$, N_2H_4/Zn, N_2H_4/$FeCl_3$ and so on.[41, 44-47]

However, most of these nitration-reduction systems are either incompatible or inefficient with PCP. Conventionally, a five-step procedure is used to synthesize 4-amino[2,2]paracyclophane from PCP.[48] This approach affords poor yields of 4-amino-PCP, and does not produce the diamino-PCP product. In another work in 1997, Cipiciani[49] conducted a three-step procedure to synthesize 4-amino-PCP in 46% yield. They first synthesized halogenated PCPs using the method initially described by Cram.[47] Successive metallation of 4-bromo[2,2]paracyclophane with n-butyllithium resulted in the 4-lithio derivative that was subsequently aminated by methyllithium-methoxyamine to provide amino-substituted PCP. Nevertheless, attempts to synthesize amino-substituted PCPs directly by nitration and subsequent reduction of nitrated PCPs were not very successful. This is due to the poor stability of PCPs in harsh oxidation conditions during the nitration reaction, which results in numerous side reactions (e.g. polymerization and oxidation of PCP). Cram[50] was the first to directly synthesize amino-PCPs, by nitration and successive reduction, with 26% yield for the mono- and 8% for the di-substituted products. However, purification of the products from polymeric byproducts was difficult and isolation of the products required repeated chromatography steps giving rise to a limited application of this approach for preparing the amino-PCPs in quantitative scales. They subsequently utilized platinum oxide catalysis in absolute methanol to reduce the 4-nitro[2.2]paracyclophanes.[47] Recently, Lahann[51] reported the ability to nitrate the PCP in high yields at very low temperatures (-78 °C). They first treated fuming nitric acid (100%) with trifluoromethanesulfonic acid (triflic acid). This reaction liberates free nitronium ions that possess high nitration power even at low temperatures. Therefore, using low temperatures

and short reaction times they prevented the side reactions that are mostly favored at elevated temperatures. Finally, they reported a yield of 93% for their dinitrated product. According to the authors, stirring the reaction mixture for 20 min at -78°C followed by reaction for 2 h at -20°C delivered mainly dinitro-PCP and only traces of mononitro-PCP. These yields remained constant through the reduction process, which involved using a triiron dodecacarbonyl in toluene/aqueous KOH two-phase system with [18]crown-6 ether as the phase-transfer catalyst. However, in our attempts to reproduce the procedure using the same reactions, we were unable to obtain similar results. For the first step, as we allowed the two acids to react at -78°C, a white precipitate appeared in the acidic solution and quickly solidified in the flask. Ignoring the precipitate and proceeding with the reaction did not lead to acceptable yields. Also, reducing the nitrated PCP using triiron dodecacarbonyl catalyst afforded negligible yields of amino-PCP. Failing to quantitatively reduce the nitro-PCP, we then tested a related model compound, 2-nitro-para-xylene, to assess reducing power of the catalyst and found that it did not yield more than maximum 53% reduced product.

Therefore, with the aim of improving both nitration and reduction reactions of [2.2]paracyclophane, we introduce a relatively simple procedure that does not suffer from the above problems. For the first nitration reaction, we propose to replace the triflic acid with triflic anhydride to avoid the formation of water that subsequently freezes at low temperatures (-78°C) and interferes with the reaction. Also, we suggest a different reducing agent for the second step that is faster, less expensive and easier to scale-up. This powerful and highly selective reduction system which benefits from the ®Raney Nickel catalysis in the presence of sodium borohydride ($NaBH_4$), has been successfully tried on a number of

aromatic nitro compounds with > 90% yields. We observed comparable yields for the reduction of 4-nitro[2.2]paracyclophane (92%) and the test compound, 2-nitro-para-xylene, (94%). Another advantage of this procedure is that it avoids strong acidic media that can degrade the starting nitrated compound, and does not require harsh reaction conditions (e.g. high hydrogenation pressures or temperature refluxing). At the end, reproducibility of the results was verified by a minimum of triplicate experiments for each set of reactions in small to large scales ranging from 25 mg to 5 g. We also present a careful and comprehensive characterization of the products at each step of the synthesis of amino-PCP and of the amino-Parylene thin films produced from it. This careful characterization has not been addressed in the literature, making the reproduction of synthesis protocols difficult and the wide applicability of amino-Parylene coatings challenging.

On the other hand, despite the frequent reports that address the synthesis of carboxyl-substituted PCP, we were unable to find any work in literature that targets the synthesis of carboxyl-PCPs as the main product. Their synthesis has been targeted in many works as intermediate PCP derivatives that can be subsequently converted to a variety of other compounds such as amines,[47, 48, 52] cyanides[52] or even more complex structures such as quinolinophane.[53] The majority of mono- and di-substituted PCPs were obtained with the aid of Friedel–Crafts electrophilic aromatic substitution either by alkylation or acylation of the pristine PCP.[47, 48, 53-56] In case of acylation, the resulting acetyl compounds have been either used as synthesized, serving as an intermediate, or further modified, often through hydrolysis, to obtain mono-substituted carboxyl-PCP or its derivatives. Like many other substituted [2.2]paracycophanes, synthesis of carboxyl-PCPs and their related ketones were

reported for the first time by Cram in 1955.[47] First, acetylation of PCP was conducted under 'very mild condition' (-20 °C, 10 min) using acetyl chloride and $AlCl_3$ in sym-tetrachloroethane solvent. The reaction was then quenched with HCl(aq.) and the extracted crude product was purified by distillation and crystallization from aqueous ethanol solution to yield 71% of 4-acetyl[2.2]paracyclophane. Following this, the isolated ketone was hydrolyzed under basic aqueous conditions. This was performed by slowly adding a solution of the ketone, from previous step, in dioxane solvent to a potassium hypobromite solution at 0° C and conducting the reaction at room temperature for less than two hours. The hydrolysis step was reported to yield 90% of 4-carboxyl[2.2]paracyclophane. Changing the solvent to dichloromethane in the first step, acylation reaction, lowered the yield to 43 % and gave rise a number of by-products which were not isolated or identified.[54] However, the authors claimed the isolation of 23% of the product by column chromatography on the filtrate of the initial crystallization step. To study the direct influence of substituents on the electrophilic substitution of [2.2]paracyclophanes, Cram carried out the acylation reaction of mono-bromo-PCP under the similar conditions with acetyl chloride/$AlCl_3$ reagents in dichloromethane solvent and obtained mainly the pseudo-para isomer in 41% yield. A similar methodology has been used by Waters.[48] In order to be able to conduct the acylation reaction of PCP at room temperature and to avoid the use of subzero cooling baths, acetyl chloride was replaced by trifluoroacetic anhydride and the reaction was allowed to continue for 30 min at room temperature. This acylation procedure has reportedly yielded 95% of 4-trifluoroacetyl[2.2]paracyclophane as crude product at the end. However, conducting the reaction at room temperature instead of controlling it at very

low temperatures is contradicted by the general considerations that Cram remarks for prevention of side reactions when doing a Friedel–Crafts acylation on PCPs.[47, 54] The subsequent hydrolysis of trifluoroacetyl-PCP, converting it to carboxyl-PCP, was carried out by refluxing in aq. KOH (10% solution) which has been reported to yield 85%.[48]

A different approach has been suggested by Yeh and Gorham starting with halogenation, more specifically bromination of PCP and converting them to carboxylated PCP in two steps.[52] In the presence of a catalytic amount of iron powder, the halogenation reaction of PCP was carried out at 40–50 °C in carbon tetrachloride to yield 91% of di-bromo-PCP which subsequently was converted to di-lithio-PCP through halogen-lithium exchange chemistry. Treatment of di-bromo-PCP with n-butyllithium in refluxing benzene under anhydrous conditions and cooling to room temperature gave a milky mixture containing di-lithio-PCP, which was used for the next reaction step by simply decanting into a beaker containing powdered dry ice. Extracting with water and acidifying with HCl resulted in 95% of di-carboxyl-PCP. Slightly different procedures can be implemented to convert the bromo groups to carboxyl groups using Grignard reagents.[57] However, addition of carbonyl groups at the end of this method was performed by bubbling of carbon dioxide, dried on $CaCl_2$, SiO_2, 5 Å molecular sieves, P_2O_5 and sulfuric acid for 18 h;[58] a procedure that required considerable time and effort compared with previous methods. In all of the above reports along with many other works, Carboxyl-PCP has been utilized as an intermediate for synthesis of further substituted PCPs. Some works, convert them to aminated PCPs,[48, 52, 53] while some introduce the possibility of synthesizing aminoacids through multi step di- or multi-substitution mechanisms.[57, 59]

Among the above methods for substitution of PCPs with carboxyl groups, we selected the Friedel–Crafts acylation approach as it does not implicate laborious experimental conditions and has proved successful in some works. The first acylation reaction was carried out following the procedure described by Waters,[48] a method that appeared to be the most straight forward reaction of all methods and reported to have a high product yield. Unfortunately, different results were obtained in our work than what is reported. In our hands, the acylation of PCP with trifluoroacetic anhydride at room temperature resulted in the production of polymers in larger proportion than the desired product. Hence, we attempted to improve this reaction by controlling it at very low temperatures. In spite of controlling the inappropriate side reactions, the low reaction temperature prolonged the main reaction as well and we recovered the majority of unreacted starting material at the end of the reaction. Furthermore, we attempted to use Cram's method for acylation of PCP using acetyl chloride/$AlCl_3$ in dichloromethane.[54] As reported, the yield of this reaction is not expected to be more than 70% and the product is contaminated with several by-products that needs to be isolated. To do this, Cram distilled the crude product at 200 °C, crystalized in methanol and performed column chromatography. To date, we have not been able to develop a reproducible method for isolation of the product and as a result, we have not yet proceeded to the next step of these reactions to convert the synthesized acetyl group to carboxyl acid derivative. Since we were mostly focused on the synthesis of amine-functionalized PCPs as the main goal of this project, we lacked of time to complete all the reactions required for the synthesis of carboxyl-PCP and here we only report the best of our obtained results by to date.

Chapter two: Experimental

2-1- Materials

Anhydrous sodium sulphate, sodium bicarbonate, sodium hydroxide, potassium hydroxide, concentrated hydrochloric acid (38%), glacial acetic acid (99.7%) and solvents including toluene, dichloromethane, chloroform, diethyl ether, n-pentane, absolute ethanol, and methanol were purchased from Caledon Laboratories Ltd. [2.2]Paracyclophane (97%), 2-nitro-para-xylene (99%), sodium nitrate (99%), sodium nitrite (97%), sodium borohydride (98%), sodium bisulfite (mixture of $NaHSO_3$ and $Na_2S_2O_5$), anhydrous aluminum chloride (99.99%), fuming nitric acid (99.5%), trifluoromethanesulfonic (triflic) acid (99%) and anhydride (99%), trifuoroacetic acid (99%) and anhydride (99%), acetyl chloride (99%), bromine (99.5%), [18]crown-6 ether (99%), triirondodecacarbonyl (contains 1-10% methyl alcohol) and Raney ® Nickel 2800, slurry in H_2O, active catalyst were obtained from Sigma-Aldrich. Dichloromethane was distilled from calcium hydride (CaH_2) immediately prior to use. All other solvents and reagents were used as received.

2-2- Instrumentation

All glassware was dried in an oven prior to use and reactions were performed under argon atmosphere where an inert atmosphere was needed. Flash chromatography was performed on a Silica gel (230–400 mesh, Silicycle Inc.) column. Thin Layer Chromatography (TLC) was carried out on pre-coated Aluminum-Backed TLC Sheets

(EMD Millipore). Spots were visualized using short-wave ultraviolet light (254 nm) or by iodine vapor. Low temperature baths were prepared by making a mixture of NaCl/ice (-20 °C) and a slurry of solid carbon dioxide (dry ice) with acetone (-78 °C). Chemical vapor deposition polymerization of Parylene films was performed in a Labcoater2® Parylene Deposition System (Specialty Coating Systems). The cold trap of the CVD machine was cooled down using a mechanical chiller probe of FTS Systems Flexi-Cool, model FC100.

2-3- Synthesis of 4-nitro[2.2]paracyclophane

2-3-1- Nitration with triflic acid/anhydride

Similar conditions were employed using both triflic acid and triflic acid anhydride. In a sample reaction DCM (30 mL) and triflic acid anhydride (3.5 mL, 20.803 mmol) were mixed for 5 min in a 100 mL round bottom flask equipped with a magnetic stir bar and then fuming nitric acid (1.6 mL, 38.343 mmol) was added to the solution and stirred for another 15 min at room temperature under argon atmosphere. The super-acidic solution was then cooled to -78 °C followed by slow addition of PCP (1.000 g, 4.805 mmol) solution in DCM (40 mL). The reaction mixture was stirred for 20 min at -78 °C and an additional 120 min at -20 °C under argon atmosphere. The reaction was stopped by quenching in ice water (700 mL) and subsequent neutralization with sodium bicarbonate. Sodium bicarbonate was added until the solution became neutral or slightly basic. The crude mixture was extracted with 3 x 250 mL of diethyl ether (Et_2O). All organic phases were combined and dried over anhydrous Na_2SO_4, filtered and evaporated under vacuum to afford the brown crude

product. Dry flash chromatography was performed on a silica gel column to isolate the nitrated products. To be able to dry load the compound, it was adsorbed onto the minimal amount of silica gel by dissolving in DCM, adding silica gel (ca. 5 g) into the solution and removing the solvent. Elution with n-pentane:Et_2O gradient (97.5:2.5, 95:5, 90:10, 80:20, 60:40, 20:80, 100% Et_2O, methanol) afforded 10 different fractions among which the third fraction was identified as 4-nitro-[2.2]paracyclophane as a yellow brittle powder after removing the eluent (1.021 mg, 84%). Rf=0.67 (60:40 n-pentane:Et_2O); m.p. = 150 – 152 °C; IR (KBr): ῡ= 868 (CN), 1196 (NO_2), 1338 and 1516 (N-O stretches), 1422, 1599, 2849 and 2920 (CH, sp^3), 3036 (CH, sp^2) cm^{-1}; ^1H NMR (600 MHz, $CDCl_3$): δ= 7.22, (1H), 6.80(1H), 6.63 (2H), 6.55 (2H), 6.47 (1H), 4.03 (1H), 3.04-3.23 (4H), 2.92 (2H), 2.87(1H). ^{13}C NMR (151 MHz, $CDCl_3$): δ= 149.57, 142.36, 140.04, 139.60, 138.05, 137.61, 136.72, 133.47, 133.40, 132.68, 130.24, 129.81, 36.27, 35.25, 35.06, 34.73; MS (EI+, 70 eV): m/z (%)= 253 [M^+], 150 [$C_8H_8NO_2^+$], 104 [$C_8H_8^+$], 103 [$C_8H_7^+$], 78 [$C_6H_6^+$]; HRMS (Found: 253.1121), $C_{16}H_{15}NO_2$ requires 253.1103.

2-3-2- Nitration with sodium nitrate/nitrite

Similar pathways were examined using both sodium nitrate and sodium nitrite salts. Various concentrations of nitrating salts, reaction times (5-60 min) and temperatures (0-60 °C) were tested for the nitration reactions. In an example reaction, to a solution of PCP (0.100 g, 0.481 mmol) in TFA (10 mL) was added $NaNO_2$ (0.063 g, 0.900 mmol) under argon at 0 °C. The reaction mixture was stirred for 10 min and then quenched in ice/water (50 mL). The mixture was extracted with DCM (3x25 mL). Then, the organic layers were combined and washed once with 5% aq. solution of $NaHCO_3$ (50 mL) and once with water

(50 mL), dried over anhydrous Na_2SO_4 and concentrated with rotary evaporator to afford a dark brown residue. TLC of the crude product in 60:40 n-pentane:Et_2O solvent system showed 11 different compounds. The fourth fraction was identified as 4-nitro[2.2]paracyclophane (maximum yields of 12 and 8% with $NaNO_2$ and $NaNO_3$ salts respectively).

2-4- Synthesis of 4-amino-[2.2]paracyclophane

2-4-1- Reduction with Raney Ni/$NaBH_4$

As-synthesized 4-nitro-[2.2]paracyclophane (1.000 g, 3.951 mmol) was dissolved in ethanol (160 mL). Then, Raney Ni (0.100 g, ca. 1 mL of the slurry) was added into the solution and stirred for 5 min at room temperature. The reduction reaction was started with the subsequent addition of $NaBH_4$ in excess amounts (0.747 g, 19.760 mmol, 5 equiv.). To better control the hydrogenation over the time of reaction, addition of $NaBH_4$ was conducted slowly and very carefully in a few portions, and the reaction vessel was kept at room temperature using a water bath. After stirring for 30 min, the catalyst was removed via vacuum filtration and washed with copious amount of methanol. Due to the pyrophoric nature of Raney Ni, immediately after washing, the catalyst was transferred to a beaker of distilled water, followed by neutralization with HCl to prevent auto ignition. The filtrate was evaporated and the solid residue was partitioned between DCM (100 mL) and water (100 mL). The organic layer was removed and the aqueous layer was further extracted with 2 x 50 mL of DCM. The organic layers were combined and dried over anhydrous Na_2SO_4,

filtered and evaporated to obtain the pure 4-amino-[2.2]paracyclophane as a tan rigid powder (0.811 g, 92%). Rf=0.33 (60:40 n-pentane:Et_2O); m.p. = 220 – 222 °C; IR (KBr): IR (KBr): ῡ= 722, 800, 1286, 1422, 1498, 1509, 1562, 1610, 2857, 2928 and 3002 (CH, sp^3), 3032 and 3061 (CH, sp^2), 3375 and 3473 (NH stretches, primary amine) cm^{-1}; ^1H NMR (600 MHz, $CDCl_3$): δ = 7.17 (1H), 6.59 (1H), 6.41 (2H), 6.27 (1H), 6.15 (1H), 5.43 (1H), 3.40- 3.99 (2H), 3.06-3.16 (3H), 3.01-3.04 (2H), 2.94-2.98 (1H), 2.81- 2.86 (1H), 2.63-2.72 (1H); ^{13}C NMR (151 MHz, $CDCl_3$): δ = 144.80, 141.11, 139.01, 138.96, 135.31, 133.49, 132.48, 131.53, 126.86, 124.63, 123.01, 122.39, 35.41, 34.99, 33.06, 32.27; MS (EI+, 70 eV): m/z (%)= 223 [M^+], 119 (main) [$C_8H_7NH_2^+$], 91 [$C_7H_7^+$], 78 [$C_6H_6^+$], 65 [C5H5]; HRMS (Found: 223.1356), C_{16} H_{17} N requires 253.1361.

2-4-2- Reduction with triiron dodecacarbonyl

In a 50 mL round bottom flask equipped with a magnetic stirrer, were dissolved 4-nitro[2.2]paracyclophane (0.100 g, 0.395 mmol), triiron dodecacarbonyl (0.199 g, 0.395 mmol) and [18]crown-6 ether (0.005 g) in toluene (10 mL). The reaction commenced by adding 10 mL of 1N KOH at room temperature under vigorous stirring. After 2 h, the green mixture was extracted with diethyl ether (2x10 mL) and then the combined organic layers were washed once with water (10 mL), dried over anhydrous Na_2SO_4, filtered and concentrated under vacuum to leave a green residue. In order to purify the reduced product from crude, the residue was dissolved in minimal amount of n-pentane:Et_2O solvent mixture (95:5 v/v) and flash chromatographed on a 1.23 cm (I.D.) x 20.32 cm (E.L.) silica gel column. First, the soluble catalyst was removed by elution with n-pentane (250 mL). Once the green color disappeared, i.e. the entire catalyst was removed, the remaining

material was eluted with 60:40 of n-pentane:Et_2O (250 mL), which resulted in 3 different compounds. The first two corresponded to the starting material and triiron dodecacarbonyl catalyst, but the combined pure fractions of the third compound delivered 0.004 g (<5% yield) of 4-amino[2.2]paracyclophane after evaporation of the solvent.

2-5- Reduction of 2-nitro-para-xylene

Reduction of 2-nitro-para-xylene was conducted in similar conditions to 4-nitro[2.2]paracyclophane as follows:

- **Raney Ni/$NaBH_4$ catalysis**: To a solution of 2-nitro-para-xylene (0.028 g, 25 µL, 0.185 mmol) in methanol (2 mL) was pipetted Raney Ni (0.1 g, ca. 1 mL of the slurry) at room temperature. After stirring for 2 min, $NaBH_4$ (0.014 g, 0.370 mmol, 2 equiv.) was added in a few portions at 2-minute intervals over a period of 10 minutes. Through the subsequent vacuum filtration, the catalyst was removed and washed with copious amounts of methanol. The solvent was removed under vacuum and the residue was partitioned between DCM (10 mL) and water (10 mL). The aqueous layer was extracted again with DCM (2 x 5 mL) and the organic layers were combined before being dried over anhydrous Na_2SO_4. Evaporation of the solvent yielded a dark yellow oil (0.022 g), characterized as 2-amino-para-xylene (96%). Rf=0.47 (60:40 n-pentane:Et_2O; visualized by iodine vapor as the product was not UV-detectable); b.p. = 216-218 °C. ^{1}H NMR (600 MHz, $CDCl_3$): δ = 6.95-6.97 (1H), 6.55-6.57 (1H), 6.54 (1H), 3.53-3.67 (2H, broad), 2.27 (3H), 2.16 (3H).

- **Triiron dodecacarbonyl catalysis**: 1 N KOH (5 mL) was added to the solution of 2-nitro-para-xylene (0.028 g, 25 µL, 0.185 mmol), triiron dodecacarbonyl (0.094 g, 0.187 mmol) and [18]crown-6 ether (0.004 g) in toluene (5 mL) and the mixture was stirred vigorously for 2h at room temperature. Extraction with Et_2O and subsequent column chromatography as described for 4-amino[2.2]paracyclophane delivered 0.012 g (52.9 %) of 2-amino-para-xylene.

2-6- Synthesis of 4-trifluoroacetyl[2.2]paracyclophane

In a two-neck round bottom flask, equipped with an argon inlet, dropping funnel and a magnetic stirrer, anhydrous aluminum chloride (0.114 g, 0.863 mmol) was dispersed in DCM (3 mL) and cooled to -78 °C. A solution of trifluoroacetic anhydride (135 µL, 0.955 mmol) in DCM (2 mL) was added dropwise over 1 min through the dropping funnel under argon at -78 °C. After the mixture was stirred for 15 min under argon at -78 °C, [2.2]paracyclophane (0.100 g, 0.480 mmol) was added over 1 min and the mixture was stirred for an additional hour. The reaction was quenched by transferring into a mixture of ice/conc. HCl (5 mL) and washed with water (2 x 5 mL), 1 N NaOH (2 x 5 mL), and water (5 mL). The combined aqueous layers were extracted with 5 mL of DCM and then the organic layers were combined, dried over anhydrous Na_2SO_4, filtered and concentrated under reduced pressure to yield 0.117 g of white residue. TLC of the crude compound showed a mixture of two compounds under UV. The more polar compound that was isolated by recrystallization from methanol was a light brown solid and characterized to be

4-trifluoroacetyl[2.2]paracyclophane (0.440 g, 28%) Rf=59.1 (80:20 n-pentane:Et_2O); m.p. 81-83 °C. ^{1}H NMR (600 MHz, $CDCl_3$): δ = 7.12 (m, 1H), 6.80 (dd, 1H), 6.64 (d, 1H), 6.53 and 6.59 (dABq, 2H), 6.38 and 6.43 (dABq, 2H), 3.94-3.98 (m, 1H), 3.18-3.25 (m, 4H), 3.01-3.07 (m, 2H), 2.91-2.96 (m, 1H). ^{13}C NMR (151 MHz, $CDCl_3$): δ = 181.04, 145.43, 140.27, 139.92, 139.40, 138.90, 136.97, 134.68, 132.97, 132.42, 131.36, 130.07, 117.49, 115.54, 36.31, 35.08, 35.05, 34.53.

2-7- Synthesis of 4-acetyl[2.2]paracyclophane

A solution of acetyl chloride (0.066 g, 60 µL, 0.842 mmol) in anhydrous DCM (1 mL) was added dropwise to a stirred anhydrous mixture of aluminum chloride (0.114 g, 0.856 mmol) in DCM (3 mL) under argon at -10°C. To the resulting homogenous solution, was added [2.2]paracyclophane (0.100 g, 0.480 mmol) over 1 minute followed by stirring for another 15 min at -10°C. The reaction mixture was poured onto a slurry of ice and concentrated HCl (5 mL) and the aqueous phase was separated and extracted with DCM (2 x 5 mL). The organic phases were combined, washed with water (2 x 5 mL), dilute (5%) bicarbonate solution (2 x 5 mL) and water (5 mL), then dried over anhydrous Na_2SO_4 and filtered prior to evaporation of the solvent under vacuum to afford the crude product.

2-8- CVD polymerization

A piranha solution with the following recipe was prepared to clean Si wafers cut into squares of size: 0.5×0.5, 1×1, and 2×2 cm^2. 200 mL of concentrated sulfuric acid

(H_2SO_4) was heated to approximately 80 °C. Then, hydrogen peroxide (H_2O_2) was added to H_2SO_4 in approximately 1/3 of the volume of the acid. Once the solution reached to 100°C, wafers were dipped into the solution for 10 min. This was followed by two successive 5-min rinses in Mili-Q water. At the end, wafers were rinsed and kept in methanol before being dried under N_2 stream. (**CAUTION!** Extra care is needed when handling Piranha solution as it is extremely dangerous and highly reactive with organic compounds. For a safe disposal of the solution it is usually diluted with 5 folds of distilled water).

The clean wafers were sputtered with chromium (20 nm) and gold (200 nm) layers and then cleaned in acetone, methanol and ethanol baths (10 min each). The gold-sputtered wafers, were placed in the deposition chamber of the CVD machine and 0.250 g of the dimer precursor was used to coat the wafers with corresponding Parylene film. Temperature and pressure at different zones of the machine were kept constant at 170°C and 1 Torr for the sublimation zone, 690°C and 0.5 Torr for the pyrolysis furnace, and room temperature and 0.1 Torr for the deposition chamber. Vacuum pressure of 0.001 Torr was created with the vacuum pump and the cold trap was cooled down to -70°C with the aid of a mechanical chiller probe.

2-9- Characterization of precursors

Melting points were determined on a MPA160 Melting Point Apparatus (Stanford Research Systems, Inc.) and were uncorrected. Fourier transform infrared (FT-IR) spectra

were recorded on a Thermo Scientific Nicolet 6700 FT-IR Spectrometer and processed in transmission mode using OMNIC software (version 7.4.127) after 64 scans. The samples of dimer precursors were oven dried at 110 °C for 2 h prior to incorporation into KBr pellets (~1 wt%). ^{1}H and ^{13}C NMR spectra were recorded on a Bruker Avance 600 spectrometer at 600 MHz and 150 MHz for proton and carbon NMR, respectively. All experiments were performed in deuterated chloroform at room temperature, unless otherwise noted. Chemical shifts in ^{1}H and ^{13}C NMR spectra are reported in parts per million (ppm) on the δ scale from an internal standard of residual chloroform ($CDCl_3$=7.26 ppm for ^{1}H NMR and $CDCl_3$=77.36 ppm for ^{13}C NMR[60]). Data are reported as follows: chemical shift, multiplicity (with the following abbreviations: s = singlet; br s = broad singlet; d = doublet; t = triplet; q = quartet; dd = doublet of doublets; dq= doublet of quartets; dt= doublet of triplets; ABq = AB quartets, dABq = doublet of AB quartets; m = multiplet), and integration. Low resolution and high resolution mass spectra (HRMS) were obtained at the McMaster Regional Centre for Mass Spectrometry using a Waters GCT system EI and a Waters Micromass Global Ultima (MALDI/CapLC-ESI Quadrupole Time of Flight) mass spectrometer, respectively.

2-10- Surface characterization

The surface energy (hydrophilicity) of the coated surfaces was assessed through static water contact angle (WCA) measurements with the sessile drop technique using a Ramé-Hart NRL C.A. goniometer, model 100-00-115, (Mountain Lakes, NJ) equipped with an automated dispensing system and a Sanyo VC8−3512T camera. The above-

mentioned FT-IR instrument could also be equipped with a narrow band Mercury Cadmium Telluride (MCT) detector (cooled with liquid N2) and a smart SAGA (Smart Apertured Grazing Angle) accessory to obtain the grazing-angle specular reflectance IR spectroscopy of the thin polymer films. The p-polarized light was incident at 70 ° relative to the surface normal of the substrate The spectra were acquired in a single reflection mode and were reported in the %reflectance mode at a resolution of 4 cm^{-1} relative to a clean gold surface. 128 scans were accumulated to achieve an acceptable signal/noise ratio. X-ray photoelectron spectroscopy (XPS) data were collected using a Kratos AXIS Ultra with monochromatic Al Kα X-ray excitation at 1486.7 eV.High resolution C1s, N1s and Cl2p (200 µm spot size, 50W beam) spectra were acquired to find the elemental composition of the deposited Parylene films.

Chapter three: Results and Discussion

3-1- Preparation of Amine-functionalized Paracyclophanes and Paraxylenes

Synthesis of amine-functionalized Parylene films has been a challenge since the initial investigations of Cram.[47] Between the two general approaches that have been utilized to this end, the direct nitration-reduction method suffers from the nitration step. This is due to the low yields and difficult purification of nitrated PCPs from the large number of by-products that result from the poor stability of [2.2]paracyclophane to oxidation and polymerization in acidic conditions. Recently, Lahann[51] developed a procedure to control the side reactions of PCP in acidic conditions and therefore improve the yield of the nitration reaction and allow the large-scale preparation of the amino-PCP precursor. Their fundamental contribution was to cool down the reaction to temperatures as low as -78 °C to suppress side reactions (e.g. polymerization) that are favored at higher temperatures, while using a superacidic condition at the same time to push the nitration reaction and produce acceptable yields. Under these conditions, the authors reported the synthesis of mainly two isomers of dinitro-PCP (93%) and only traces of mononitro-PCP.[51, 61] In principle, only four different isomers of dinitro[2,2]paracyclophane can be synthesized through the direct nitration method. According to the work of Reich the four isomers could be created by substitution of the second nitro group on four open positions of the unsubstituted ring (2bI-2bIV in **Scheme 4**).[50, 62] The NMR spectra of dinitro[2,2]paracyclophanes allowed only the assignment that they are heteroannularly disubstituted [2,2]paracyclophanes.[50] Since the two rings of the [2.2]paracyclophanes

cannot rotate with respect to each other, four dinitro [2.2]paracyclophanes with nitro groups in different rings can be drawn.[63] During column or thin layer chromatography, the pseudo-gem isomer is consistently more polar than the other known isomers. The pseudo-para and pseudo-meta isomers are inseparable by chromatography but usually have a sufficient solubility difference to allow reasonable separation on this basis. The pseudo-ortho isomers are generally more polar than the pseudo-para isomers, as expected, since they should have a higher dipole moment.[62]

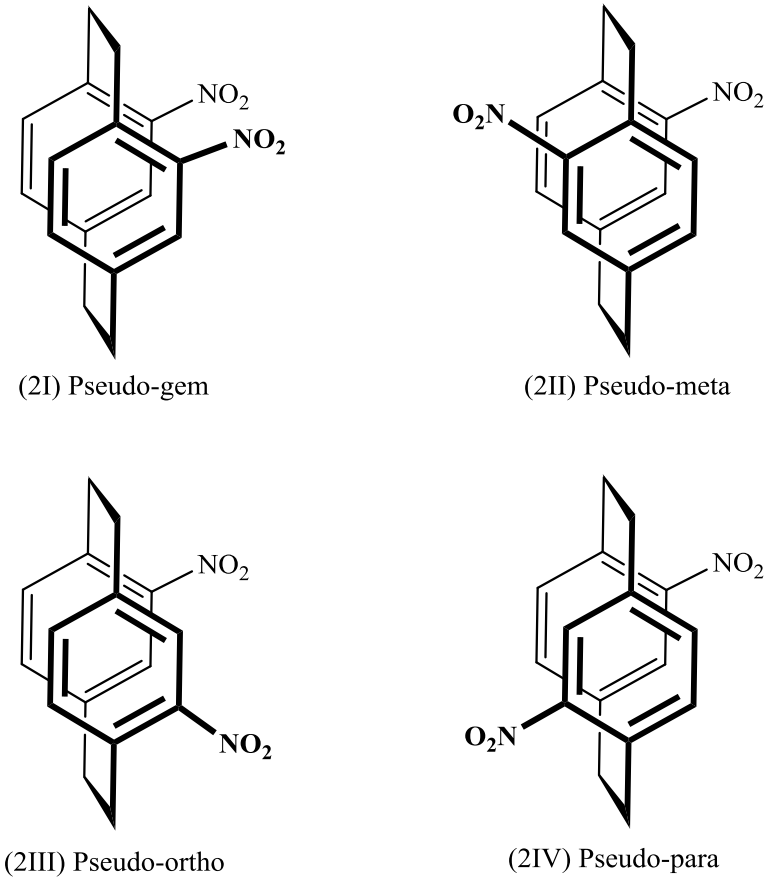

Scheme 4. Isomers of Dinitro[2.2]paracyclophane

Although the approach used in Lahann's work was expected to produce mainly two pseudo-meta and pseudo-para isomers (at yields of ~20% and 70%, respectively), minor amounts of pseudo-gem and pseudo-ortho isomers, and traces of monosubstituted product,[51] different results were obtained in our work. Following Lahann's procedure failed to reproduce the reported results and, under most conditions, the major products were identified as mononitro-PCP or polymeric by-products. Furthermore, varying reaction conditions including reaction time (from 0.5 to 6 h), temperature (-78 to 60 °C), and molar ratio of acid:PCP (1:1 to 20:1) did not result in noticeable amounts of dinitro-PCP. Based on our observation, the main problem was the immediate precipitation of the acidic mixture when cooled down to -78 °C. As the fuming anhydrous nitric acid was added to the solution of triflic acid in anhydrous DCM and cooled down to subzero temperatures, we observed a precipitate formed in the reaction vessel that gave rise to inefficient stirring as the stir bar was trapped inside the precipitates. Considering the mechanism of formation of nitronium ions (**Scheme 5**), we attributed the presence of precipitates to the formation of water as a consequence of the reaction of triflic and nitric acids, which is not miscible with DCM and freezes at subzero temperatures.

On the other hand, close scrutiny of the published results for the synthesis of dinitro-PCP[51] revealed that some spectroscopic data were inaccurately reported, which reduces the reliability of the published method. These inaccuracies can be found for instance in NMR data where almost the same shifts for ^{1}H NMR and completely identical shifts for ^{13}C NMR of dintro-PCP and mononitro-PCP have been reported. This is despite the reasonable expectation of more than one deshielded aliphatic proton in ^{1}H NMR and two deshielded

carbons in ^{13}C NMR of dinitro-PCP. In addition, the amount of dinitro-PCP that has been used for the following reduction step is based on the same molecular weights as that of the mononitro-PCP.

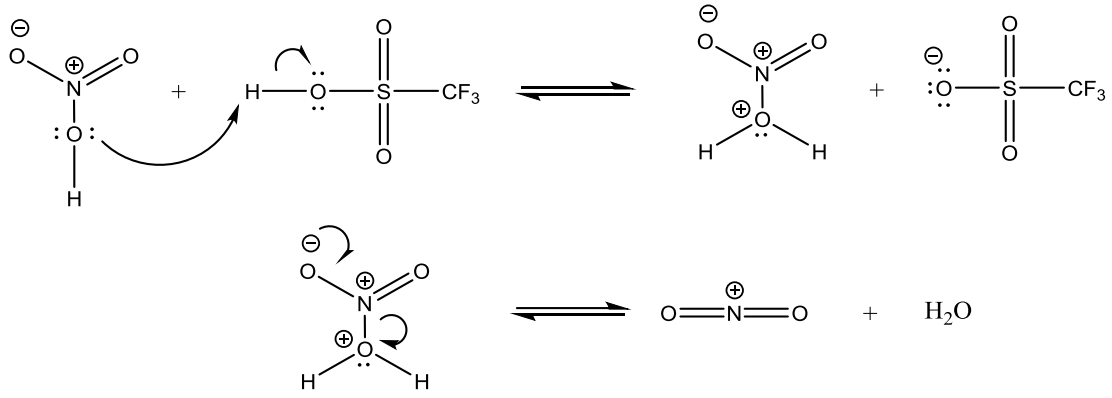

Scheme 5. Reaction of nitric acid with triflic acid and formation of nitronium ions

In order to overcome the precipitation problem, we replaced the triflic acid with triflic anhydride to minimize the water content in the nitration reaction. Varying the time of reaction and concentration of the acid, we found that the highest yield of mononitro-PCP was obtained when PCP is reacted with respectively 8 and 4 equivalents of nitric acid and triflic anhydride for 20 min at -78 °C and for an additional 2 h at -20 °C. The alternative nitration reaction is presented in **Scheme 6**.

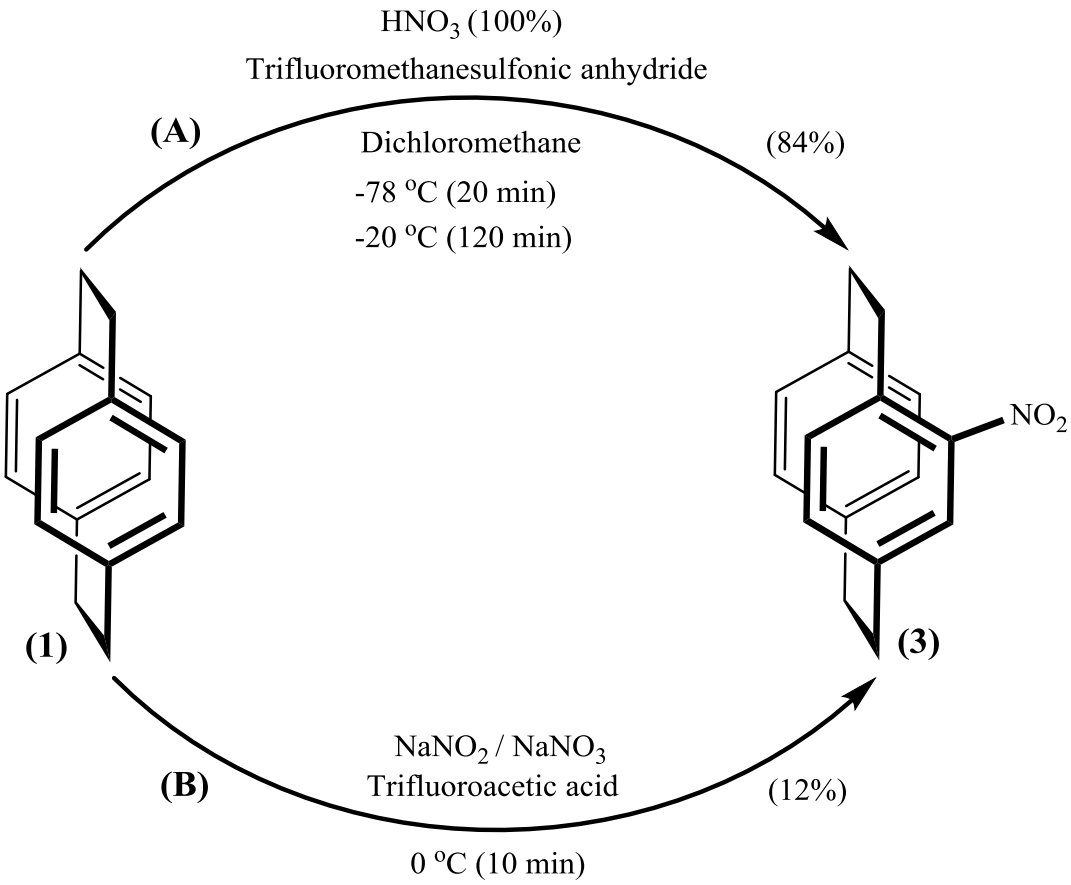

Scheme 6. Nitration reaction of PCP using i) fuming nitric acid and triflic anhydride (84%); and ii) TFA and nitrite or nitrate salts (12%)

In addition to the nitrating acid reactions (the most frequently used method), two other nitrating systems have been proposed for aromatic compounds: nitrating salts and solid acids. Following a procedure described by Luguya[41] for the synthesis of meso-(para-nitrophenyl)porphyrins, we explored the nitration of PCP using nitrate/nitrite salts (**Scheme 6**). This method involves treatment of a concentrated solution of PCP in TFA with $NaNO_2$. The proposed electrophiles for the electrophilic substitution reaction are both NO_2^+ and

N_2O_3.[40] High yields of nitrated products have been reported in nitration of benzene and substituted benzenes under these conditions.[39, 40]

However, following the reported procedure, [41] using either $NaNO_3$ or $NaNO_2$ at room temperature, did not produce more than 8% of nitro-PCP. Also, varying the reaction temperature, time, and the amount of $NaNO_2$ or $NaNO_3$ did not lead to significant progress so that the maximum yield that we achieved using this method was 12%. This was carried out with 2 equiv. of $NaNO_2$ at 0°C for 10 minutes. One of the restrictions of this method is the comparatively high freezing points of acetic acid (16°C) and trifluoroacetic acid (-15.4°C) that limit the reaction temperature. As a consequence, this approach resulted mainly in polymer by-products rather than the desired nitrated products due to poor control of side reactions. The reaction conditions for different nitrating systems and the obtained results with each method as well as special remarks on each method are summarized in **Table 1**. As shown in the table, the highest yield of mono-nitro PCP was achieved when 8 equivalents of fuming nitric acid is used along with triflic anhydride to treat a solution of PCP in dichloromethane at very low temperatures under stringent prevention of moisture and oxygen in the reaction medium.

For the reduction of the synthesized nitro-PCP, we first followed the procedure described by Lahann.[51] However, the reduction reaction of the nitro-PCP with triiron dodecacarbonyl under organic/aqueous phase-transfer condition, shown in **Scheme 7Ai**, did not yield quantitative amounts of the desired amino-PCP product. In addition, triiron dodecacarbonyl is a homogeneous catalyst that completely dissolves in the reaction solvent and consequently complicates the isolation of products. To isolate the products, the crude

mixture was chromatographed on a tall silica gel column and the catalyst was washed thoroughly with a nonpolar solvent (n-pentane) before starting elution of the compounds. This reaction and purification process yielded only 5% of 4-amino[2.2]paracyclophane.

Table 1. Summary of different nitration reaction conditions and their results

Methods	Nitrating system	Yield	Remarks
Nitrating acid	HNO_3/H_2SO_4	N.A.	- Water formation - Difficult Purification
	Fuming HNO_3/ Triflic Acid	26%	- Water formation (precipitation) - Difficult Purification
	Fuming HNO_3/ Triflic anhydride	84 %	- Very sensitive to moisture and O_2 - No precipitation problem - Easier extraction
Nitrate/Nitrite salts	$NaNO_3$/TFA	8%	- Limited to high temperatures (minimum -15°C) - Appropriate for regioselective nitration
	$NaNO_2$/TFA	12%	
Solid acids	Silica based solid acids	N.A.	- Less pollution - Appropriate for more reactive materials

The low yields from this approach to the reduction step, prompted us to reexamine the ability of the catalyst and the phase transfer approach to reduce nitrated aromatic compounds. For this purpose, as shown in **Scheme 7Aii**, reduction of 2-nitro-para-xylene, a similar compound, was attempted using the same procedure. Although 2-nitro-para-xylene is much more reactive than 4-nitro[2.2]paracyclophane and it is expected to reduce quantitatively in an efficient reduction reaction, it was reduced only in moderate yields (~53%). The lack of efficiency of triiron dodecacarbonyl catalysis, motivated us to search for a more efficient and compatible reducing agent.

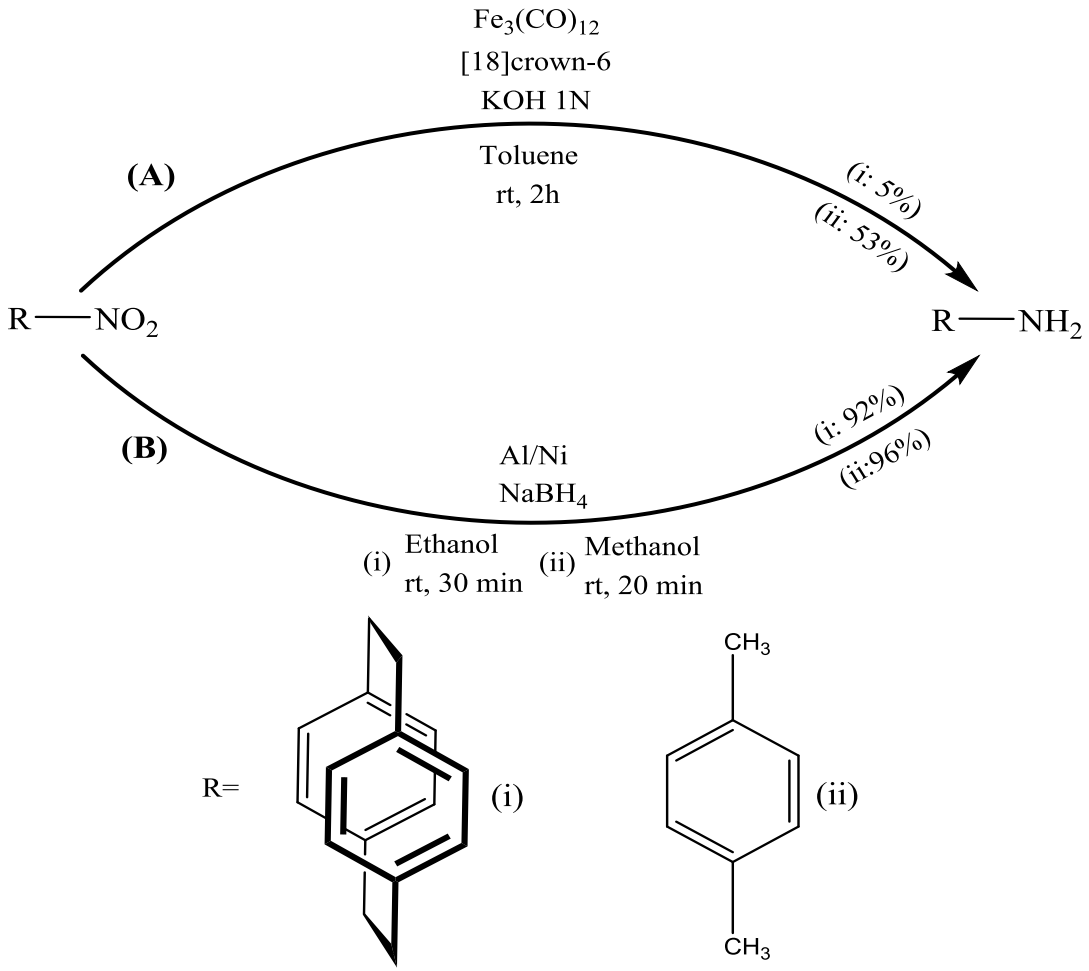

Scheme 7. Reduction of i) 4-nitro[2.2]paracyclophane and ii) 2-nitro-p-xylene via A) Raney Ni/$NaBH_4$ and B) triiron dodecacarbonyl/[18]crown-6 catalyses

In this regard, many of the traditional reduction systems such as Fe/HCl or $SnCl_2$/HCl were unsuitable for our system. The main reasons for this were the insolubility of nitro-PCP in the reaction medium and that the use of co-solvents (e.g. methanol) did not have a considerable effect on the reduction nitro-PCP. In addition, agents that have been reported to be efficient in the reduction of many nitro compounds (e.g. Pd/C/H_2) were avoided because they involved harsh conditions such as high pressure of hydrogenation or

refluxing at high temperatures.[64] Eventually, an alternative method was adapted from the work of Pogorelić,[43] where a number of aromatic nitro compounds were successfully reduced to corresponding aniline molecules using Raney Nickel/$NaBH_4$ system. This method was first employed in reduction of 2-nitro-para-xylene (**Scheme 7Bii**) to examine the efficiency of Raney Ni catalysis and similar to the work of Pogorelić,[43] a very high yield (96%) was obtained. As the reduction of the model compound showed promising results, the method was used in the reduction of 4-nitro[2.2]paracyclophane. Although we obtained acceptable yields (78 – 82%) following the reported reaction conditions, we observed that 4-nitro[2.2]paracyclophane was not completely soluble in the reaction solvent, methanol. While the authors report that this reduction system performs best in methanol, our best yields (92%) were obtained using ethanol, which more effectively dissolves nitro-PCP (**Scheme 7Bi**) A summary of reaction conditions, their results and selected remarks for all reduction systems that were considered in this work is given in **Table 2**. A simple comparison of these methods suggest that the only drawback of the latter method is pyrophoric nature of the Raney Ni catalyst that requires some care in handling to avoid its autoignition. However, if care is taken to prevent its exposure to air, it has many advantages over other reduction systems that make this reaction an ideal method for scale-up productions. First, this method is straightforward and inexpensive. It does not require harsh conditions such as high pressures for hydrogenation or refluxing at high temperatures. In addition, it can be carried out in a short time (10-20 min) and affords a high purity crude product, which obviates the need for chromatographic purification. All of these advantages

alleviate the difficulties of scaling-up and in overall make this reaction a simple and practical method.

Table 2. Summary of reduction reaction conditions and their results

Reduction System	Yield	Remarks
$SnCl_2$/HCl or Fe/HCl	-	Not soluble in HCl
Pd/C/H_2	N.A.	High pressure of hydrogenation
$Fe_3(CO)_{12}$/Toluene/aq. KOH	5%	Difficult isolation from the dissolved Catalyst
Raney Ni/$NaBH_4$	92%	High purity of crude products Pyrophoric catalyst waste

3-2- Preparation of Carboxyl-functionalized Paracyclophanes

Synthesis of carboxyl-functionalized PCP has been reported in some works as useful intermediate compounds.[47, 48, 52] The multistep procedures, generally involve halogenation of the parent PCP followed by transformation of bromine groups to carboxyl groups usually via organometallic chemistry in a few steps.[52, 57, 58] However, simpler approaches exploit the Friedel-Crafts acylation of PCP followed by hydrolysis of the resultant ketones to convert to corresponding carboxylic acids.[47, 48, 54] In the investigations of Cram on the chemistry of PCPs, it is advised to conduct such reactions under controlled conditions to avoid polymerization of PCPs.[54] However, recently Waters[48] reported quantitative acylation of PCP using trifluoroacetic anhydride/$AlCl_3$ at room temperature. Subsequent hydrolysis of the obtained 4-trifluoroacetyl[2.2]para-cyclophane in refluxing KOH solution converted the acetyl groups to carboxylic acids. This method was originally developed by Cram[54] using acetyl chloride/$AlCl_3$ at very low temperatures (-40 to -20 °C).

Additionally, the second step was carried out by the hydrolysis of the acetyl-substituted PCP with hypobromite solution.

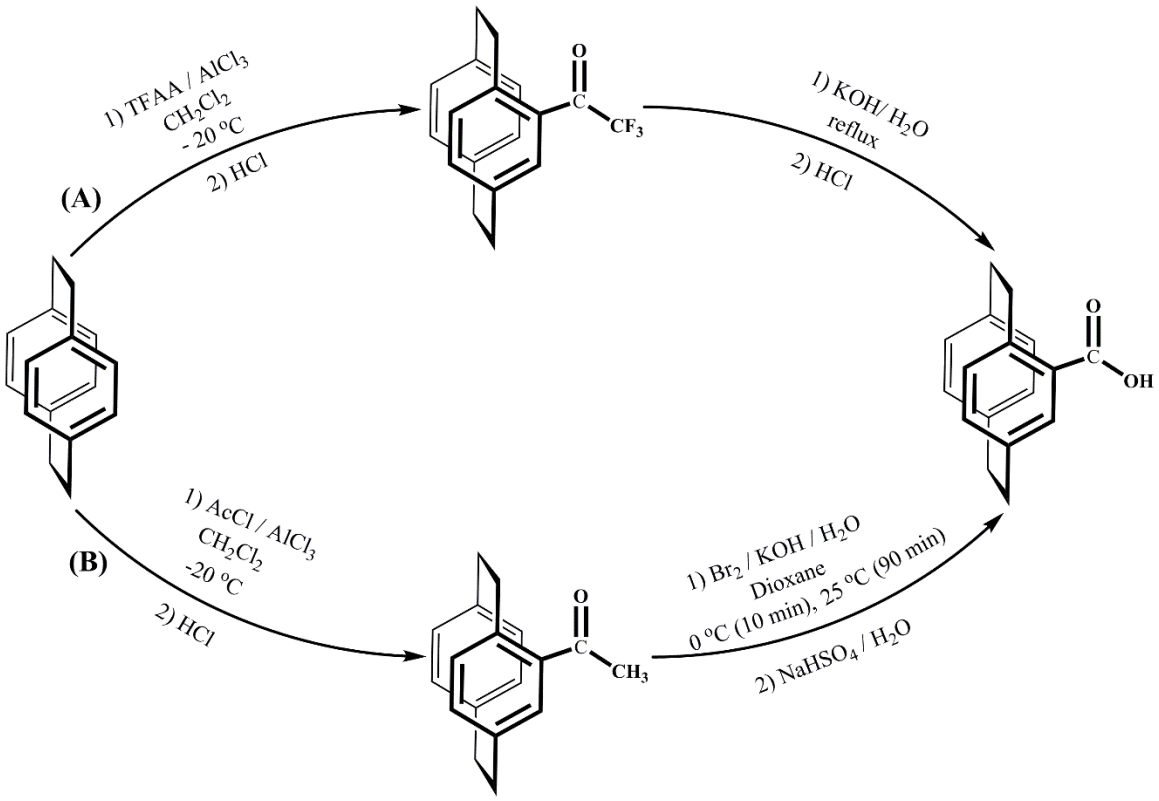

Scheme 8. Carboxylation of [2.2]paracyclophane via A) trifluoroacetyl and B) acetyl functionalized intermediates

We adapted our synthetic route toward the carboxyl-PCP with a slight variation of conditions in the last two procedures described for Friedel-Crafts acylation.[48, 54] These two approaches are illustrated in **Scheme 8.** In our experience, following the approach A as originally reported[48] led mostly to the polymerization of PCP, which required post-

purification steps by column chromatography. Nevertheless, very low amounts of 4-trifluoroacetyl-[2.2]para-cyclophane (<10%) was collected. Neither changing the amounts of reagents nor shortening the reaction time prevented the production of polymers. Therefore, considering the general remarks of Cram[54, 63] we lowered the reaction temperature to -78 °C to avoid side reactions. Despite succeeding in reducing the side reactions, we have not been able so far to optimize the reaction condition to achieve the highest yield of the desired 4-trifluoroacetyl-PCP. The majority of PCP (~75%) is yet unreacted at the end of the reaction. Allowing the reaction to continue for longer periods (3-5 h) at -78 °C or warming to room temperature for short periods (10-30 min) did not increase the yield considerably.

Because of the inefficiency of the above method that still needs to be optimized and pushed toward higher yields, the second step, hydrolysis of the synthesized 4-trifluoroacetyl-PCP, is not attempted yet. Also, in approach B, we have only been able to try the first step so far. Purification of acetyl-PCP from the crude product in this method is reported to require distillation at high temperatures (~200 °C).[47] In a different method a combination of column chromatography and distillation has been utilized to isolate the product.[54] We failed in our initial experiments to effectively isolate a completely pure product; however, this seems attainable by running a few experiments and finding the optimized condition to purify the product. Due to the lack of time carboxylation of PCP could not be studied completely and here, we only report our preliminary results and observations of these reactions.

3-3- Characterization of functional compounds

3-3-1- Amine-functionalized para-xylene

All of the functionalized compounds and some byproducts were characterized by traditional physical, chemical and spectrometric characterization techniques. In most cases, the preliminary analytical identification was conducted with ^{1}H NMR and once promising results were found, the samples were subjected to further characterization. For example, ^{1}H NMR spectrum of 2-amino-p-xylene synthesized by direct nitration with fuming nitric acid and triflic anhydride followed by Raney Ni/$NABH_4$ reduction is shown in **Figure 1**. According to the spectrum, the most characteristic chemical shift is shown at δ=3.62 with the integration of 2, corresponding to two protons of amino-para-xylene.[65] In total the following shifts are seen in the spectrum: δ= 2.16 (3H), δ= 2.27 (3H), δ= 3.62 (2H), δ= 6.54 (1H), δ= 6.55 - 6.57 (1H), δ= 6.95 – 6.97 (1H); that are in a good agreement with the literature and the spectrum provided by the manufacturer of the same compound.[65, 66]

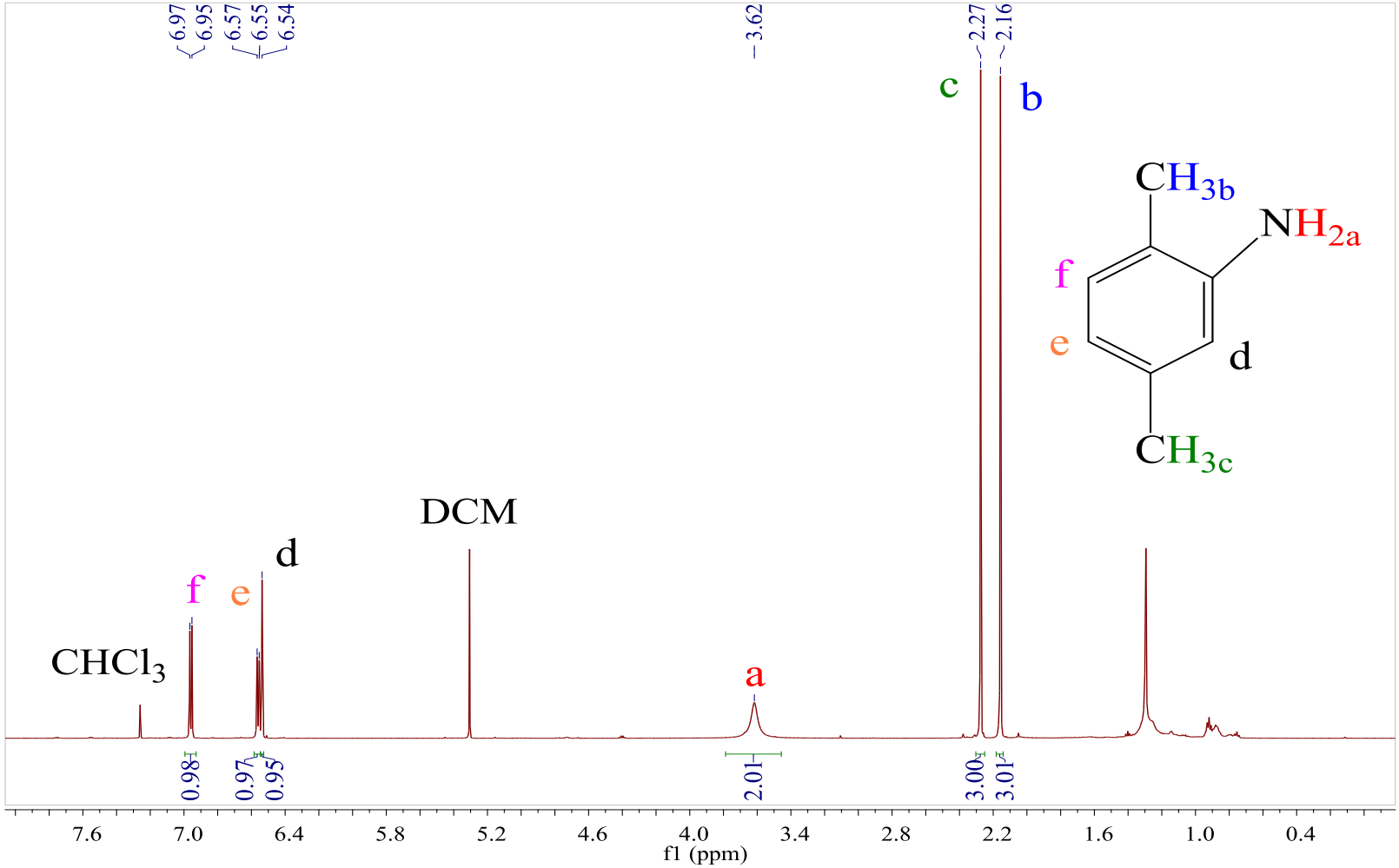

Figure 1. ^{1}H NMR spectrum of 2-amino-para-xylene synthesized by Raney Ni catalysis (crude)

As stated above, one of the advantages of the Raney Ni/$NaBH_4$ reduction system was its pure crude products. This is in contrast to most other procedures, which entail further purification steps such as chromatographic separation. For example, the homogenous catalysis system of $Fe_3(CO)_{12}$ resulted in difficult isolation of the final reduced product. This can be observed ^1H NMR spectra acquired from 2-amino-para-xylene synthesized via both pathways. The ^1H NMR spectrum of 2-amino-para-xylene synthesized via $Fe_3(CO)_{12}$ /[18]crown-6/ aq. KOH reduction system and purified on a tall silica gel chromatography column is depicted in **Figure 2**. Compared to the spectrum in **Figure 1**, a large number of impurities is observed in the spectrum of the $Fe_3(CO)_{12}$ mediated reduction, and integration of protons associated with primary amine group only reaches a value of 1.7. MS was used to further prove the successful synthesis of 2-amino-para-xylene. **Figure 3** shows low resolution mass spectrum of 2-amino-para-xylene. The parent ion was detected at = 122.1, which coupled with the NMR spectra indicates the successful synthesis of the product. MS of the commercial analogous compound had a similar pattern, but with more intense fragmentation peaks. This could be related to purity of the synthesized compound.

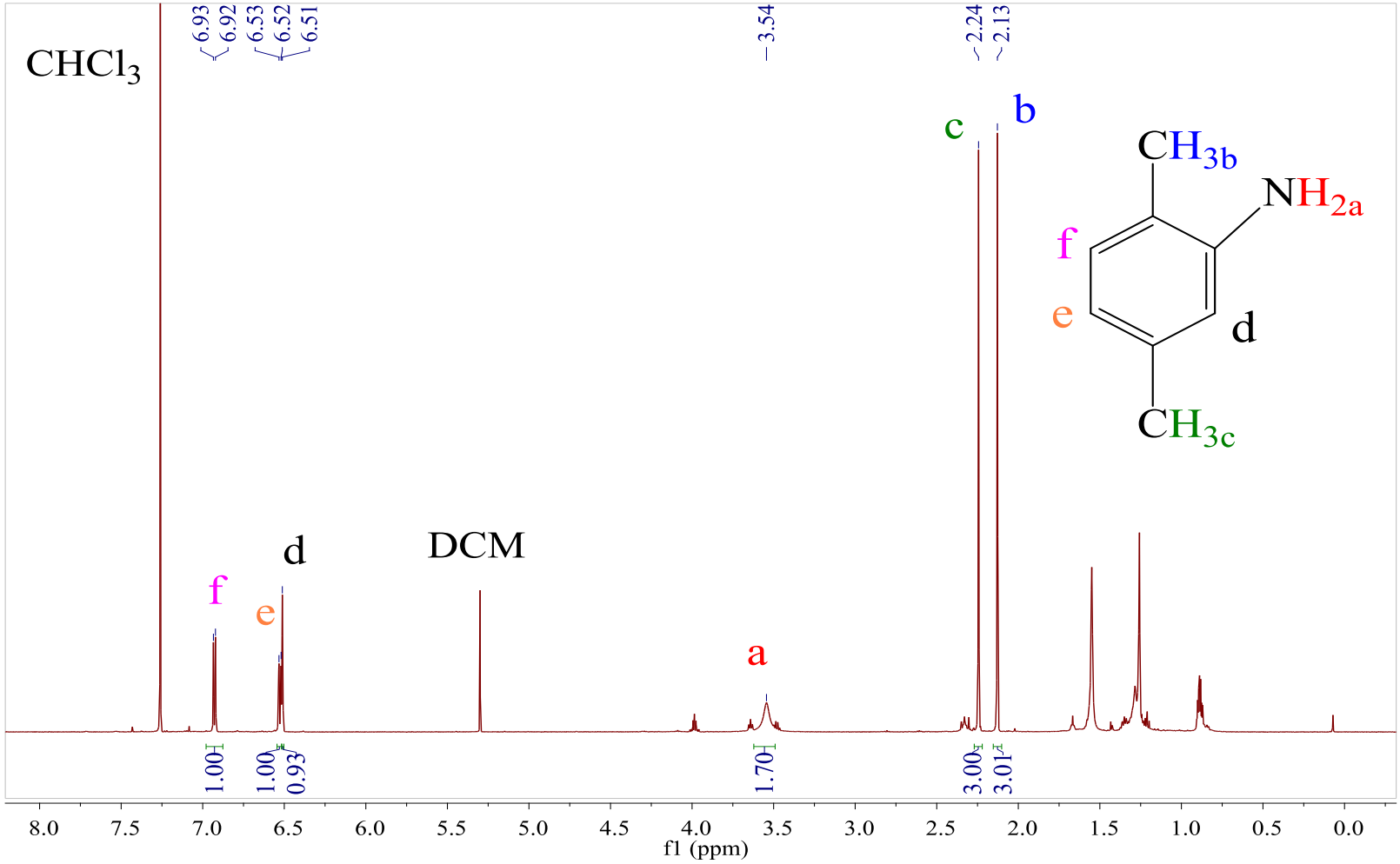

Figure 2. ^{1}H NMR spectrum of 2-amino-p-xylene synthesized by $Fe_3(CO)_{12}$ catalysis (purified by column chromatography)

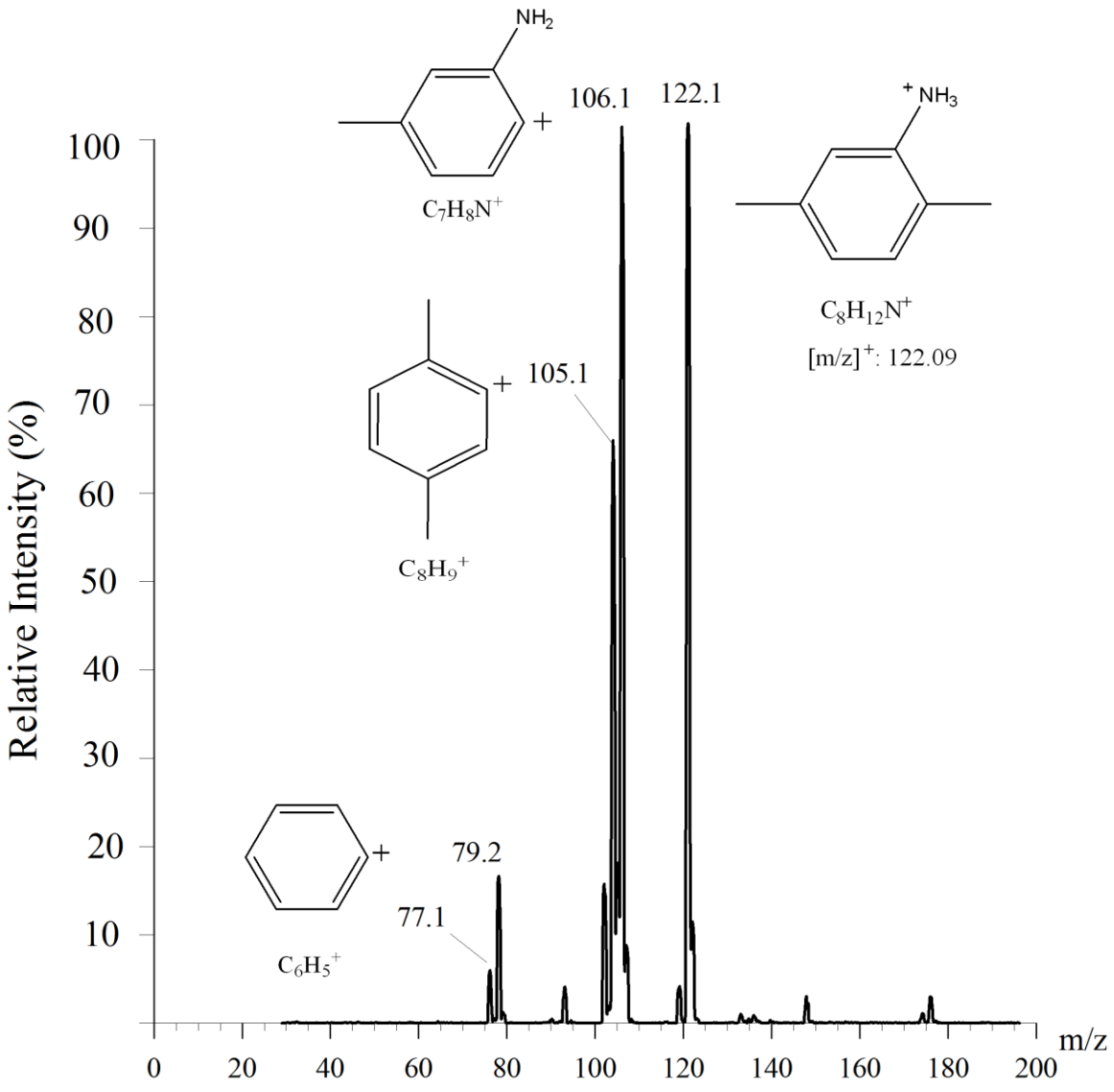

Figure 3. ESI Mass spectrum of 2-amino-p-xylene synthesized by Raney Ni catalysis (crude)

3-3-2- Nitro-PCP, amino-PCP and related by-products

To verify the successful production of amine-substituted PCPs, we characterized the monosubstituted and pristine PCPs, and their physical properties were compared. The correlation between substitution and structure of the PCP is clearly reflected in its physical

properties. Pristine PCP has a symmetric and crystalline structure. Therefore, it is insoluble in polar solvents and has a relatively high melting point (286°C). In contrast, Cram[47] reported the melting point (m.p.) of mono-substituted PCPs at low temperature ranges (e.g. 155.5-156.5°C m.p. for 4-nitro[2,2]para-cyclophane), but did not specify the heating rate for these measurements. The m.p. of our synthesized nitro-PCP was measured to be 150-152.5°C at a rate of 10°C/min. Furthermore, solubility of mono-substituted PCPs is generally improved compared to un-substituted PCP. The decrease in m.p. and improvement of solubility is expected, because introducing a substitution on one of the rings disturbs the symmetry of the molecule, resulting in a more amorphous structure of the bulk material due to weaker molecular interactions.[62] However, symmetry of the PCP is not always the dominant parameter. The correspondence between the structure and physical properties of substituted PCPs is also related to the nature of the substituents. For example, changing the substituent from nitro to amino group, gives rise to about 90°C higher m.p. for amino-PCP. Although, this is still lower than the m.p. of highly crystalline PCP, the hydrogen bonding between the molecules of amino-PCP compensates to a great extent for the effects of symmetry disturbance. For the same reason, solubility of the more polar amino-PCP is further improved in solvents such as methanol which only partially dissolves nitro-PCP. Isolation of all compounds produced in the nitration reactions by column chromatography was a laborious task and almost always failed, since the polarity of the compounds is too similar and they tend to co-elute from the column. Nevertheless, by running three consecutive chromatography columns starting with a very non-polar solvent system, and also using the solubility differences of compounds in some of the mixed

fractions that never became pure by column chromatography, we isolated entire fractions of one of the samples for characterization. We observed that the different nitration reaction conditions conducted by triflic acid/anhydride produced similar products and by-products but with different abundances. In addition to the major mono-nitrated product, 10 other compounds were eluted through various experiments. Their R_f values (60:40 n-penntane:Et_2O solvent system) lie between 0.15 and 0.79 for polymer by product and unreacted PCP respectively. In the optimized condition, that yielded 84% of 4-nitro[2.2]paracyclophane, none of the other fractions exceeded more than 5%.

Regardless of their quantity, NMR spectra of the other compounds did not show a consistent pattern, and the di-nitro-[2,2]paracyclophane could not be isolated under any of the tested conditions. However, according to their NMR spectra, starting material (PCP) and two other byproducts of the reaction can be assigned in addition to the main product. The rest is attributed to polymer by-products through ^{1}H NMR spectroscopy. The ^{1}H NMR spectrum of the first fraction, the least polar compound, showed 2 singlets at δ=3.05 (8H) and δ=6.5 (8H) that are attributed to two types of aliphatic and aromatic positions in un-substituted [2,2]paracyclophane (**Figure 4**). However, this fraction was not seen in all runs and it was totally absent when longer reaction times or higher acid/PCP ratios were used.

^{1}H NMR spectrum of the second fraction (**Figure 5**), showed a singlet at δ=10.76 integrating to 1 proton. Also, rather than a deshielded proton, three protons shifted upfield, suggesting that one of the rings is substituted with an electron donating substituent. Cram[63] reported that during the nitration of PCPs, hydroxyl groups could be created on the phenyl rings while the other or the same ring is already substituted with NO_2 group. Although the

direct synthesis of such disubstituted PCPs has not been attempted yet, the authors reported its formation as a byproduct of the nitration reaction. Studying the NMR spectra of some commercial nitrophenols[67] suggests that the deshielding effect of the NO_2 group on the phenolic proton can cause a large downfield shift (~10 ppm). According to this, we assigned might attribute the second fraction to 4-hydroxyl-13-nitro[2,2]paracyclophane in which the two substitutions are on different rings. Other chemical shifts are as follows: δ=1.9 (1H), 2.14 (1H), 2.47 (1H), 2.79 (2H), 3.14 (3H), 5.78 (1H), 5.96 (1H), 6.10 (1H), 7.18-7.22 (2H), 7.51 (1H) and 10.76 (1H).

In addition to these two fractions and the main nitro-PCP product collected in the third fraction, we found that all the remaining fractions are polymers or oligomers of PX with various molecular weights. This was determined by the appearance of too many alkyl protons in the ^{1}H NMR spectra of these fractions. Usually, linear polymers are rich in methylene groups in their backbones. Therefore, presence of very large amounts of aliphatic protons compared to other types of protons reflects the formation of polymeric chains. The ^{1}H NMR spectrum of the fourth fraction (**Figure 6**) shows a reasonable ratio of integration for aromatic and those aliphatic protons that are connected to aromatic moiety, but appearance of a few extra alkyl protons indicates that an oligomer of nitro-PX has been synthesized. However, from fraction 5 to the final collected fraction, the abundances of these alkyl protons increase to greater extent. They all have similar ^{1}H NMR spectra but with different alkyl protons suggesting that a variety of polymers with different chain lengths are generated as byproducts. For an example, ^{1}H NMR spectrum of the tenth fraction is shown in **Figure 7**. Since the reaction is carried out under inert atmosphere,

degradation of the PCP via strong acids or interference of the reaction solvent (dichloromethane) could be considered as potential sources of alkyl units. Further to these spectral characterization, physical appearance of most of these fractions resembled a pasty malleable solid which is indicative of their large molecule sizes.

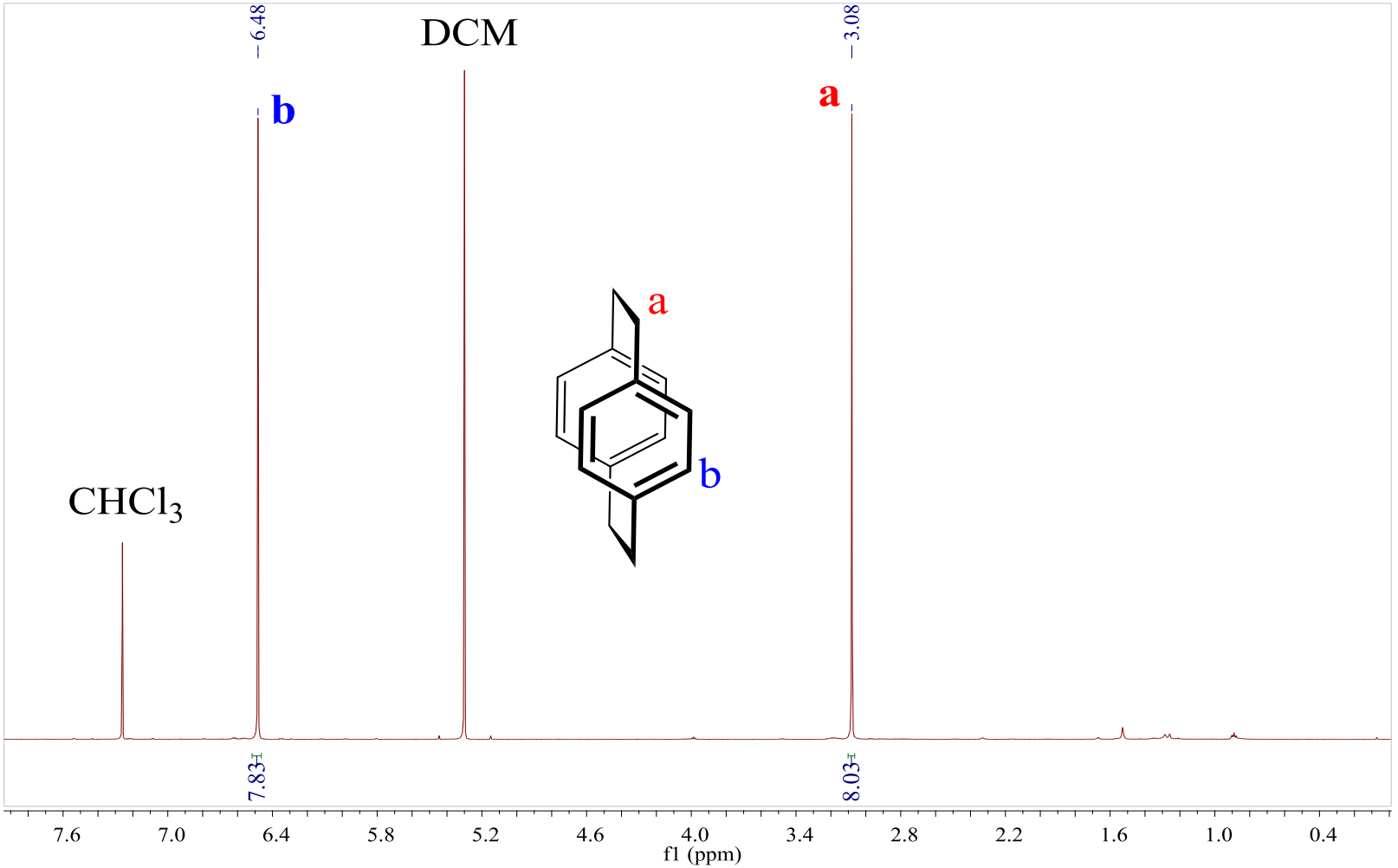

Figure 4. ^{1}H NMR spectrum of the first fraction in nitration reaction of PCP, identified as unreacted [2.2]paracyclophane

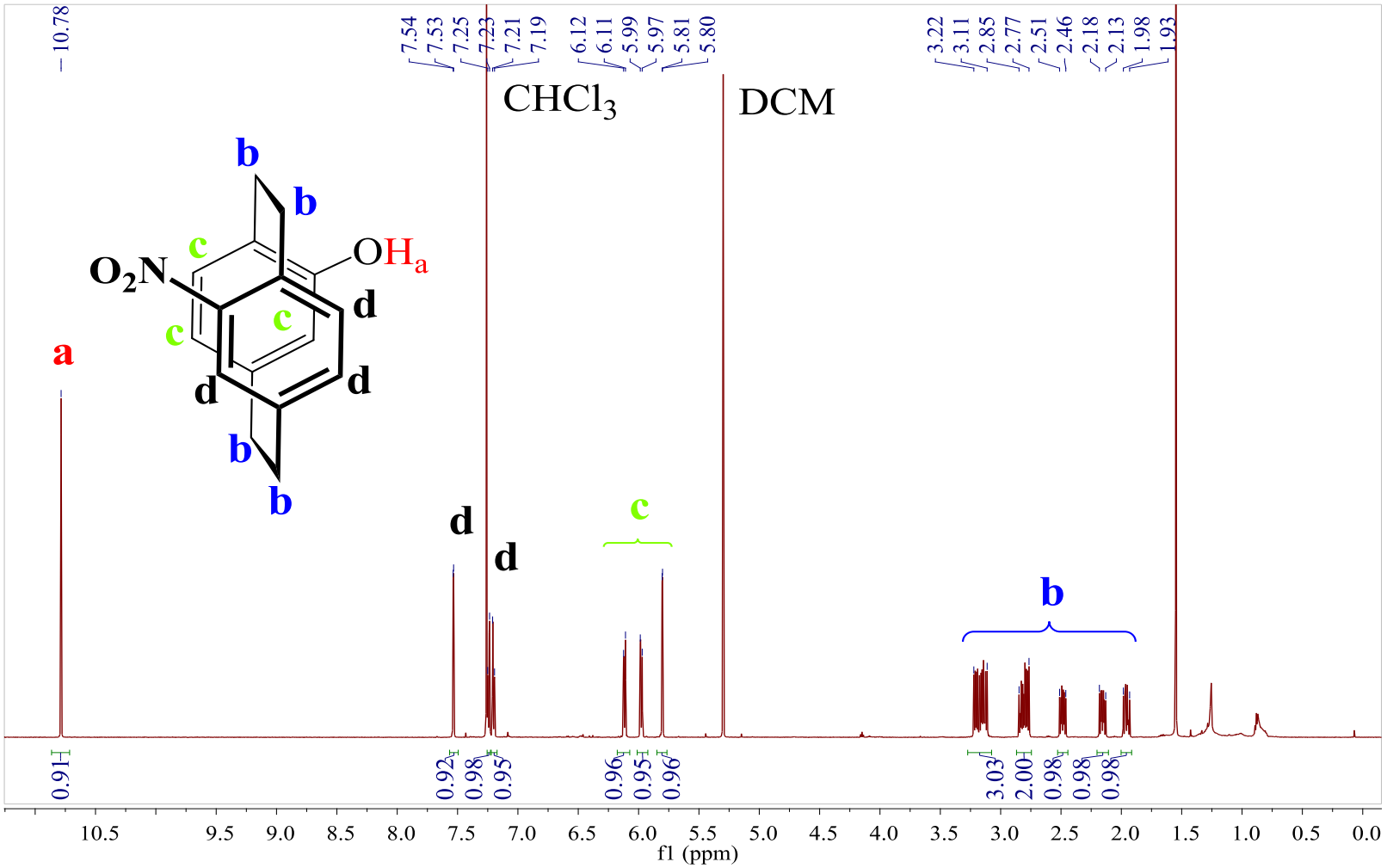

Figure 5. ^{1}H NMR spectrum of the second fraction of nitration of PCP, identified as 4-hydroxyl-13-nitro[2.2]paracyclophane

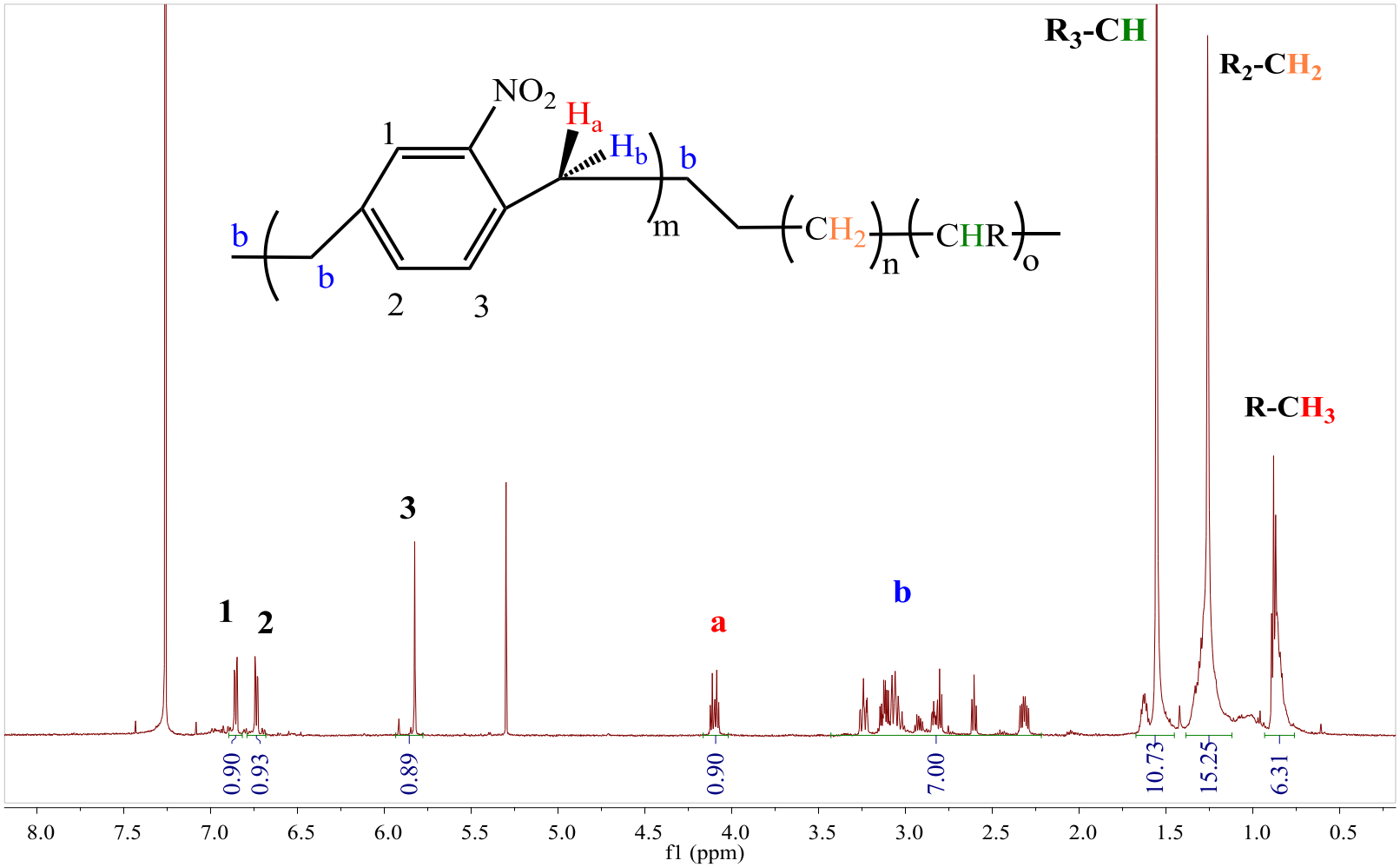

Figure 6. ^{1}H NMR spectrum of the fourth fraction of nitration of PCP, Oligomer of Nitro-para-xylylene

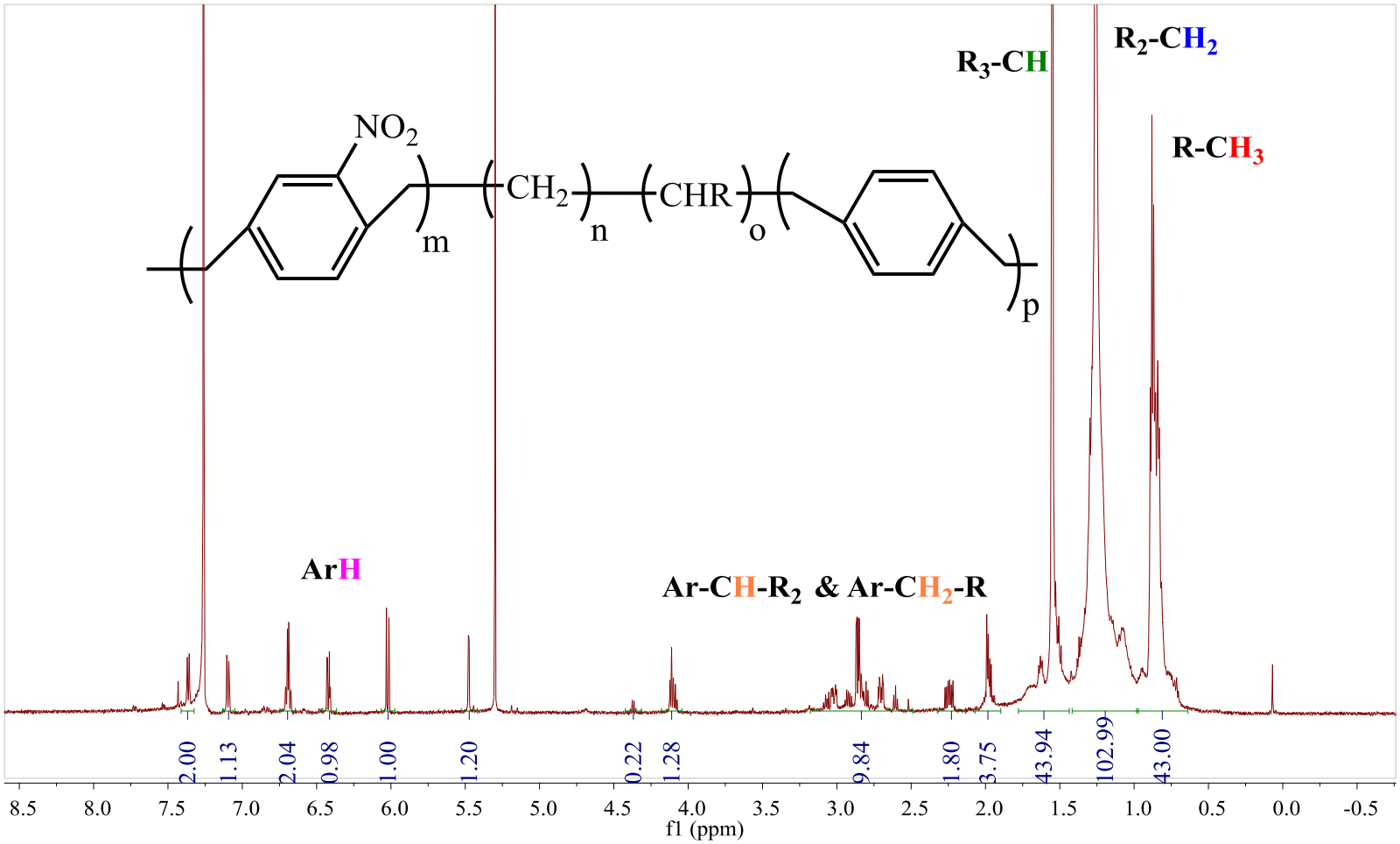

Figure 7. ^{1}H NMR spectrum of the polymer by-products produced in nitration of PCP

Eventually, ^{1}H and ^{13}C NMR spectra of the third fraction confirmed the successful synthesis of nitro-PCP. To compare the results of nitro- and amino-PCP, their spectroscopic data is shown either together or after each other throughout the rest of the text. **Figures 8 and 9** demonstrate ^{1}H NMR spectra of 4-nitro[2.2]paracyclopane and 4-amino[2.2]paracyclophane, respectively, while their ^{13}C NMR spectra are shown in **Figures 10 and 11**. Characteristic shifts at δ=4.01 (1H, **Figure 8**) for nitro-PCP and δ=2.63-2.72 (1H, **Figure 9**) for amino-PCP are associated to the protons cis to the substituent in the aliphatic bridge. Presence of the NO_2 electron-withdrawing group in the nitro-PCP and the NH_2 electron-donating group in the amino-PCP give rise to downfield and an upfield shifts, respectively. The broad singlet at δ=3.40-3.99 (2H, **Figure 9**) is characteristic of two protons of the primary amine substituent in the amino-PCP. A marked shift of aromatic protons is seen in the transition from nitro substituent to amino substituent. The proton ortho to the substituent is shifted downfield by the nitro substituent which is an electron withdrawing group, while it is shifted upfield by amine substituent, an electron donating group. In addition, all protons in the other aromatic ring are shifted in the same direction as the ortho proton. This is characteristic of monosubstituted-PCPs in which a substitution on one aromatic ring, shifts the protons of other aromatic moiety due to transannular electronic interactions.[62] Similar shielding/de-shielding behavior of carbons is observed in the ^{13}C NMR spectra (**Figures 10 and 11**).

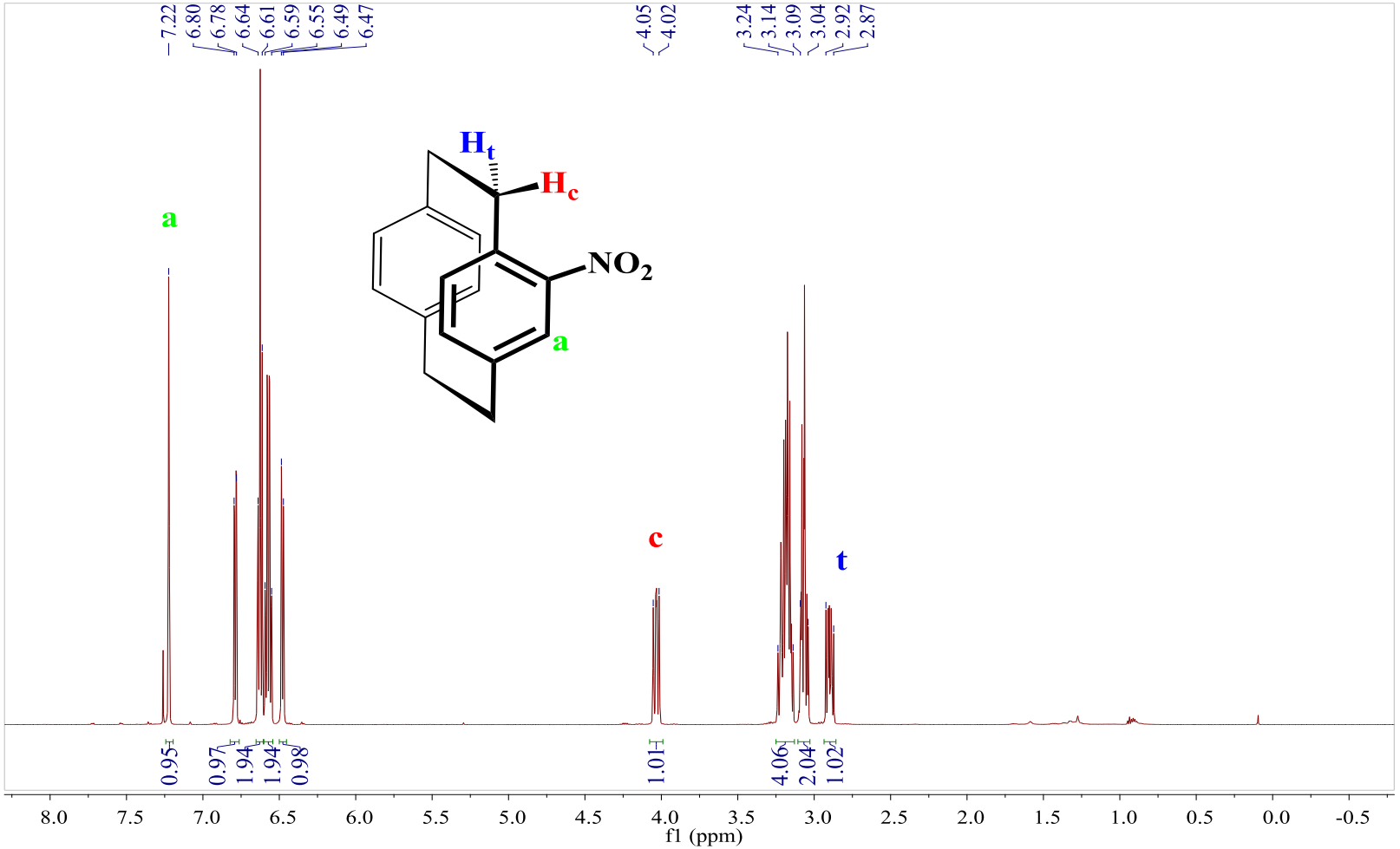

Figure 8. ^{1}H NMR spectrum of 4-nitro[2.2]paracyclophane

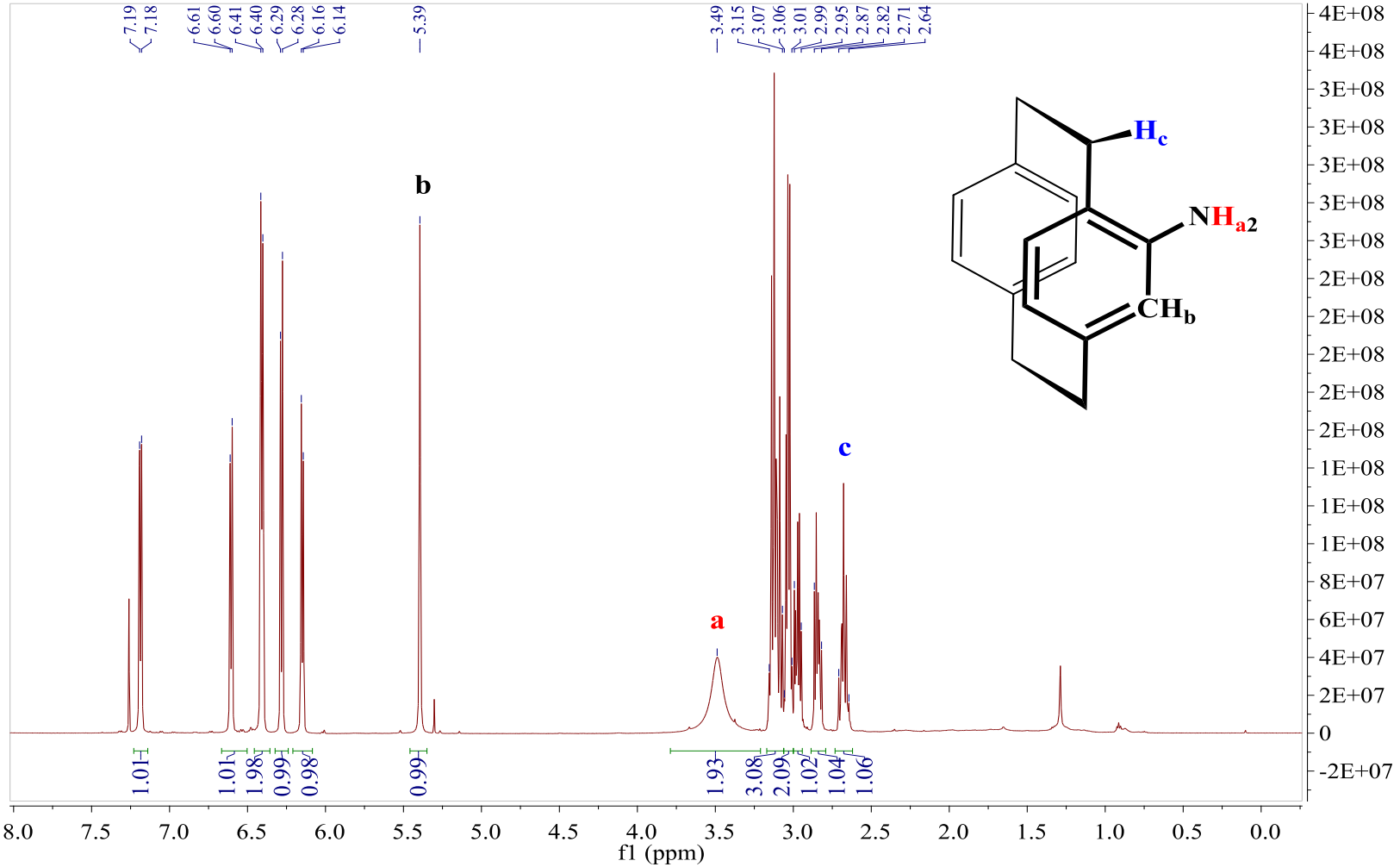

Figure 9. ^{1}H NMR spectrum of 4-amino[2.2]paracyclophane.

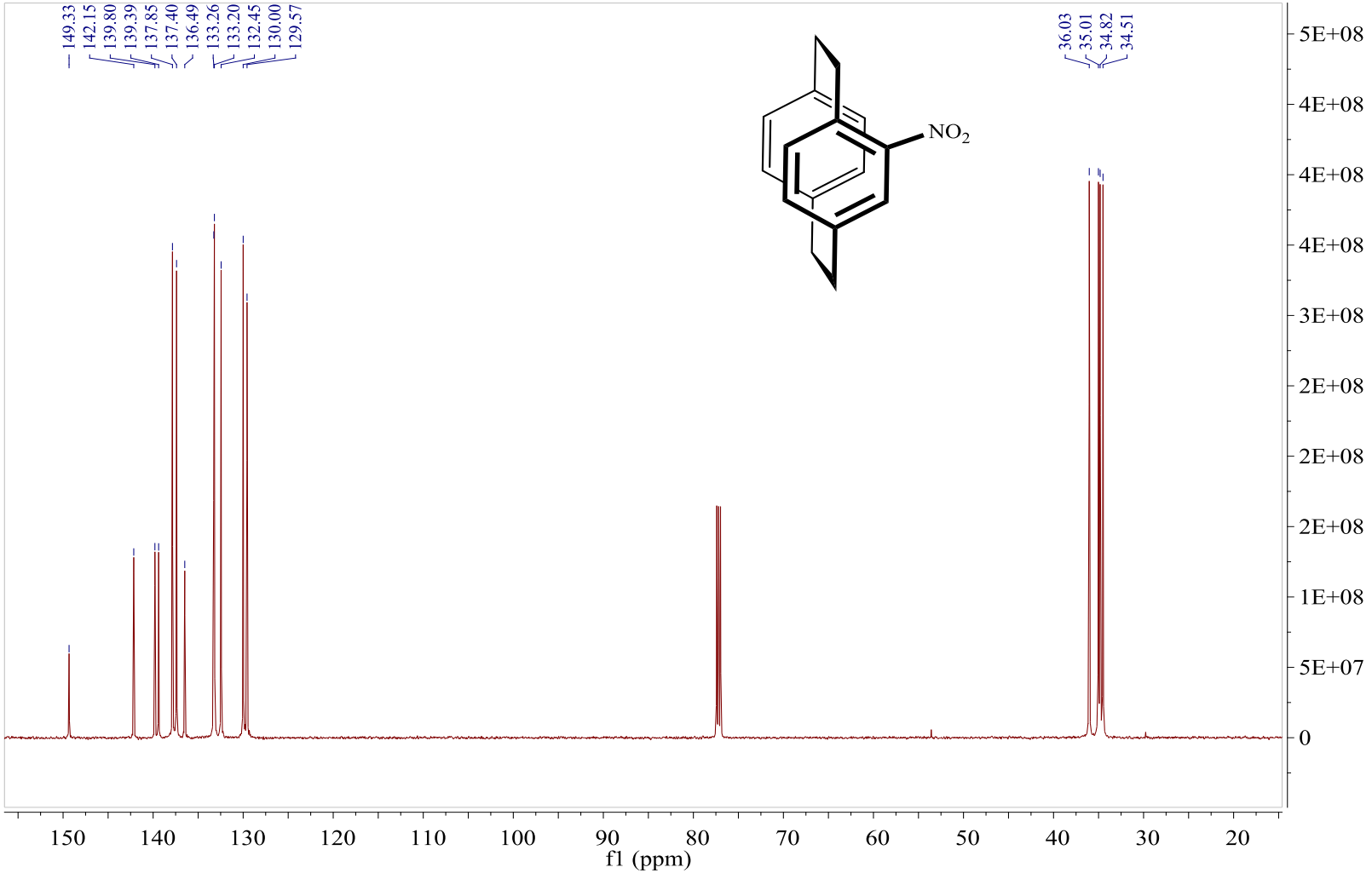

Figure 10. ^{13}C NMR spectrum of 4-nitro[2.2]paracyclophane.

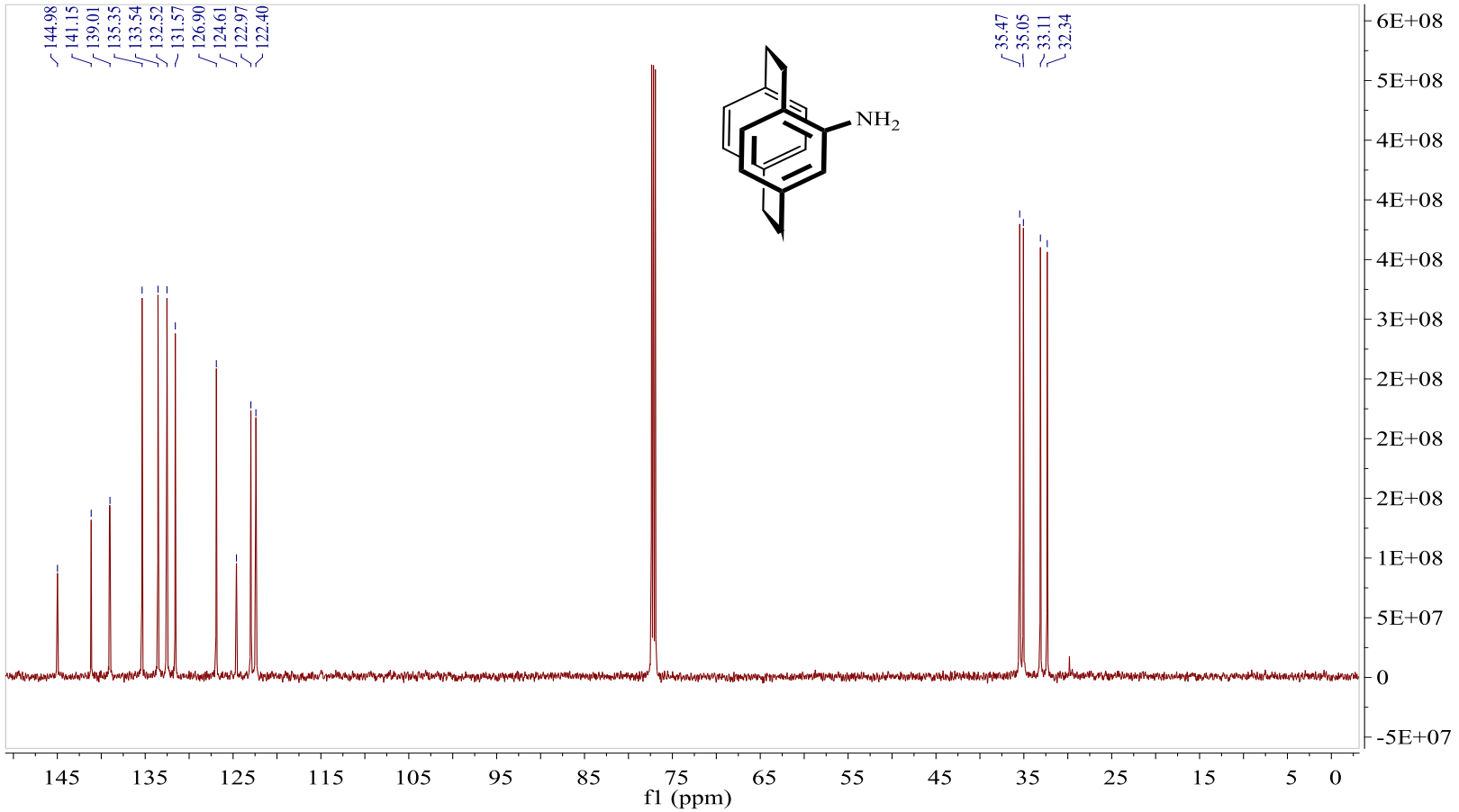

Figure 11. ^{13}C NMR spectrum of 4-amino[2.2]paracyclophane.

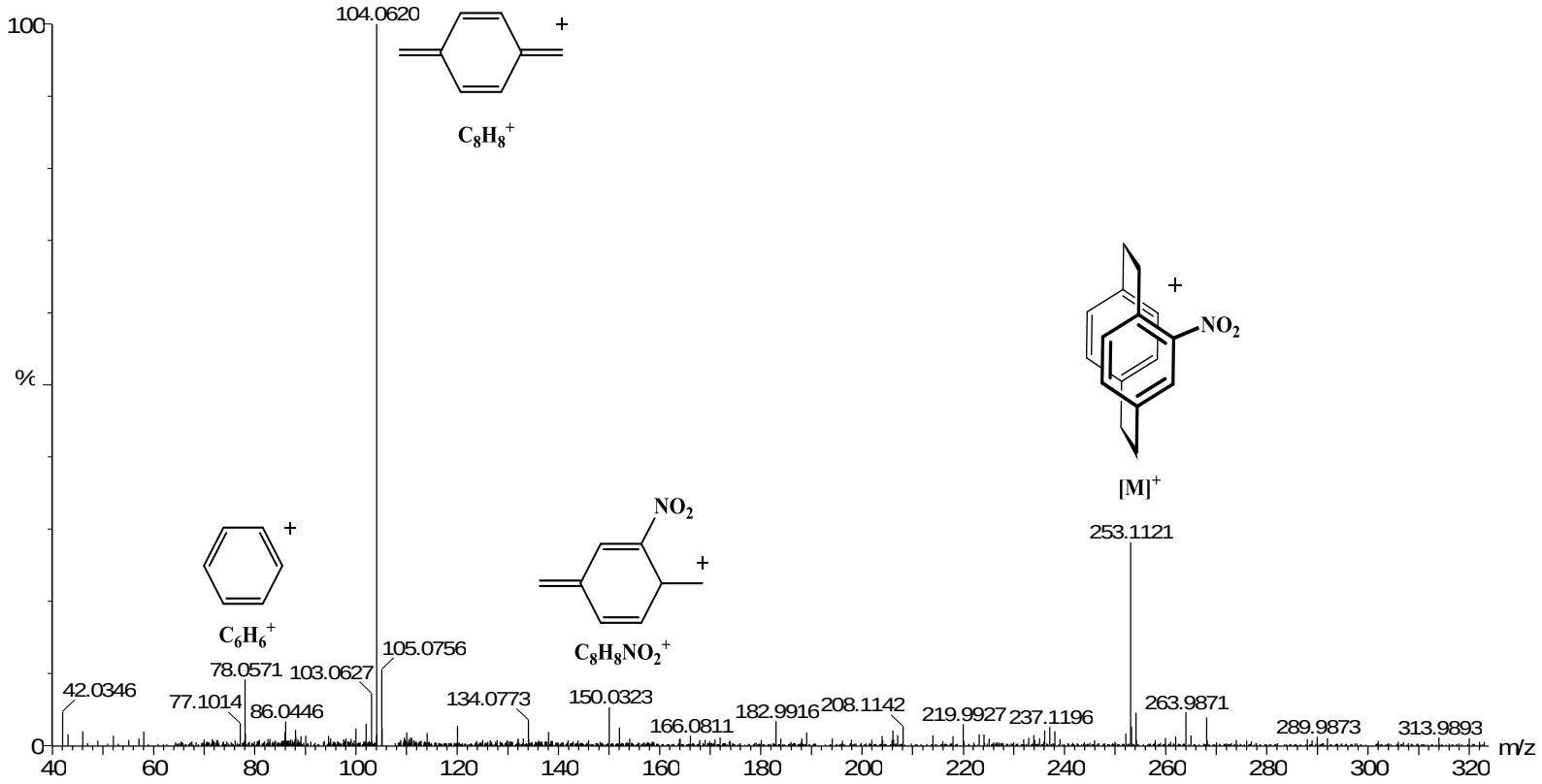

Figure 12. Mass spectrum of 4-nitro[2.2]paracyclophane with corresponding fragment ions

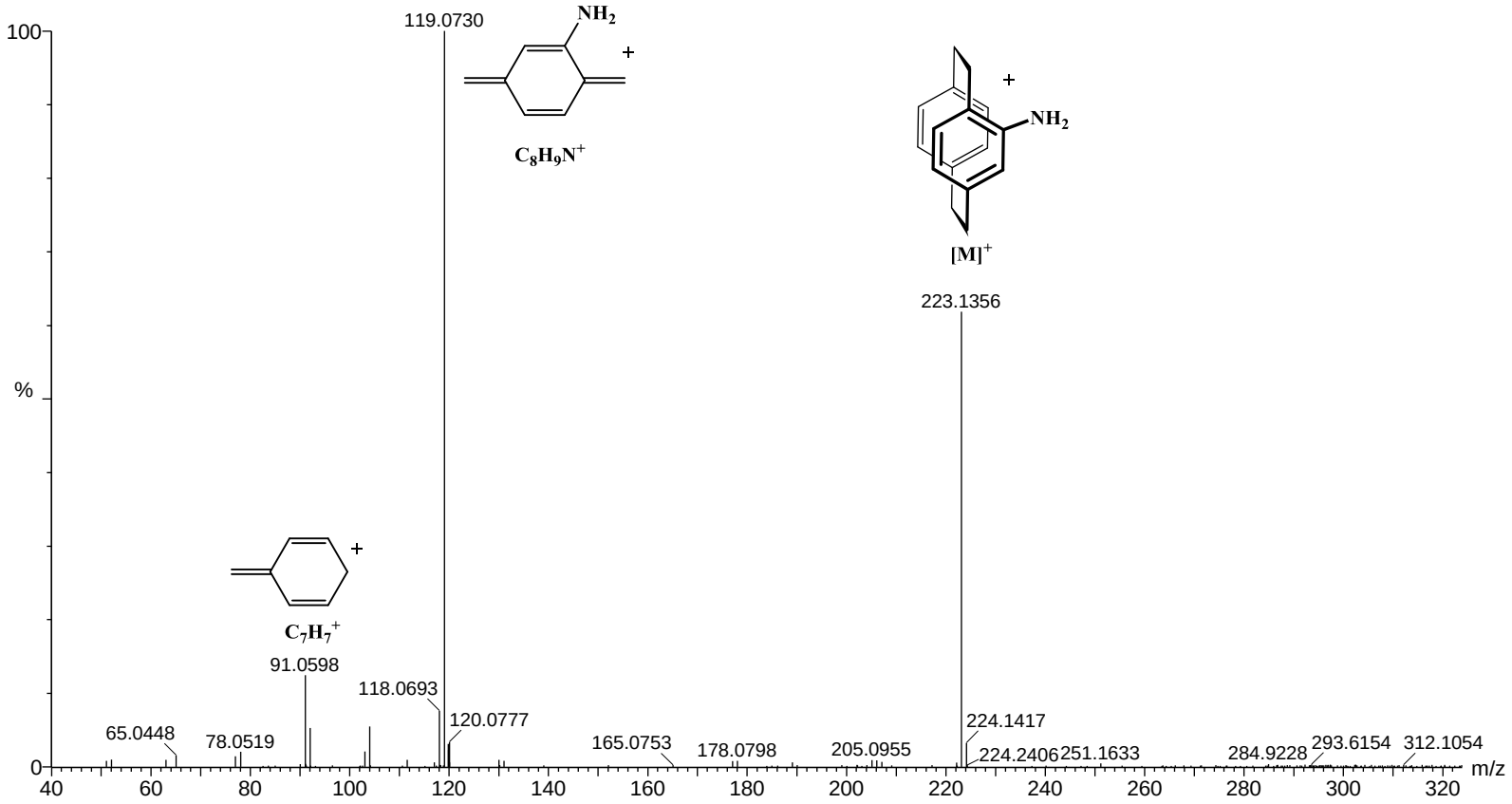

Figure 13. Mass spectrum of 4-amino[2.2]paracyclophane with corresponding fragment ions

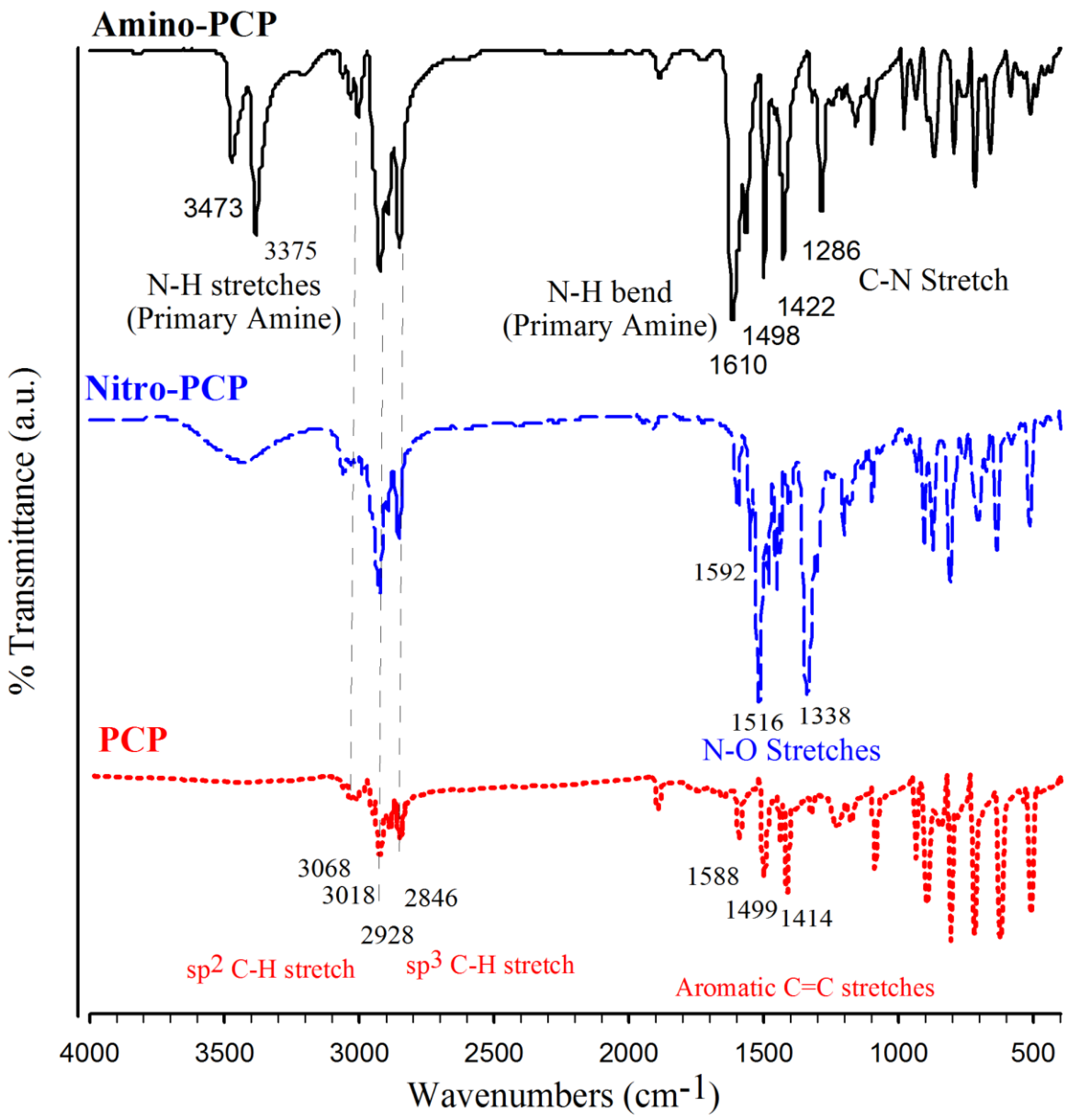

Figure 14. FT-IR spectra of PCP, Nitro-PCP and Amino-PCP

Mass spectrometry of substituted PCPs, exhibited peaks at m/z values representing the relevant parent and characteristic fragment ions (**Figures 12 and 13**). In accordance with the literature of substituted PCPs,[62] the predominant peak at each spectra is related to

either of the substituted (nitro- or amino-PCP) or un-substitued para-xylylene halves. In addition, FT-IR spectra of PCP, nitro-PCP and amino-PCP are shown at **Figure 14**. Compared with PCP, which mainly shows aromatic C=C stretches at 1499 and 1588 cm^{-1}, and sp^3 and sp^2 C-H stretches at 2846-2928 cm^{-1} and 3000-3100 cm^{-1}, the spectrum of the nitro-PCP has two distinct sharp peaks of N-O stretches at 1338 and 1516 cm^{-1}, while the amino-PCP shows a sharp peak at 1610 cm^{-1} attributed to the N-H bend and two peaks at 3375 and 3473 cm^{-1} corresponding to N-H stretches of the primary amine.

3-3-3- 4-trifluoroacetyl-[2.2]para-cyclophane

As discussed earlier, acylation of PCP with trifluoroacetic anhydride/$AlCl_3$ at -78°C gave us a mixture of two easily separable compounds monitored by TLC (80:20 n-pentane:Et_2O system). We found out that these two fractions have sufficient solubility differences allowing them to be separated by dissolving in methanol. The first band in TLC corresponded to pristine PCP which is insoluble in methanol. The NMR spectra taken from this fraction are not shown here as they were identical to those of the PCP fractions obtained previously in nitration reaction. But the second fraction was identified as 4-trifluoroacetyl-[2.2]paracyclophane. The ^1H NMR and ^{13}C NMR of this fraction are shown in **Figures 15 and 16**. As expected, its ^1H NMR spectrum resembles that of other mono-substituted PCPs with electron-withdrawing substituents. Similar to nitro-PCP, we observe the proton cis to the substituent shifted distinctly downfield (δ=3.95) while the proton trans to the substituent is shifted upfield (the first aliphatic proton at δ=2.91). Also, there is an obvious downfield shift in the aromatic protons of the substituted moiety, particularly protons at orto (δ=7.22)

and para (δ=6.85) positions to the substituent. A similar pattern can be seen for carbons in ^{13}C NMR spectrum with the exception that for trifluoroacetyl-PCP we expect two more distinctive peaks; one at the very high chemical shift (δ=181.04), characteristic of carbonyl group, and one at aliphatic region which is significantly shifted downfield (δ=50.86), associated with $-CF_3$ group on the substituent.

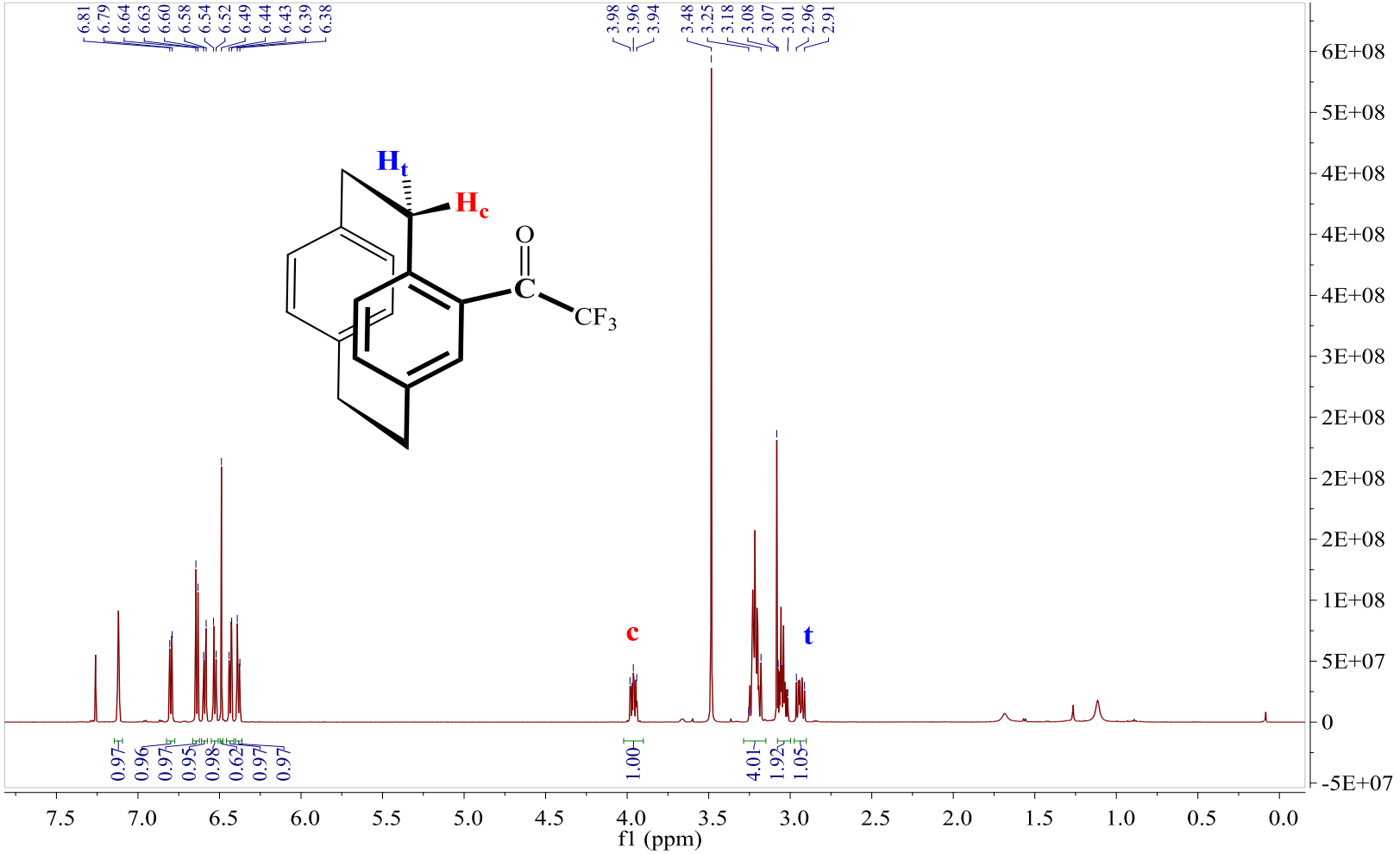

Figure 15. ^{1}H NMR spectrum of 4-trifluoroacetyl[2.2]paracyclophane

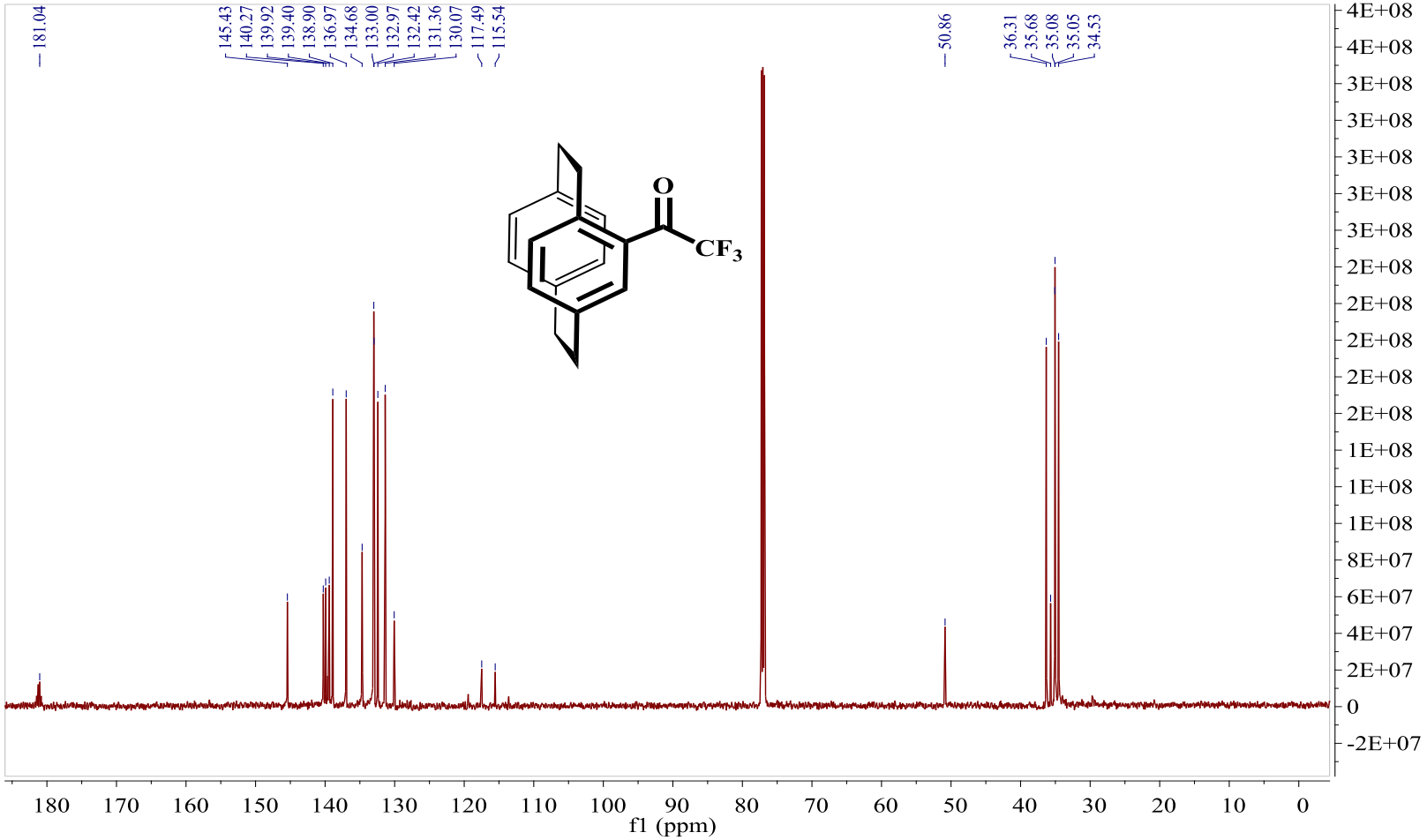

Figure 16. ^{13}C NMR spectrum of 4-trifluoroacetyl[2.2]paracyclophane

3-4- Preparation of functionalized thin films

In order to investigate and compare the film properties of amine-functionalized PPX-A with two well-known un-substituted PPX and chlorine-substituted PPX-C films manufactured from commercially available precursors, CVD polymerization was carried out using a procedure described by Gorham.[13] As illustrated in **Scheme 9**, poly(para-xylylene) films were obtained from the direct pyrolysis of the corresponding PCP precursors. Briefly, the process commences with sublimation of powder-loaded dimer precursors at 170°C. The vapor of sublimated dimer is then flowed into a pyrolysis furnace where the dimer is heated to 690°C to ensure cleavage of the aliphatic C-C bonds yielding the reactive para-xylylene monomers. Cooling the reactive material to room temperature polymerizes the monomers adsorbed onto the surface of any products placed in the coating chamber. Throughout the operation, excess process gas travels from the coating chamber into an external cold trap. Different coating sets with various amounts of each precursor were performed on piranha-cleaned SiO_2 wafers.

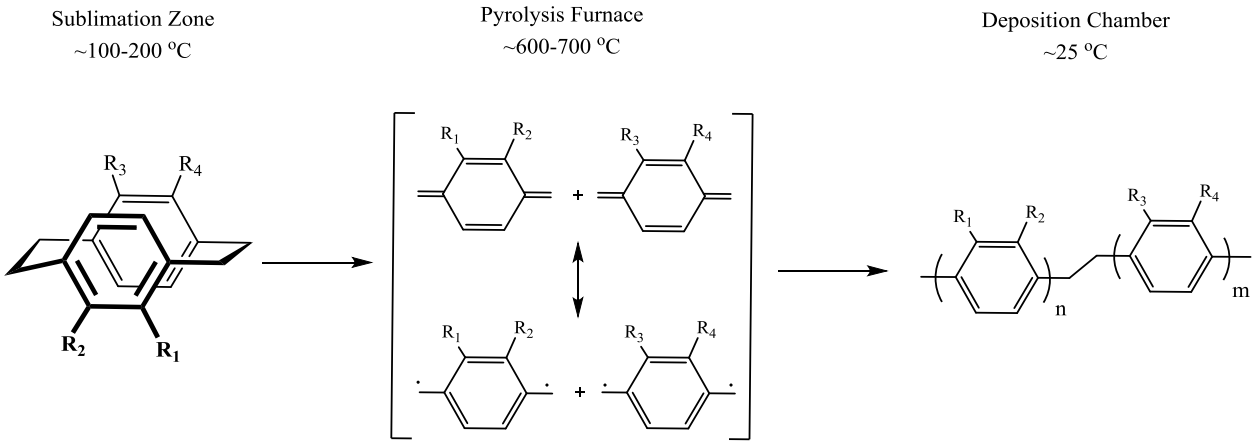

Scheme 9. CVD polymerization of Parylene

3-4-1- Characterization of the functional thin films

One of the major effects of substituting PPX films is the change of surface properties such as optical and electrical properties, wettability, roughness and chemical composition. In this regard, contact angle (CA) measurement is one of the most useful techniques for surface analysis because only the top nanometer of the surface determines the surface energy. Parameters that influence the CA of a liquid on a solid are both surface roughness and chemistry.[68] Water contact angle (WCA) measurements (**Figure 17**) show the changes in wettability of the surface of the SiO_2 wafers coated with different PPX films. The amount of dimer precursor loaded in the CVD machine was 0.250 g for all samples. According to WCA values, coating the surface of SiO_2 wafers with all organic thin films increased the hydrophobicity; however, introducing the hydrophilic amine group, improved wettability of the wafers compared with the un-substituted and chlorine-substituted films. This is reflected in surface energy of the polymer coating. Using the well-known Neumann

equation[69] the surface energy of these hydrophobic coatings was estimated. As noted in **Figure 17,** introduction of primary amine groups on PPX films, increased the surface energy considerably from 30.22 to 38.61 mJ/m^2.

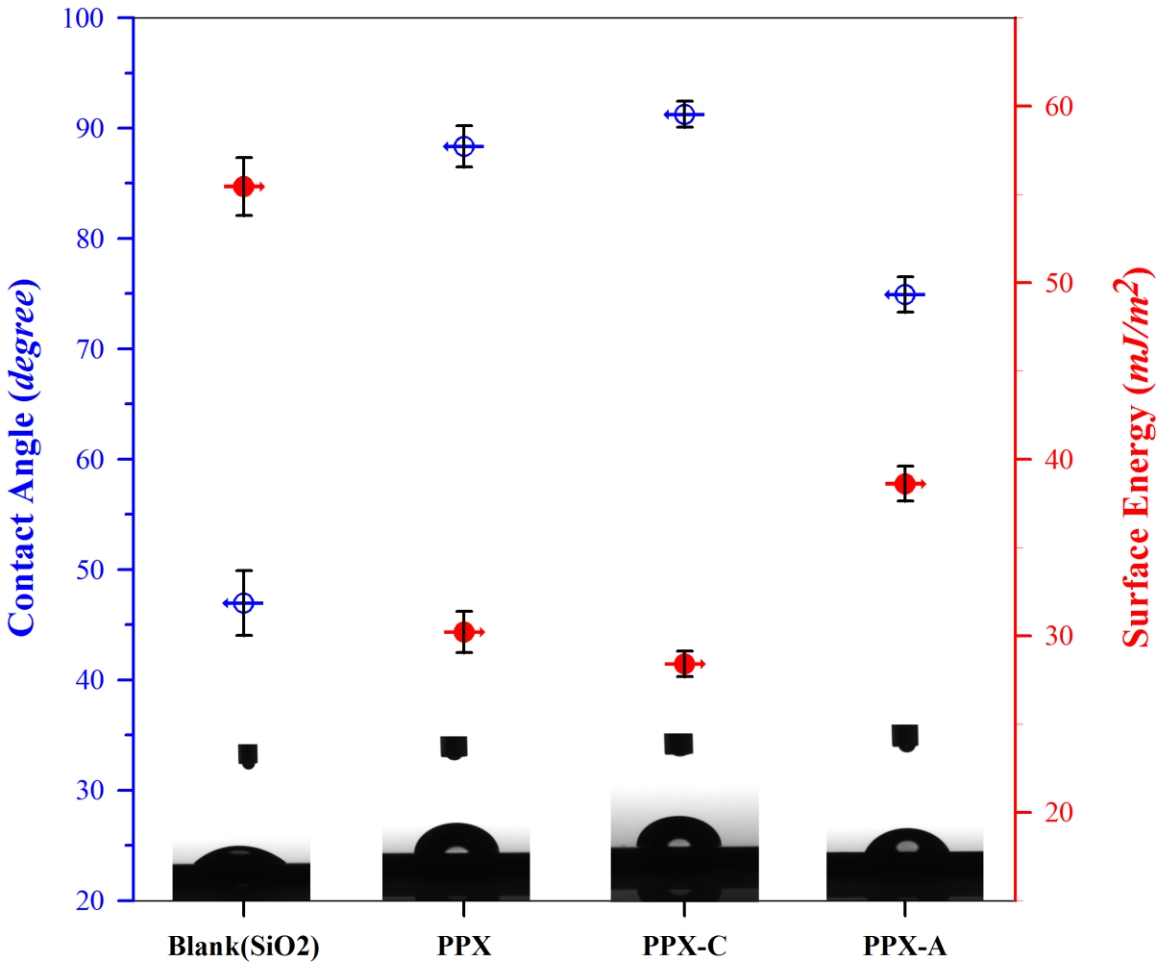

Figure 17. WCA of uncoated (Blank) and coated SiO_2 wafers with PPX, PPX-C and PPX-A. Error bars represent standard deviations (n = 9).

One of the advantages of CVD polymerization is its compatibility with a variety of functionalities. Pyrolysis of precursor dimers, usually cleaves the aliphatic C-C bonds without altering the functionalities on the aromatic moieties. This enables us to engineer the surface properties of the polymer films through a comparatively simpler chemistry of the smaller corresponding molecules. IR specular reflectance provides a means of analyzing thin films on reflective substrates such as metals. This non-contact technique can be performed quickly, and requires no sample preparation or a definite sample size, maintaining the samples intact for other purposes.[70]

To confirm the integrity of the functional groups in PPX-A films after polymerization, we studied the reflectance spectra of thin films deposited on Si wafers that were pre-coated with 200 nm of gold layer. Spectra that closely resemble those of their corresponding precursors were obtained after CVD polymerization. As shown in **Figure 18**, the spectrum of un-substituted PPX film showed aliphatic and aromatic C-H stretches at 2846 and 2928 cm^{-1}, and 3018 and 3068 cm^{-1}, respectively. In general, multiple weak to medium peaks at 1400-1600 cm^{-1} are assigned to aromatic C=C stretches, with aromatic ring vibrations seen as a pair of bands at ~1550 cm^{-1} and ~1610 cm^{-1}. Although, halogen substituted aromatic compounds show no well-defined C-X absorptions, the presence of a halogen atom on a benzene ring can be recognized by its electronic impact on the in-plane C-H bending vibrations. The in-plane C-H bending vibrations of aromatic compounds occur in the region 950-1150 cm^{-1}, where many organic functional groups show multiple bands that make this region very crowded and infrequently used.[71] Yet, due to the high electronegativity of the chlorine atom, the intensity of these vibrations at 960 cm^{-1} and 1051

cm^{-1} in PPX-C is enhanced and shifted to higher frequencies relative to the absorptions in PPX. Similar to its precursor, the spectrum of PPX-A in addition to frequencies related to aliphatic and aromatic C-H stretches, shows a sharp peak at 1629 cm^{-1} and two peaks at 3363 and 3460 cm^{-1}, which are attributed to N-H bend and N-H stretches of primary amine group.

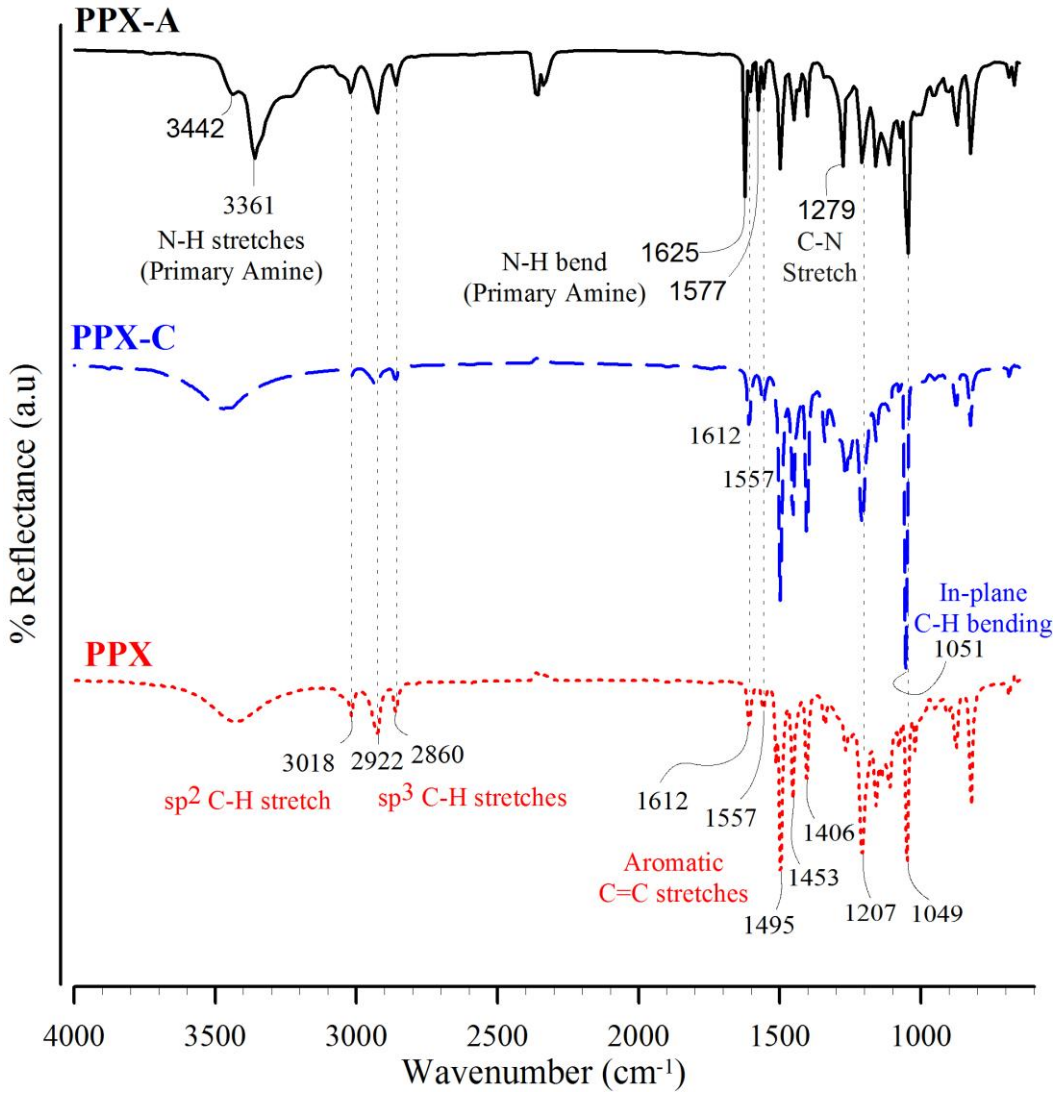

Figure 18. Grazing-angle specular reflectance IR spectra of thin PPX, PPX-C and PPX-A films

In addition to above characterizations, X-ray photoelectron spectroscopy (XPS) provides a very powerful means of analyzing surface chemistry and the chemical composition of thin films. In XPS, high-energy X-ray photons are directed to the surface of the material and in response, electrons of the specimen are excited and ejected from the sample via the photoelectric effect.[72] Then, electron (or binding) energy of the ejected electrons is measured through a detector, and because binding energy of electrons is specific to each atom, it is attributed to its corresponding element. Therefore, XPS enables the identification and relative quantification of the elements which is vital for many areas of surface sciences.

The XPS spectra of uncoated and PPX-coated Si wafers and the relative elemental composition of PPX films on each sample are presented in **Figure 19** and **Table 3**, respectively. The spectrum of the blank wafer showed peaks at 103.1, 154.2, 283.9, and 533.2 eVs which correspond to Si_{2p}, Si_{2s}, C_{1s} and O_{1s} signals, respectively. Although the wafers were piranha cleaned before the application, non-negligible C_{1s} signal in the spectrum of uncoated SiO_2 wafer is indicative of organic contaminants, which could have been adsorbed from the environment during the transportation and storage before performing the measurement. As expected, the peaks related to Si_{2p} and Si_{2s} signals are absent in the spectra of PPX-coated samples. PPX-N, shows only characteristic signal of C_{1s} at 283.9 eV. PPX-C however, shows additional peaks at 199.2 and 269.9 eV attributed to the Cl_{2p} and Cl_{2s} signals. In addition to the above C_{1s} peak, the PPX-A spectrum in **Figure 19** exhibits a characteristic signal of N_{1s} at 398.7 eV, and does not exhibit the Cl_{2p} and Cl_{2s} peaks of PPX-C. Appearance of O_{1s} signal at 530.3 eV, which is absent from the other PPX

films, implies that either some water vapor is adsorbed onto the surface of the film or the amine group has been oxidized.

Table 3. Elemental composition of Parylene films

Elements / Thin Films	C 1s		N 1s		O 1s		Cl 2p	
	Found	**Calcd.**	**Found**	**Calcd.**	**Found**	**Calcd.**	**Found**	**Calcd.**
PPX	100	100	-	-	-	-	-	-
PPX-C	87.63	88.89	-	-	0.96	-	11.42	11.11
PPX-A	89.81	94.12	9.74	5.88	0.45	-	-	-

Comparison of the measured and calculated elemental compositions for PPX and PPX-C, shows good agreement between the experimental and theoretical amounts. This suggests the successful deposition of functionalized films with no loss of functional groups during the CVD polymerization. However, there is an appreciable discrepancy between the obtained and theoretically expected amounts of N atom for PPX-A film. This amount (9.47) is closer to the theoretical amount of di-amino-PPX (11.11%). The higher abundance of N atoms on the surface than expected suggests that the substituted and un-substituted PX units are not equally distributed throughout the polymer, such that a high fraction of the polymer consists of amino-PX rather than un-substituted PX. This implies that amino-PX had a higher tendency to participate in polymerization under our conditions. This finding is not reported elsewhere and could be specific to our CVD conditions. A reasonable answer for that lies in the different deposition rates of the two moieties. Since amino-PX is denser than PX, its deposition rate is believed to be faster than PX. The optimal conditions for CVD polymerization of substituted PCPs have been reported in the literature.[61] However, our

CVD instrument is adjusted to different condition with lower pyrolysis and vaporizer temperatures and lower pressure vacuum pressure, which could give rise to higher rate of deposition and polymerization of amino-PX moieties.

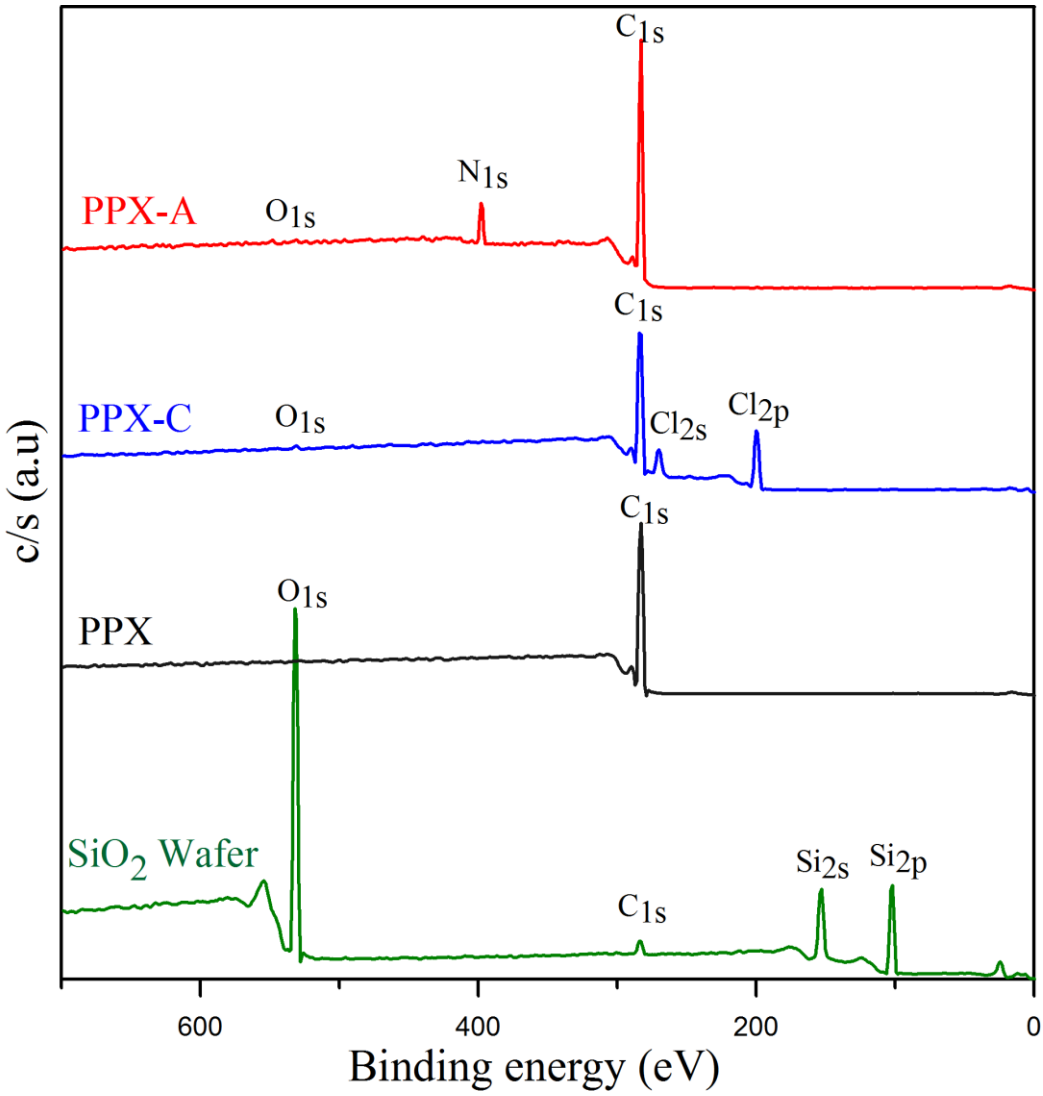

Figure 19. XPS spectra of gold-sputtered Si wafers; uncoated (blank) and coated with PPX, PPX-C and PPX-A thin films

In addition to XPS surveys from the surface of PPX films, high resolution XPS spectra at C1s, N1s, O1s and Cl 2p regions provide more information about the chemical structure of the films. Furthermore, once it is carried out carefully, deconvolution of these spectra and fitting at characteristic binding energies of these elements, will disclose the chemical bonds in which that specific element is contributed. The results of high resolution XPS spectra and contribution of each chemical bond is presented in **Table 4**. All of the chemical bonds are fitted in good correspondence with the characteristic binding energies reported in the literature. Presence of a minimal amounts of N-C=O band in both C1s and N1s spectra of the films show that a small amount of amines are converted to amide prior to the measurement.

Table 4. Contributions of each chemical bond type in the surface of Parylene thin films

	PPX		PPX-C		PPX-A	
	BE (eV)	**Atomic %**	**BE (eV)**	**Atomic %**	**BE (eV)**	**Atomic %**
C 1s	**100 %**		**87.63 %**		**89.81 %**	
C-C	283.1	100.00	283.4	44.97	284.4	59.95
C-N					285.3	20.22
C-Cl			283.9	42.66		
N-C=O					286.5	0.64
N 1s					**9.74 %**	
N-C					391.2	9.03
N-C=O					400.9	0.71
O 1s			**0.96 %**		**0.45 %**	
Cl 2p			**11.43 %**			
Cl-C ($2p_{1/2}$)			199.1	7.34		
Cl-C ($2p_{3/2}$)			200.7	4.09		

3-5- Stability of the amine groups

As described in the Introduction, there is considerable interest in developing amine-rich surfaces for a wide variety of biotechnological applications,[22, 25, 27, 28, 73] including protein synthesis[74] and cell cultures in orthopaedic[75] and cardiovascular medicine.[76] It has been shown that the presence of a high density of primary amines [$–NH_2$] on the surface is essential for applications such as promoting the adhesion of primer layers used for metallized plastics,[77] and for effective cell adhesion.[78] For example, no adhesion of cells was observed when human U-937 monocytes were applied on the surface of a thin organic film bearing less than a critical [$–NH_2$] concentration of 4.2 atomic % (per 100 atoms of C, N and O).[79] These functional surfaces have been prepared through different approaches including direct chemical modification of the surface,[26, 28] or addition of a thin organic coating that readily contains the desired functionality. The latter, could be done via plasma assisted techniques and ultraviolet photopolymerization[24, 26] or via CVD polymerization of functional precursors.[30, 80] Utilization of the last category for this purpose only applies for Parylene coatings so far.

A challenge to the use of amine-rich surfaces is that amines have poor stability[73] and can be oxidized by being exposed to air. Hence, many organic compounds such as amine hydrochlorides and drugs that contain amine groups are either stored under inert atmospheres or sold as salts. Various products, primarily nitro, nitroso and amide groups, can result from the oxidation of amines, though the mechanisms of these reactions are yet to be characterized. Therefore, many of the reports in the literature dedicate significant efforts to address the question of whether the amine-rich surfaces are stable in the specific

operational conditions; of particular interest is the stability of amine groups in air and/or in aqueous solutions.[73] In all the categories described for fabrication of functional surfaces, radicals are involved throughout the coating or modification processes. These free radicals can sometimes be trapped in the bulk of a polymer and can react with oxygen or water, causing drastic changes in the functional groups and/or their densities. Although the kinetics and mechanisms relating to these reactions are not clearly known, various researchers have studied the time-dependent stability of surface functional groups.[30, 73, 81, 82] The mechanisms proposed in these studies for the reaction of these bulk-trapped radicals with O_2 are shown in **Scheme 10**.[73]

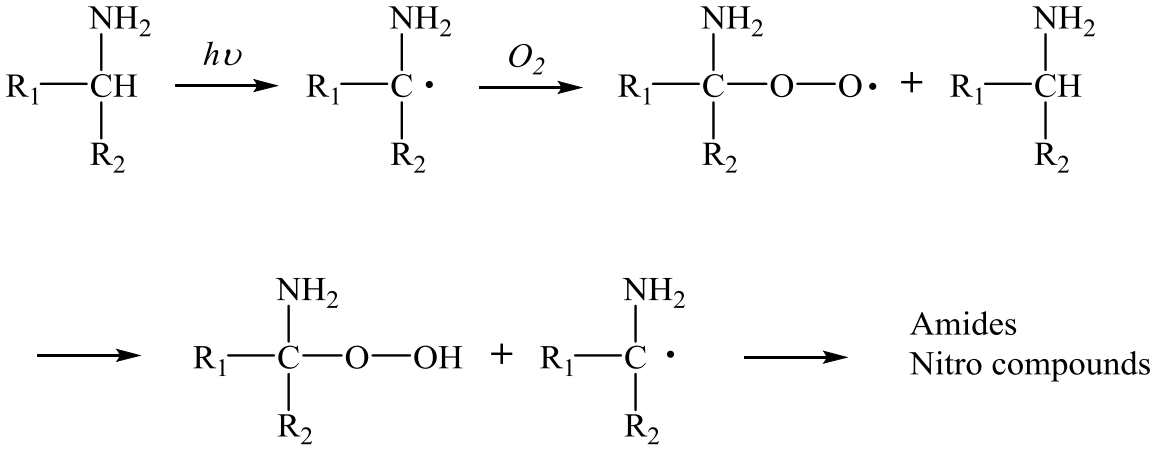

Scheme 10. Proposed mechanism for aging of polymers containing primary amines and trapped-free radicals.[73]

In contrast with the plasma polymers and Vacuum-unltraviolet polymers, which are rich in buried free radicals,[83] PPXs have shown no detectable electro-spin resonance

signal,[30] suggesting that no trapped radicals are present after their deposition. Despite the absence of free radicals in the surface of such films, the decay of surface primary amine functionalities over the storage time (aging) has been also reported for amine-functionalized PPXs. To the best of our knowledge, there is only one work in the literature that has studied the aging of an amine-bearing PPX, commercially known as Parylene diX AM, which is synthesized by the CVD polymerization of 4-aminomethyl[2.2]para-cyclophane.[30] In this work, adhesion of U-937 monocytes on different amine-functionalized polymer surfaces including Parylene diX AM and also aging of the surface functionalities in air and mili-Q water were studied. The results of Parylene diX AM showed that for each NH_2 group lost, exactly one oxygen atom appeared in the structure of the film. In other words, during the storage time, amine decay and oxygen take-up occur at the same rate and time constant. This was reflected in the time-evolving curves of $[NH_2]/[C]$ and [O]/[C]measured at the surface over the same period of aging in ambient air, in the darkThe two curves for Parylene diX AM were mirror images of one another.

Therefore, considering that certain functional groups such as primary amines are inherently reactive, a mechanism that does not rely on the reaction of trapped-free radicals is presumed. **Scheme 11a** presents a possible mechanism for the conversion of highly reactive primary amines to oxygen-bearing groups. For polymers that still contain the trapped-free radicals both aging mechanisms, presented in **Schemes 10** and **11**, are valid and are expected to occur at a same time. The so-called parallel aging mechanisms justify the lower time constants (or higher speeds) of oxygen take-up, ([O]/[C]) (t) observed in amine-bearing polymers that also contain trapped radicals. Also, it is stated that when all

of these functional films were immersed in Mili-Q water, not only the previous reactions took place with dissolved O_2 (akin to atmosphere O_2), but water molecules were also incorporated in the structure as shown in **Scheme 11b**.[30] Indeed, both phenomena can occur in either media, with the consideration that the abundance of oxygen and water, and consequently the percentage of these reactions might be reversed.

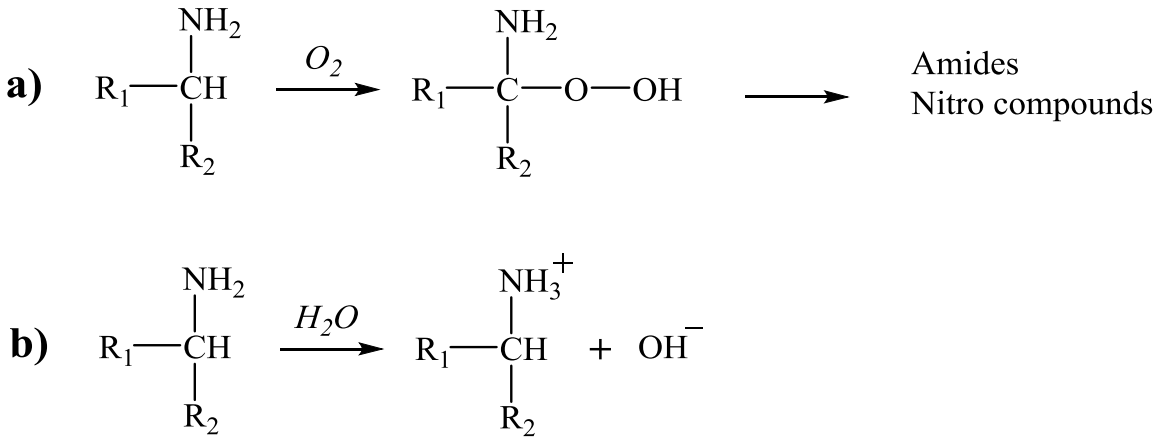

Scheme 11. Proposed mechanisms for aging of amine-bearing polymers without the interference of free radicals;a): reactions with O_2, and b) reaction with water. [30]

3-5-1- Stability of amino-PCP

In light of the instability of amine-bearing coatings, we studied the aging of Parylene A. The first observation in the course of our work refers to functionalization of [2.2]-paracyclophane. Although no evidence of anomalies was found in the early characterizations of 4-amino[2.2]paracyclophane that were performed immediately after its synthesis, a color change from tan to very dark brown was observed in the compounds

stored for a few days in the lab environment. Solutions of 50 mg of as-synthesized and aged (30 days) amino-PCP in dichloromethane (4 mL) are shown in **Figure 20**. Also, the TLC spots that were not detectable unless a short wavelength UV light was used, turned to dark smudges after only a few hours of finishing the TLC experiment. These basic laboratory observations prompted us to re-examine the synthesized compounds.

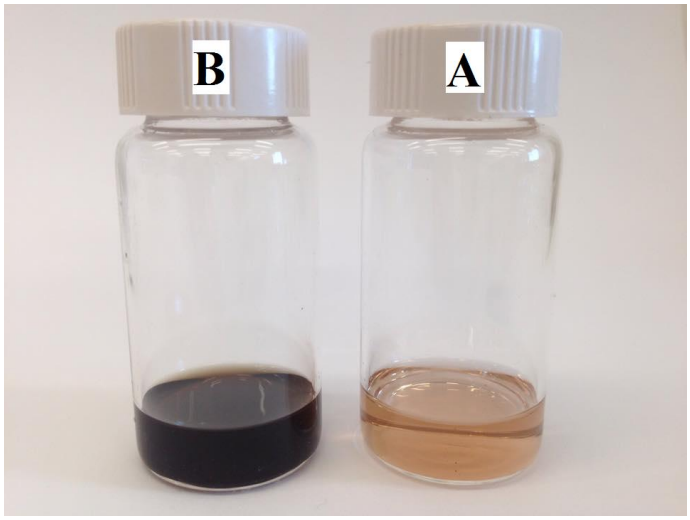

Figure 20. Solutions of amino-PCP (50 mg) in dichloromethane (4mL); A) as-synthesized amino-PCP, B) aged amino-PCP (30 days)

In order to obtain more reliable results, we carefully repeated the synthesis of amino-PCP to produce high purity amino-PCP. The nitro-PCP synthesized in the first nitration step was crystallized twice from methanol to assure its high purity prior to the reduction step. The synthesized amino-PCP was immediately dried and stored under argon. We then investigated the effect of aging on the chemical structure of amino-PCP via NMR

spectroscopy. For this purpose, a small quantity of amino-PCP (50 mg) was set aside and exposed to air for one day in the laboratory environment. Another 50 mg of the compound was soaked in mili-Q water for 30 min, followed by a rapid vacuum filtration. The filtered compound was re-dissolved in chloroform and dried over Na_2SO_4 prior to evaporation of the solvent under vacuum and subsequent NMR measurements. Also, it is crucial to purge the NMR test tubes with an inert gas (e.g. Ar) and seal the cap with Parafilm to minimize the probability of further oxidation during or before the test. NMR samples that were not kept under inert condition showed unreliable results. The superimposed ^{1}H NMR spectra of as-synthesized, aged for one day in air, and water-treated amino-PCPs are shown in **Figure 21**. The spectra of these three samples were almost identical regarding the chemical shifts and the number of protons. However, the chemical shift that is associated with primary amine and its integration are different for these samples. As denoted on the spectra, the relative integration of the protons on amine group is reduced from 1.95 (δ=3.18–3.80), to 1.72 (δ=3.21–4.04) and to 1.64 (δ=3.40–4.22) respectively for aged and water-treated samples indicating the decrease in the amount of primary amine groups. Furthermore, the decrease of intensity of the chemical shifts is accompanied by broadening to downfield. The latter might result from the presence of electron withdrawing moieties such as carbonyl groups of amides, supporting the hypothesis that the primary amine groups of the amino-PCP are prone to oxidation in air and aqueous solutions. We did not observe any additional chemical shift in the ^{13}C NMR of these samples so far. This might be due to the very low concentrations of the oxidized molecules at this early stages of aging.

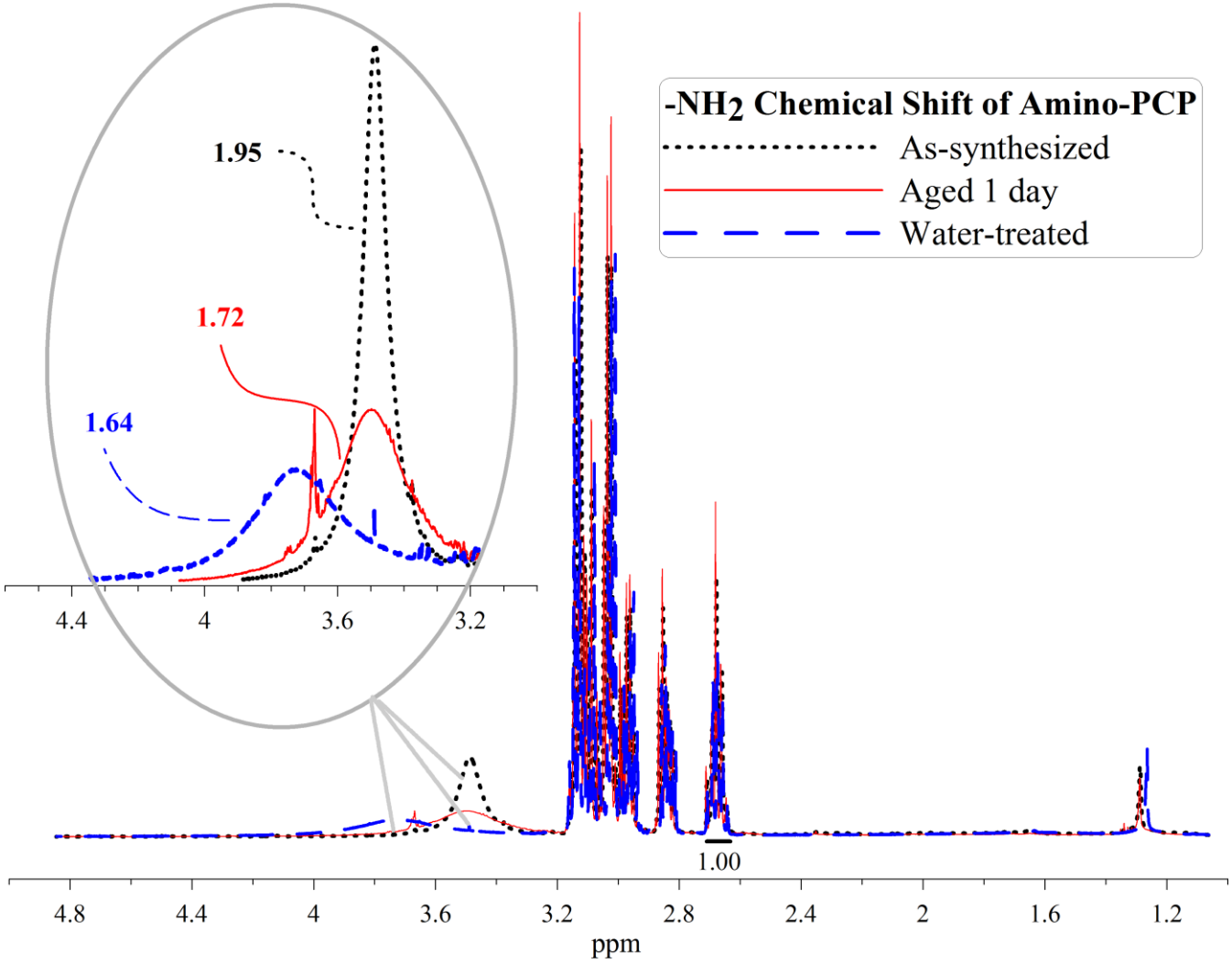

Figure 21. Superimposed ^{1}HNMR spectra of Amino-PCP; Decay of protons associated with primary amine groups.

3-5-2- Stability of Parylene films

As discussed earlier, the XPS and FTIR characterizations demonstrated that CVD polymerization successfully transferred the functionality of the precursors, as well as primary amine groups, onto the surface of deposited PPX-A films. However, we have recently found out that XPS surveys performed on old PPX-A films depict different chemical composition than that of the freshly-deposited films. Following that, a careful literature review including all aspects of amine-functionalized surfaces, revealed that these surfaces are subject to evolution of their functional groups during the storage times, in a similar fashion to the precursor aging discussed above. We studied the evolution of primary amine groups in the structure of PPX-A films by aging them for several days in ambient air followed by XPS measurements.

The results of the XPS survey from the surface of aged PPX-A films are shown in **Figure 22** comparing with the fresh (as-deposited) PPX-A. Also, the detailed elemental composition on the surface of these films are given in **Table 5.** As shown in their XPS spectra, after only 1 day O atoms appear on the surface (2.27 at. %) and within 4 days it reaches to 12.63 % (relative to C and N). The appearance and buildup of O is accompanied by a 3.4 % decrement in the abundance of N atoms over 4 days. This is much lower (~ 1/4) than the amount of Oxygen take-up suggesting that N atoms (and similarly, C atoms, **Table 5**) are not lost but its overall percentage is decreased due to the incorporation of O atoms and introduction of other chemical bonds in the structure. Conversion of chemically unstable amine groups to more stable functionalities such as amides or oximes without

significant variations in the overall concentration of [N] on the surface is evidenced by XPS studies in other works [77, 84]

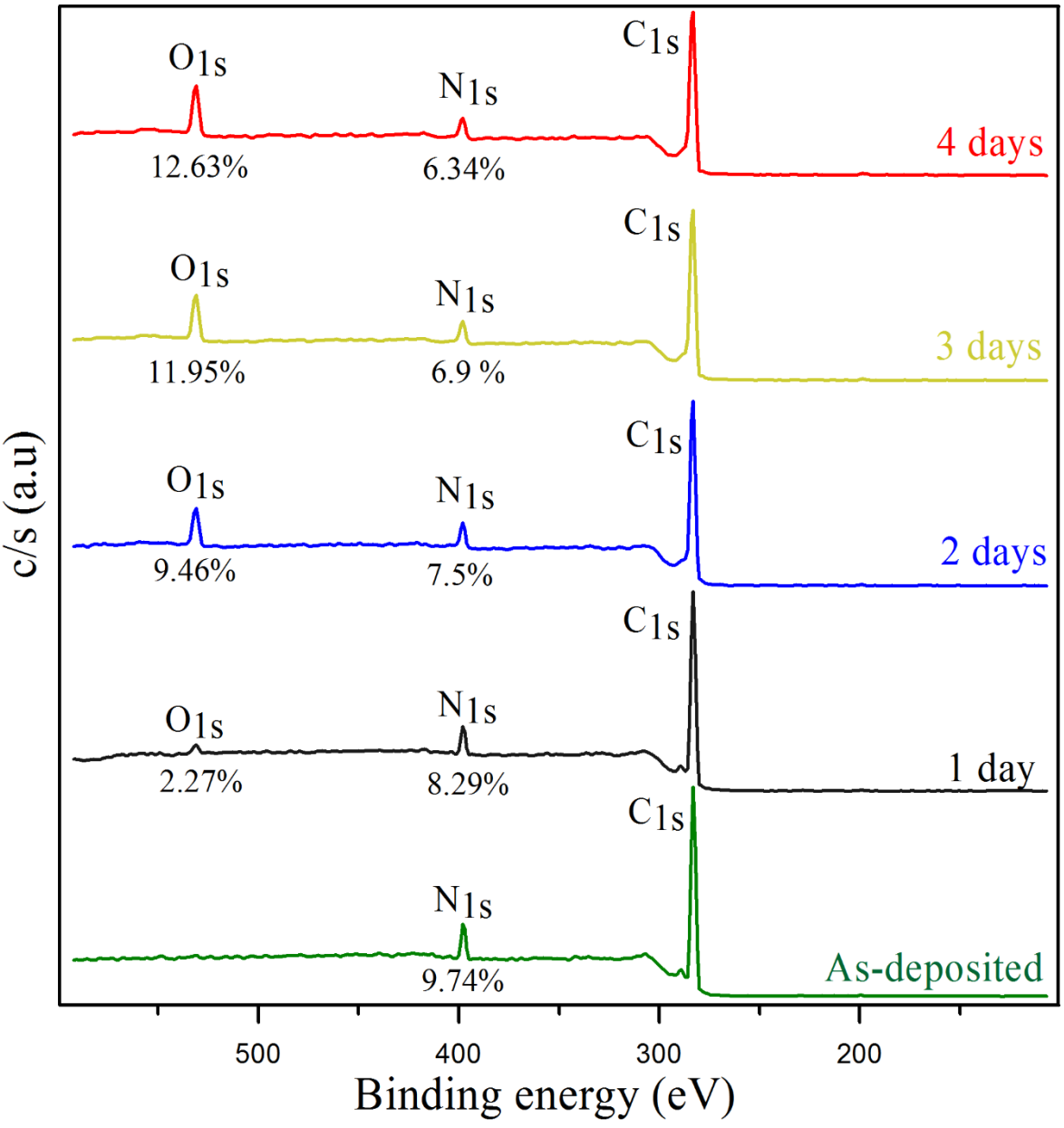

Figure 22. XPS spectra of aged PPX-A thin films; Evolution of the surface composition over the storage time in air

Table 5. Evolution of chemical composition during the aging of PPX films

		Pre-Etch				Post-Etch		
Sample code	**Condition**	**C 1s**	**N 1s**	**O 1s**	**Cl 2p**	**C 1s**	**N 1s**	**Other**
PPX 30	**PPX** 30 days in air	98.24	-	1.76	-	100	-	-
PPX-C 30	**PPX-C** 30 days in air	87.32	-	1.75	10.33	88.74	-	Cl 2p (11.26)
PPX-A	**PPX-A** As-deposited	89.81	9.74	0.45	-	89.69	10.31	
PPX-A 1	**PPX-A** 1 day in air	89.38	8.29	2.27	0.07	89.92	10.08	
PPX-A 2	**PPX-A** 2 days in air	82.79	7.5	9.46	0.25	93.19	6.21	Ag 3d (0.61)
PPX-A 3	**PPX-A** 3 days in air	81.12	6.9	11.95	0.3	94.53	5.47	-
PPX-A 4*	**PPX-A** 4 days in air	80.53	6.34	12.63	0.33	96.7	3.3	-
PPX-A 1 W	**PPX-A** 1day in mili-Q water	90.24	8.69	0.95	0.12	NA	NA	NA

* Comprised also 0.18 % S2p trace impurity prior to etching

In addition to aging in air, we examined the durability of PPX-A in aqueous media by dipping a PPX-A-coated Si wafer in mili-Q water for one day. Based on the observation of the faster decay of amines of amino-PCP in mili-Q water compared to air, we expected a high degree of oxidation even after one day. But, the results were different than our expectations as less than 1 % O was detected in the XPS analysis of PPX-A thin film stored in mili-Q water for 1 day. If we consider that O_2 molecules are the predominant source of oxidization, this observation aligns well with the lower content of dissolved O_2 in water compared to air but the reverse rates of oxidization of amino-PCP and PPX-A in water and

air yet needs to be justified. A simple reason for this observation could be related to technical errors as such these samples had different availabilities to the test media. In case of amino-PCP, the precursor was appropriately dispersed in water, but for the air-aged sample we failed to disturb the clumps of the precursor powder and to spread it over a large flat surface to provide it with comparable availability to O_2 as it had in water.

Aging of amine-bearing surfaces has been studied in some works in the literature; however, no in depth study of these aging phenomena have been performed on PPX-A polymer films. We found that the chemical composition of the films not only on the surface, but also in the bulk of the films are subject to variation due to the oxidation phenomena during aging of PPX-A films. In order to study the evolution of the chemical composition in bulk of the aged films we applied an argon etch for 6s, followed by an immediate XPS survey from the resultant films. The post-etch XPS spectra of aged PPX-A films (shown in **Figure 23**) exhibits a significant decrease in the overall N at. % over the storage time. Decay of nitrogen in the bulk (post-etch) of the aged films is presented in more detail in **Table 5.** Since no other element contributed to XPS spectra of etched films, we can simply conclude that variation of chemical composition is on the account of reduction in the amount of [N] atoms. While, its content was almost constant in the bulk of un-aged PPX-A films or samples that were prevented from aging by storing under argon in tightly sealed containers. This observation was not changed by repeating the argon etch (6 s) depth surveys and no meaningful variation in the amount of [N] was observed after 5 consecutive etches for the un-aged PPX-A films. The difference in the resistance of bulk N atoms to etching in aged and un-aged samples indicates that oxidization of PPX-A films can also

occur in depth of the films. Such that, at least a part of the new chemical bonds that are formed after oxidation are not as strong as the parent chemical bonds and are etched faster. However, since the only contributing atoms to the XPS spectra of etched films are C and N, elucidation of the oxidation mechanisms and consequently identification of the chemical bonds that are formed seem infeasible even with high resolution XPS.

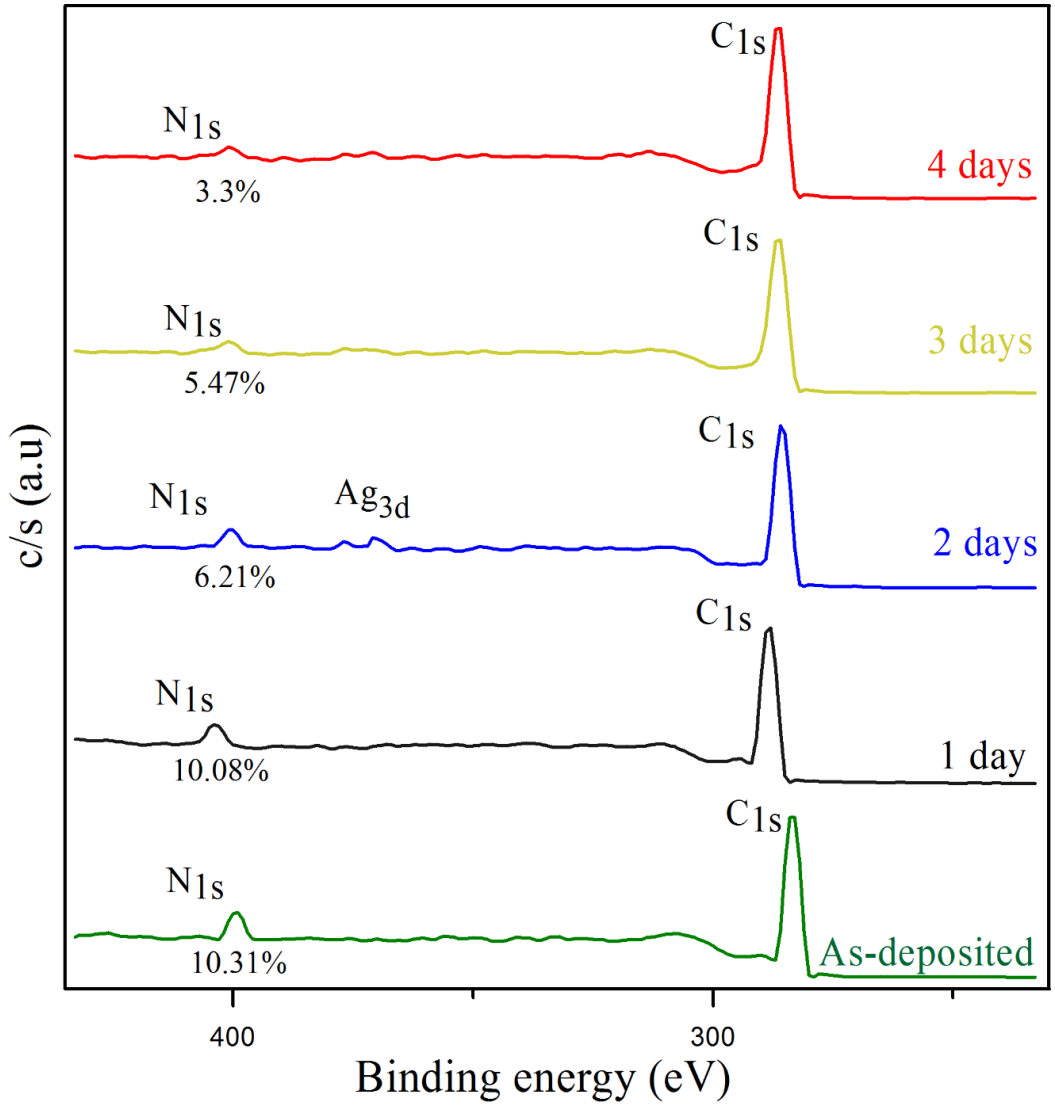

Figure 23. XPS spectra of aged PPXA thin films after an argon etch for 6 s; Decay of nitrogen atomic % in the bulk over the storage time in air

We were not able with these preliminary experiments to track a consistent pattern for the evolution of the composition in the bulk and consequently justify the decay of nitrogen amines in bulk. However, considerable attention has been paid in literature to investigate the effect of aging on the surface chemistry of amine-bearing polymers that helped us to correlate the evolution of chemical composition on the surface of our PXX-A films. For this purpose, we studied the high resolution XPS spectra acquired from the surface of aged films. **Figure 24** shows the deconvolved bands that are fitted at high resolution C1s, N1s and O1s spectra of the PPX-A sample aged 4 days. According to these high resolution spectra, various chemical bonds involving O are created after exposure of the PPX-A film to air within 4 days. C1s spectrum shows that in addition to major C-C and C-N bonds of amines, two other chemical bonds C-O and N–C =O (amide) are formed due to the oxidation of PPX-A. This is reflected accordingly in N1s and O1s spectra as NC and NC=O, and OC and O=C type bonds are detected respectively.

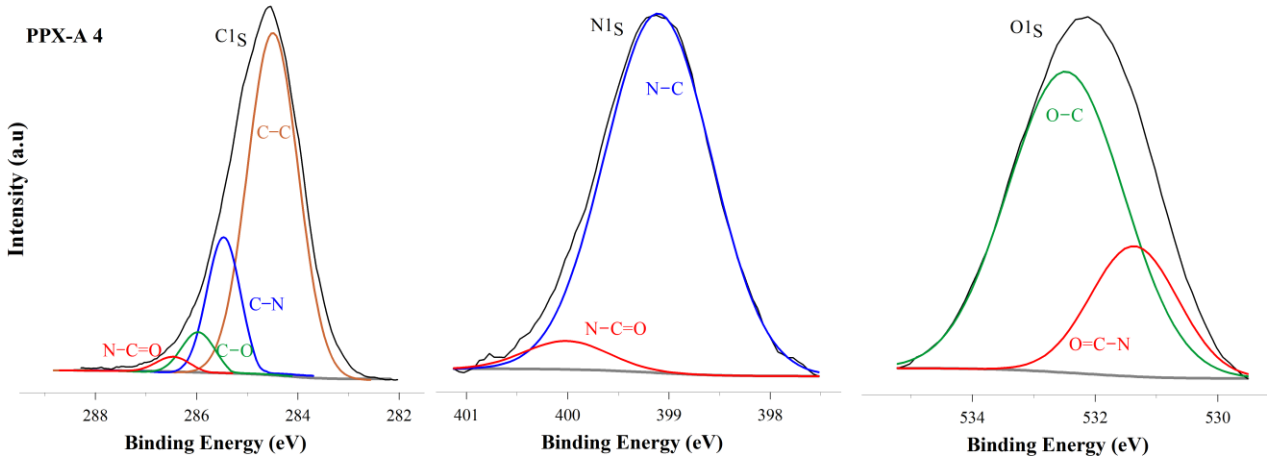

Figure 24. Deconvolved high resolution C1s, N1s and O1s spectra of the PPX-A aged 4 days.

As high resolution XPS spectra of the aged films suggest, within the exposure time to air or water, O atoms are incorporated into the structure of the films through either amide formation or oxidation of backbone (C-O).We previously stated in this section that two general mechanisms are presumed for aging of amine-bearing films. In case of PPX, however, no oxidation through the polymer backbone is expected due to the absence of trapped free radicals Therefore, oxidation is presumed to occur on amine groups only.[30] However, this was found on aminomethyl-PPX where amine groups are connected to aliphatic carbons. To further investigate this in PPX-A films, where amine groups are connected to aromatic rings instead of aliphatic carbons, we compared the aging of PPX-A with that of PPX and PPX-C films which lack amine groups in their structure. Their pre-etch and post-etch elemental composition collected after 30 days of aging in air is shown in **Table 5**. Although, a small amounts of O (1.75%) is detected on the surface of aged PPX 30 and PPX-C 30 films, their post-etch XPS surveys demonstrate similar results to un-aged samples. Meaning that the expected amounts elements (C and Cl) as well as no O were seen in the bulk of PPX 30 and PPX-C 30 samples. Presence of small quantities of O on the surface of PPX films has been observed in other works as well. Though, it has been attributed to organic contaminants rather than oxidation of backbone chains.[85-87] Comparing these results with the aging behavior of PPX-A films gives further evidences to the fact that amine-functionalized PPX films with no trapped radicals in their structure are oxidized through their pendant amine functionalities.

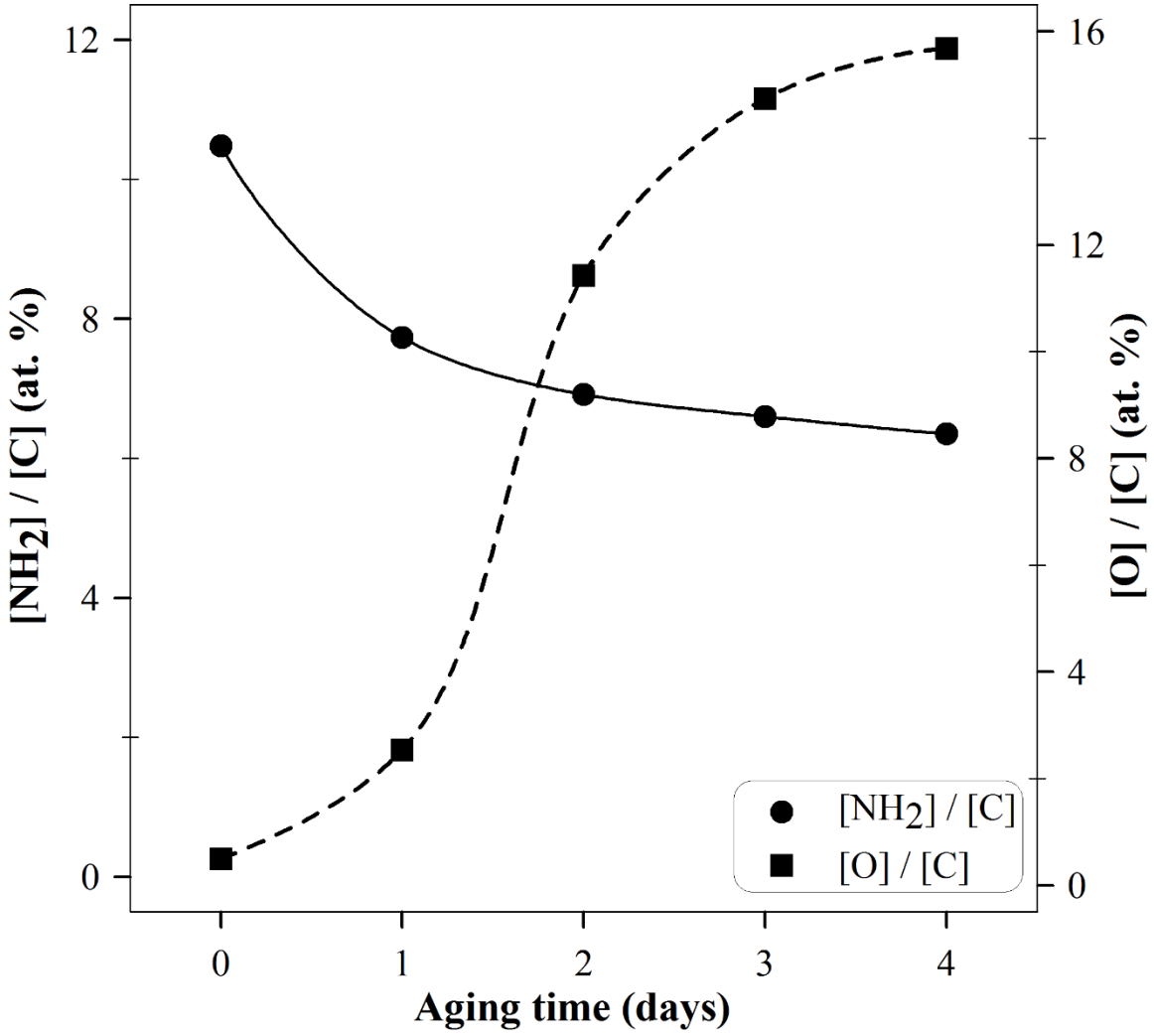

Figure 25. Decay of primary amines ([NH_2]/[C]) versus oxygen uptake ([O]/[C]) in PPXA films as a function of the storage time in laboratory ambient atmosphere.

Also, compared to the previous work on aminomethyl-PPX,[30] we found that the rates of oxygene take-up and amine's decay are not necessarily equal over the entire duration of aging. To study this we plotted the [-NH_2]/[C] % versus [O]/[C] % against the storage time in air (**Figure 25**). Our results, revealed that the decay of amines and take-up of oxygen atoms in the PPX-A films occur with different slopes. These unequal rates further

suggests that the mechanism of oxidation of these films is more complicated than a simple amidation reaction as we clearly detected that oxygen atoms are involved not only in amide groups but also in other chemical bonds such as at least O–C. The obtained experimental amounts of [N]/[C], [-NH_2]/[C], [O]/[C] and [N-C=O]/[C] are given in **Table 6**. Comparing the increasing trends of [O]/[C] and [N-C=O]/[C] in the aged films, shows that the abundance of amide groups are first increased with O take-up. However, at the later stages of aging its relative abundance is decreased indicating that either the amide groups are transformed to other groups or their rate of production is significantly reduced compared with other chemical bonds

Table 6. Relative abundance of amine and amide groups in comparison with [N] and [O] amounts during the aging of PPX-A films

Aged samples	[N]/[C] (%)	[NH2]/[C] (%)	[O]/[C] (%)	[N-C=O]/[C] (%)	Δ ([O]/[C]) (%)	Δ ([N-C=O]/[C]) (%)
PPX-A	10.84	10.48	0.50	0	-	-
PPX-A 1	9.28	7.73	2.54	0.29	2.04	0.29
PPX-A 2	9.06	6.92	11.43	2.14	8.89	1.85
PPX-A 3	8.53	6.6	14.74	1.89	3.31	- 0.25
PPX-A 4	7.87	6.35	15.68	1.35	0.94	- 0.54
PPX-A 1 W	9.63	9.07	1.053	0.56	-	-

Conclusion

CVD polymerization of [2.2]paracyclophanes, particularly when they bear functional groups, provides a general and convenient way for the preparation of functionalized thin films. In addition to simplicity, when compared to conventional solvent-based methods, thin film coating through CVD polymerization provides excellent compatibility with a wide variety of functional groups, superb adhesion to various materials, and applicability to three-dimensional substrates. A practical method that facilitates the incorporation of reactive groups without requiring post-treatment of the films is in high demand for biomaterials development. The addition of reactivity on biomaterials of interest enables the selective attachment of bio-active molecules via non-toxic aqueous chemistry, which is free of hazardous solvents or other reagents. As a result, the interfacial biocompatibility of such materials can be enhanced allowing them to be implanted or to be used in complex biological environments.

Highly reactive groups such as amines and carboxylic acids enable immobilization approaches for a wide range of biomolecules. They also influence the interfacial interactions by controlling surface charge. However, despite the promise of great benefits for biomedical applications, industrial use of vapour deposited functional films is limited due to the lack of practical methods for production of the related functional precursors. Synthesis of amine-functionalized PCP precursors through the direct nitration method has been a challenge for many years. The current thesis, contributes to this milestone of paracyclophane chemistry and represents a simple and reliable method for large-scale

production of amino-PCP. The initial obstacle in the nitration reaction of PCP was resolved by replacing the triflic acid with triflic anhydride, resulting in a higher yield of nitro-PCP. This also facilitated the extraction and purification steps of the crude product, which is a well-documented challenge. We were unable to detect any di-nitro PCP under any conditions tested, instead a mixture of oligomers and polymers of nitrated PX were eluted after nitro-PCP.

Furthermore, a very simple and efficient reduction reaction was successfully conducted for the first time on nitro-PCP. The overall yield of the suggested synthetic route was above 77%, which was successfully scaled-up to 5 g of starting material. Additionally, the synthesis of carboxyl-functionalized precursors was attempted through Freidel-Crafts acylation of PCP. Apart from the partial success in synthesizing the intermediate acetyl derivatives, our research on the carboxylation of PCP is still in its early stages and further experiments are currently being done to optimize the reaction conditions. Finally, various characterization techniques were employed to verify the successful synthesis of functionalized PCPs. Characterization of the thin films deposited from these functionalized precursors demonstrated the compatibility of CVD polymerization with primary amine functional groups.

Eventually, the more important issue of durability of amine groups was investigated for the first time for both precursors and thin films of PPX-A. NMR studies of amino-PCP showed a significant decrease in the amount of primary amines by a short treatment with water or exposure to air. Broadening of the ^{1}H NMR chemical shifts toward downfield also suggested a correlation between the decay of amines and the appearance of functional

moieties that contain electron-withdrawing groups. Oxidation of amines with aging in air or storing under mili-Q water was further observed on the surface of deposited films. Within only 4 days of storage in air, the amount of amine groups compared to C ([NH_2]/[C]) reduced from 10.48 to 6.35 which was accompanied by 15.68 % uptake of O ([O]/[C]). Also for the first time, we showed that aging of PPX-A films changes the chemical composition in their bulk as well as the surface. The XPS spectra obtained from freshly-deposited films after etching with Ar more closely matched the predicted elemental composition, with no O and an amount of N comparable to that expected from di-amino-PPX. However, the amount of N in the bulk of aged films was substantially decreased after 48 h, suggesting the evolution of new chemical bonds during the oxidation that are not resistant to Ar etch. This subsequently indicates the effectiveness of oxidation phenomena in depth of the films once a considerable time of aging has elapsed.

The current study requires to be extended to longer periods of aging to further investigate the long-term stability of amine groups. Nevertheless, it has been reported that despite the rapid O uptake of amine-functionalized films in the early stages of aging, they retain a significant fraction of amine groups over long aging periods. The overall amount of long-term stable amine groups depends on their initial density in the film. This factor may define the shelf-life and time-scale applicability of amine-functionalized coatings. Similar to commercial providers of amine-functionalized materials such as aminosilane-coated glass slides, we were able to prevent both amino-PCP and PPX-A films from aging by storing them under argon. In addition, since the CVD process is conducted under high vacuum the chances of oxidation are limited to the short times of transferring the materials

in between the processes. But, if one foresees to use PPX-A films, it is beneficial to minimize the time of fabrication and exposure to active media. Especially, if they have to be used a lengthy period after preparation, it is necessary to design a fabrication scheme that results in the best shelf-life.

Future outlook

As discussed, one of the major issues with amine-bearing surfaces is their poor resistance to oxidation in air or aqueous solutions, where most biological interactions take place. Hence, despite the successful incorporation of functional groups into PPX films, maintaining them until the time of operation is challenging. From these facts, one can infer that these amine-functionalized films are best to be prepared immediately before their final use. Here in this thesis we presented a facile heterogeneous catalysis for reduction of nitro-PCP; a reaction with mild conditions that can convert aromatic nitro compounds to corresponding amino products. As nitro groups are in oxidized state compared to amino groups they have sufficient durability in air or aqueous solutions. The nitro-PCP produced in our lab remained intact for periods as long as a year under ambient laboratory atmosphere and we predict that the nitro functionality resists the CVD conditions. Based on these observations, we propose a scheme that can minimize the potential time of aging of PPX-A films. To do this, we can coat the surface of substrates with nitro-PCP instead of amino-PCP. The thin films of nitro-PPX can be stored at normal conditions in air without worrying about further oxidation prior to use. Then the same reduction system that was used for nitro-PCP can be employed here to treat the nitrated surfaces. This method relies strictly on the high efficiency of the Raney Ni/$NaBH_4$ reduction system that can perform over mild conditions at room temperature, atmosphere pressure and short reaction time, crucial to prevention of the films from physical damages.

Recent advancements in immobilization of biomolecules provide a very powerful and versatile means to engineer the surface properties which can be useful in many aspects

of science such as molecular biology, analytical chemistry, medical diagnostics, tissue engineering and biomedical implants.[88, 89] So far, various methods including physical adsorption, self-assembly of monolayers, layer-by-layer deposition, CVD polymerization and polymer grafting have been reported for immobilizing biomolecules onto the surface of biomaterials.[90] Covalent immobilization techniques offer a long-term availability of biomolecules and does not require large amounts of modifiers, compared to non-covalent methods. Nevertheless, presence of a reactive group on the substrate surface is required, which is difficult for many materials such as polymers without functionalization. More importantly, biomedical applications require a highly defined and predictive expression of functional groups on the surface of biomaterials. In this regard, depositing organic thin films containing reactive groups onto the surface of bulk material has attracted increased attention. In particular, platforms of functionalized PPX films promise advantages for cell culture, immunoassays and covalent binding of biomolecules such as proteins.[25, 27, 30, 90-92] Owing to their ability to pattern surfaces with micro- and nanometer-precision various microarrays including DNA, peptide, tissue and cellular microarrays can be fabricated on these functionalized PPX films.

Moreover, to mimic a more in vivo like environment or to obtain a synergistic action in some advanced cases, co-immobilization of two or more biomolecules is required. One application that has been successfully investigated using PPX-C films are Parylene lift-off stencils.[93, 94] Functionalized PPX films could be used in combination with conventional PPX-C films to extend multilayer Parylene stencils.[9, 10, 95] Such platforms could enable co- or multi-culture of different cell types through the successive patterning

and lifting off steps of the layers, resulting in substrates that resemble multi-component complex structure of extra cellular matrix. Functional layers of the so-called stencil can be further modified with other molecules such as Poly(ethylene glychol) (PEG) to serve as an interlayer between two Parylene layers, or to exploit the protein repellent properties of PEG to selectively direct proteins of interest in the features of a micropatterned substrate.

In addition to multilayer stencil-based patterning, co-immobilization of biomolecules can be achieved through a multifunctional surface. Due to their good chemical reactivity, primary amine (-NH2) and carboxyl (-COOH) groups are widely used as reaction sites to covalently immobilize biomolecules.[88-92] For instance, Yang et al.[89] constructed a polyfunctional coating containing $-NH_2$, −COOH, and phenol/quinine groups by a two-step procedure assisted with Gallic acid for co-immobilization of diverse biomolecules onto the surface. Results of their work, showed that co-immobilization of vascular endothelial growth factor (VEGF) with anti-CD34 antibody promoted bioactivity of poly-functional surfaces compared with similar mono-functional substrates.

Furthermore, many applications including microfluidics and medical devices require conformal and uniform coating over nonplanar or porous substrates. As mentioned earlier, the CVD process is a suitable method to produce commercial, pinhole-free coatings used, for instance, in micro electro mechanical systems[4] and microsensors such as neural probes,[96, 97] microvalves,[98] microchips and electrospray micronozzles for mass spectrometry[99, 100]. This technique has been used to functionalize the surface of a number of microfluidic devices.[90-92] However, bonding different (usually top and bottom) parts of these devices to each other, which is conventionally performed by plasma activation of the

surface, is yet a challenge in microfluidics fabricated from polymeric substrates. It is has been recently reported that wafers containing Parylene coatings can be bonded to each other through the thermal bonding of Parylene interlayers.[101-104] So far, we have been able to examine the thermal bonding of Parylene C/Parylene C films coated on standard microscope glass slides (76 mm x 26 mm x 1 mm) at different experimental conditions varying the time and temperature of the experiment. Although, we have not yet performed a quantitative bond strength test, the primary laboratory observations including visual inspection and razor blade test were conducted following the methods reported in the literature to determine the quality of bondings.[102, 103, 105] Good bonding results, were obtained at temperatures above 150 °C and pressures of 2.5–3 MPa under vacuum, in a good agreement with litereature.[103]

However, successful thermal bonding depends strictly on applying a pressure on the two pieces and performing the experiment under vacuum, since Parylene undergoes thermal oxidation if the heating process is carried out in air.[106] These two conditions require designing a particular setup to load pressure on the samples, which can be inserted in the experiment medium such as a vacuum oven. In addition, applying even moderate pressure on delicate microfluidic devices can distort the microchannels (e.g. in PDMS-made devices). Hence, developing a relatively gentle process to bond the microfluidic devices is of great importance. In a different approach, using two complementary PPX layers, poly (4-aminomethyl-pxylylene-co-p-xylylene) and poly (4-formyl-p-xylylene-co-xylylene), Chen and co-workers [91] have demonstrated the surface modification of two different PDMS slides to form Schiff base cross-links for bonding of different pieces of microfluidic

devices. They named their bonding technique as solventless adhesive bonding (SAB) for which they utilize the chemical reaction of the surface functionalities and thus obtain a stronger attachment. More recently, two complementary polymers, namely, poly (4-aminostyrene) (PAS) and poly (glycidyl methacrylate) (PGMA), were used to modify a number of substrates such as PDMS, Si wafers, and glass using the iCVD technique.[92] In both examples, amino groups were demonstrated to be available in the formed microchannels after assembly and bonding process.

Inspiring from the previous work of Xu and Gleason,[92] we suggest an inexpensive, facile and effortless method to carry out the solventless adhesive bonding of PPX films by exploiting the amidation chemistry of pendant -NH_2 and -COOH groups on the films. To do this, amine- and carboxyl-functionalized PCPs, can be CVD (co)polymerized[35] to coat the surface of the proposed substrates with thin films bearing reactive NH_2 and COOH groups. The bonding temperature of around 50-80 °C will be used which is much lower than the T_g of polymer films. Also, no additional high-pressure load is required, and the procedure is predicted to be successful in ambient atmosphere. Then adapting the two above ideas of chemical adhesive bonding and poly-functional surfaces with our framework, we propose to poly-functionalize the surface of a variety of materials as well as PDMS to fabricate microfluidic devices. These functional groups are predicted to not only serve as bonding facilitators, but also to provide the surface of assembled microfluidic devices with two different functional groups, enabling co-immobilization of biomolecules in the microchannels.

References

1. Sirringhaus, H., Tessler, N., and Friend, R. H. (1998) Integrated Optoelectronic Devices Based on Conjugated Polymers, *Science 280*, 1741-1744.
2. Seymour, J. P., Elkasabi, Y. M., Chen, H.-Y., Lahann, J., and Kipke, D. R. (2009) The insulation performance of reactive parylene films in implantable electronic devices, *Biomaterials 30*, 6158-6167.
3. Tan, C. P., and Craighead, H. G. (2010) Surface Engineering and Patterning Using Parylene for Biological Applications, *Materials 3*, 1803-1832.
4. Kim, B. J., Chen, B., Gupta, M., and Meng, E. (2013) Three dimensional transformation of Parylene thin film structures via thermoforming, In *Micro Electro Mechanical Systems (MEMS), 2013 IEEE 26th International Conference on*, pp 339-342.
5. Junichi, M., Yuji, S., and Nobuhide, K. (2000) Adhesion-Based Cell Sorter with Antibody-Immobilized Amino-Parylene Surface, In *20th IEEE MEMS Conference*, pp 27-30, IEEE, Kobe, Japan.
6. Gleiter, R., and Hopf, H. (2006) *Modern cyclophane chemistry*, John Wiley & Sons.
7. Tan, C. P., Ri Seo, B., Brooks, D. J., Chandler, E. M., Craighead, H. G., and Fischbach, C. (2009) Parylene peel-off arrays to probe the role of cell-cell interactions in tumour angiogenesis, *Integrative Biology 1*, 587-594.
8. Kahouli, A., Sylvestre, A., Ortega, L., Jomni, F., Yangui, B., Maillard, M., Berge, B., Robert, J.-C., and Legrand, J. (2009) Structural and dielectric study of parylene C thin films, *Applied Physics Letters 94*, -.
9. Jinno, S., Moeller, H.-C., Chen, C.-L., Rajalingam, B., Chung, B. G., Dokmeci, M. R., and Khademhosseini, A. (2008) Microfabricated multilayer parylene-C stencils for the generation of patterned dynamic co-cultures, *Journal of Biomedical Materials Research Part A 86A*, 278-288.
10. Chen, C. L., Jinno, S., Moller, H., Rajalingam, B., Chao, S. H., Selvarasah, S., Khademhosseini, A., and Dokmeci, M. R. (2008) Multilayer parylene-C stencils for dynamically controlling cell interactions, In *Micro Electro Mechanical Systems, 2008. MEMS 2008. IEEE 21st International Conference on*, pp 276-279.
11. Fortin, J. B. L. T.-M. (2004) *Chemical vapor deposition polymerization : the growth and properties of parylene thin films*, Kluwer Academic Publishers, Boston [u.a.].
12. Szwarc, M. (1947) Some remarks on the CH2[graphic omitted]CH2 molecule, *Discussions of the Faraday Society 2*, 46-49.
13. Gorham, W. F. (1966) A New, General Synthetic Method for the Preparation of Linear Poly-p-xylylenes, *Journal of Polymer Science Part A-1: Polymer Chemistry 4*, 3027-3039.

14. Rogojevic, S., Moore, J. A., and Gill, W. N. (1999) Modeling vapor deposition of low-K polymers: Parylene and polynaphthalene, *Journal of Vacuum Science & Technology A 17*, 266-274.

15. Gaynor, J. F., Desu, S. B., and Senkevich, J. J. (1995) A Model for Chemical Vapor Copolymerization of p-Xylylenes with Vinylic Comonomers: Order of Initiation and Reactivity Ratios, *Macromolecules 28*, 7343-7348.

16. Errede, L. A., and Szwarc, M. (1958) Chemistry of p-xylylene, its analogues, and polymers, *Quarterly Reviews, Chemical Society 12*, 301-320.

17. Kubo, S., and Wunderlich, B. (1972) Crystallization during polymerization of poly-p-xylylene, *Journal of Polymer Science: Polymer Physics Edition 10*, 1949-1966.

18. Beach, W. F. (1978) A Model for the Vapor Deposition Polymerization of p-Xylylene, *Macromolecules 11*, 72-76.

19. Ganguli, S., Agrawal, H., Wang, B., McDonald, J. F., Lu, T.-M., Yang, G.-R., and Gill, W. N. (1997) Improved growth and thermal stability of Parylene films, *Journal of Vacuum Science & Technology A 15*, 3138-3142.

20. Lahann, J. (2006) Reactive polymer coatings for biomimetic surface engineering, *Chemical Engineering Communications 193*, 1457-1468.

21. Wu, M.-G., Hsu, H.-L., Hsiao, K.-W., Hsieh, C.-C., and Chen, H.-Y. (2012) Vapor-Deposited Parylene Photoresist: A Multipotent Approach toward Chemically and Topographically Defined Biointerfaces, *Langmuir 28*, 14313-14322.

22. Förch, R., Zhang, Z., and Knoll, W. (2005) Soft plasma treated surfaces: tailoring of structure and properties for biomaterial applications, *Plasma processes and polymers 2*, 351-372.

23. Jenkins, A. T. A., Hu, J., Wang, Y. Z., Schiller, S., Foerch, R., and Knoll, W. (2000) Pulsed Plasma Deposited Maleic Anhydride Thin Films as Supports for Lipid Bilayers, *Langmuir 16*, 6381-6384.

24. Girard-Lauriault, P.-L., Desjardins, P., Unger, W. E. S., Lippitz, A., and Wertheimer, M. R. (2008) Chemical Characterisation of Nitrogen-Rich Plasma-Polymer Films Deposited in Dielectric Barrier Discharges at Atmospheric Pressure, *Plasma Processes and Polymers 5*, 631-644.

25. Jeon, B.-J., Kim, M.-H., and Pyun, J.-C. (2010) Parylene-A coated microplate for covalent immobilization of proteins and peptides, *Journal of Immunological Methods 353*, 44-48.

26. Siow, K. S., Britcher, L., Kumar, S., and Griesser, H. J. (2006) Plasma Methods for the Generation of Chemically Reactive Surfaces for Biomolecule Immobilization and Cell Colonization - A Review, *Plasma Processes and Polymers 3*, 392-418.

27. Hu, W.-W., Elkasabi, Y., Chen, H.-Y., Zhang, Y., Lahann, J., Hollister, S. J., and Krebsbach, P. H. (2009) The use of reactive polymer coatings to facilitate gene delivery from poly (ε-caprolactone) scaffolds, *Biomaterials 30*, 5785-5792.

28. Griesser, H. J., Chatelier, R. C., Gengenbach, T. R., Johnson, G., and Steele, J. G. (1994) Growth of human cells on plasma polymers: putative role of amine and amide groups, *Journal of Biomaterials Science, Polymer Edition 5*, 531-554.

29. Schleicher, M., Hansmann, J., Elkin, B., Kluger, P. J., Liebscher, S., Huber, A. J., Fritze, O., Schille, C., Müller, M., and Schenke-Layland, K. (2012) Oligonucleotide and parylene surface coating of polystyrene and ePTFE for improved endothelial cell attachment and hemocompatibility, *International journal of biomaterials 2012*.

30. St-Georges-Robillard, A., Ruiz, J.-C., Petit, A., Wang, H. T., Mwale, F., Elkin, B., Oehr, C., Lerouge, S., and Wertheimer, M. R. (2012) Adhesion of U-937 Monocytes on Different Amine-functionalised Polymer Surfaces, *Plasma Processes and Polymers 9*, 243-252.

31. Daw, R., M. Brook, I., Jane Devlin, A., D. Short, R., Cooper, E., and J. Leggett, G. (1998) A comparative study of cell attachment to self assembled monolayers and plasma polymers, *Journal of Materials Chemistry 8*, 2583-2584.

32. Shoichet, M. S., and McCarthy, T. J. (1991) Convenient syntheses of carboxylic acid functionalized fluoropolymer surfaces, *Macromolecules 24*, 982-986.

33. Dias, A. J., and McCarthy, T. J. (1987) Introduction of carboxylic acid, aldehyde, and alcohol functional groups onto the surface of poly(chlorotrifluoroethylene), *Macromolecules 20*, 2068-2076.

34. Costello, C. A., and McCarthy, T. J. (1987) Surface-selective introduction of specific functionalities onto poly(tetrafluoroethylene), *Macromolecules 20*, 2819-2828.

35. Pu, H., Wang, Y., and Yang, Z. (2007) Chemical vapor deposition copolymerization of 4-carboxyl-[2,2] paracyclophane and 4-amino-[2,2] paracyclophane, *Materials Letters 61*, 2718-2722.

36. Cram, D. J., and Steinberg, H. (1951) Macro Rings. I. Preparation and Spectra of the Paracyclophanes, *Journal of the American Chemical Society 73*, 5691-5704.

37. Hosseini-Sarvari, M., Tavakolian, M., and Ashenagar, S. (2010) Nitration of aromatic compounds using alumina sulfuric acid (ASA) as a novel heterogeneous system and $Mg(NO_3)_2.6H_2O$ as nitrating agent in water, *Iranian Journal of Science & Technology 34*.

38. Laszlo, P., and Pennetreau, P. (1987) Vastly improved para preference in the nitration of halobenzenes, *The Journal of Organic Chemistry 52*, 2407-2410.

39. Spitzer, U. A., and Stewart, R. (1974) Trifluoroacetic acid as a medium for aromatic nitration using sodium nitrate, *The Journal of Organic Chemistry 39*, 3936-3937.

40. Uemura, S., Toshimitsu, A., and Okano, M. (1978) Nitration of aromatic hydrocarbons and ipso-nitrosodemetallation of arylmetal compounds in sodium nitrite-trifluoroacetic acid, *Journal of the Chemical Society, Perkin Transactions 1*, 1076-1079.

41. Luguya, R., Jaquinod, L., Fronczek, F. R., Vicente, M. G. H., and Smith, K. M. (2004) Synthesis and reactions of meso-(p-nitrophenyl)porphyrins, *Tetrahedron 60*, 2757-2763.

42. Riego, J. M., Sedin, Z., Zaldívar, J., Marziano, N. C., and Tortato, C. (1996) Sulfuric acid on silica-gel: an inexpensive catalyst for aromatic nitration, *Tetrahedron Letters 37*, 513-516.

43. Pogorelić, I., Filipan-Litvić, M., Merkaš, S., Ljubić, G., Cepanec, I., and Litvić, M. (2007) Rapid, efficient and selective reduction of aromatic nitro compounds with sodium borohydride and Raney nickel, *Journal of Molecular Catalysis A: Chemical 274*, 202-207.

44. Bellamy, F. D., and Ou, K. (1984) Selective reduction of aromatic nitro compounds with stannous chloride in non acidic and non aqueous medium, *Tetrahedron Letters 25*, 839-842.

45. Tafesh, A. M., and Weiguny, J. (1996) A Review of the Selective Catalytic Reduction of Aromatic Nitro Compounds into Aromatic Amines, Isocyanates, Carbamates, and Ureas Using CO, *Chemical Reviews 96*, 2035-2052.

46. Chandrappa, S., Vinaya, K., Ramakrishnappa, T., Rangappa, and S., K. (2010) *An Efficient Method for Aryl Nitro Reduction and Cleavage of Azo Compounds Using Iron Powder/Calcium Chloride*, Thieme, Stuttgart, ALLEMAGNE.

47. Cram, D. J., and Allinger, N. L. (1955) Macro Rings. XII. Stereochemical Consequences of Steric Compression in the Smallest Paracyclophane1, *Journal of the American Chemical Society 77*, 6289-6294.

48. Waters, J. F., Sutter, J. K., Meador, M. A. B., Baldwin, L. J., and Meador, M. A. (1991) Addition curing thermosets endcapped with 4-amino [2.2] paracyclophane, *Journal of Polymer Science Part A: Polymer Chemistry 29*, 1917-1924.

49. Cipiciani, A., Fringuelli, F., Mancini, V., Piermatti, O., Pizzo, F., and Ruzziconi, R. (1997) Synthesis of Chiral (R)-4-Hydroxy- and (R)-4-Halogeno[2.2]paracyclophanes and Group Polarizability. Optical Rotation Relationship, *The Journal of Organic Chemistry 62*, 3744-3747.

50. Reich, H. J., and Cram, D. J. (1969) Macro rings. XXXVII. Multiple electrophilic substitution reactions of [2.2]paracyclophanes and interconversions of polysubstituted derivatives, *Journal of the American Chemical Society 91*, 3527-3533.

51. Lahann, J., Höcker, H., and Langer, R. (2001) Synthesis of Amino[2.2]paracyclophanes—Beneficial Monomers for Bioactive Coating of Medical Implant Materials, *Angewandte Chemie International Edition 40*, 726-728.

52. Yeh, Y. L., and Gorham, W. F. (1969) Preparation and reactions of some [2.2] paracyclophane derivatives, *The Journal of Organic Chemistry 34*, 2366-2370.

53. Ricci, G., Ruzziconi, R., and Giorgio, E. (2005) Atropisomeric (R,R)-2,2‘-Bi([2]paracyclo[2](5,8)quinolinophane) and (R,R)-1,1‘-Bi([2]paracyclo[2](5,8)isoquinolinophane): Synthesis, Structural Analysis, and Chiroptical Properties, *The Journal of Organic Chemistry 70*, 1011-1018.

54. Cram, D. J., and Fischer, H. P. (1965) Macro Rings. XXX. Structure of Anomalous Products of Acylation of [2.2]Paracyclophane*,1, *The Journal of Organic Chemistry 30*, 1815-1819.

55. Cram, D. J., Wechter, W. J., and Kierstead, R. W. (1958) Macro Rings. XVIII. Restricted Rotation and Transannular Electronic Effects in the Paracyclophanes1, *Journal of the American Chemical Society 80*, 3126-3132.

56. Psiorz, M., and Schmid, R. (1987) Cyclophane, I. Ein einfacher Zugang zu funktionalisierten [2.2]Paracyclophanen, *Chemische Berichte 120*, 1825-1828.

57. Pelter, A., Kidwell, H., and A. N. C. Crump, R. (1997) N-Methyl- and N-benzyl-4-amino[2.2]paracyclophanes as unique planar chiral auxiliaries, *Journal of the Chemical Society, Perkin Transactions 1*, 3137-3140.

58. Marchand, A., Maxwell, A., Mootoo, B., Pelter, A., and Reid, A. (2000) Oxazoline Mediated Routes to a Unique Amino-acid, 4-Amino-13-carboxy[2.2]paracyclophane, of Planar Chirality, *Tetrahedron 56*, 7331-7338.

59. Pelter, A., Crump, R. A. N. C., and Kidwell, H. (1997) Chiral [2.2]paracyclophanes—III. The preparation of unique homochiral amino-acids derived from [2.2]paracyclophane, *Tetrahedron: Asymmetry 8*, 3873-3880.

60. Fulmer, G. R., Miller, A. J. M., Sherden, N. H., Gottlieb, H. E., Nudelman, A., Stoltz, B. M., Bercaw, J. E., and Goldberg, K. I. (2010) NMR Chemical Shifts of Trace Impurities: Common Laboratory Solvents, Organics, and Gases in Deuterated Solvents Relevant to the Organometallic Chemist, *Organometallics 29*, 2176-2179.

61. Lahann, J., and Langer, R. (2002) Novel Poly(p-xylylenes): Thin Films with Tailored Chemical and Optical Properties, *Macromolecules 35*, 4380-4386.

62. Reich, H. J., and Cram, D. J. (1969) Macro rings. XXXVIII. Determination of positions of substituents in the [2.2]paracyclophane nucleus through nuclear magnetic resonance spectra, *Journal of the American Chemical Society 91*, 3534-3543.

63. Cram, D. J., Bauer, R. H., Allinger, N. L., Reeves, R. A., Wechter, W. J., and Heilbronner, E. (1959) Macro Rings. XXI. Mono- and Polysubstituted [2.2]Paracyclophanes1, *Journal of the American Chemical Society 81*, 5977-5983.

64. Merlic, C. A., Motamed, S., and Quinn, B. (1995) Structure Determination and Synthesis of Fluoro Nissl Green: An RNA-Binding Fluorochrome, *The Journal of Organic Chemistry 60*, 3365-3369.

65. Zou, X., and Gu, K. (1990) Synthesis of fluoromethoxythrin and its insecticidal activity, *Journal of fluorine chemistry 46*, 507-513.

66. Sorribes, I., Wienhöfer, G., Vicent, C., Junge, K., Llusar, R., and Beller, M. (2012) Chemoselective Transfer Hydrogenation to Nitroarenes Mediated by Cubane-Type Mo3S4 Cluster Catalysts, *Angewandte Chemie 124*, 7914-7918.

67. Preiß, A., Lewin, U., Wennrich, L., Findeisen, M., and Efer, J. (1997) Analysis of nitrophenols and other polar nitroaromatic compounds in ammunition wastewater by high-field proton nuclear magnetic resonance (1H-NMR) spectroscopy and chromatographic methods, *Fresenius' Journal of Analytical Chemistry 357*, 676-683.

68. Taylor, M., Urquhart, A. J., Zelzer, M., Davies, M. C., and Alexander, M. R. (2007) Picoliter Water Contact Angle Measurement on Polymers, *Langmuir 23*, 6875-6878.

69. Li, D., and Neumann, A. W. (1992) Contact angles on hydrophobic solid surfaces and their interpretation, *Journal of Colloid and Interface Science 148*, 190-200.

70. Wong, J. S., and Yen, Y.-S. (1988) Intriguing Absorption Band Behavior of IR Reflectance Spectra of Silicon Dioxide on Silicon, *Applied Spectroscopy 42*, 598-604.

71. Coates, J. (2006) Interpretation of Infrared Spectra, A Practical Approach, In *Encyclopedia of Analytical Chemistry*, John Wiley & Sons, Ltd.

72. Seah, M. (1980) The quantitative analysis of surfaces by XPS: a review, *Surface and Interface Analysis 2*, 222-239.

73. Ruiz, J. C., St-Georges-Robillard, A., Thérésy, C., Lerouge, S., and Wertheimer, M. R. (2010) Fabrication and Characterisation of Amine-Rich Organic Thin Films: Focus on Stability, *Plasma Processes and Polymers 7*, 737-753.

74. Gigout, A., Levasseur, S., Girard-Lauriault, P. L., Buschmann, M. D., Wertheimer, M. R., and Jolicoeur, M. (2009) CHO Cells Adhering to Nitrogen-Rich Plasma-Polymerised Ethylene Exhibit High Production of a Specific Recombinant Protein, *Macromolecular bioscience 9*, 979-988.

75. Girard-Lauriault, P. L., Truica-Marasescu, F., Petit, A., Wang, H. T., Desjardins, P., Antoniou, J., Mwale, F., and Wertheimer, M. R. (2009) Adhesion of Human U937 Monocytes to Nitrogen-Rich Organic Thin Films: Novel Insights into the Mechanism of Cellular Adhesion, *Macromolecular bioscience 9*, 911-921.

76. Lerouge, S., Major, A., Girault-Lauriault, P.-L., Raymond, M.-A., Laplante, P., Soulez, G., Mwale, F., Wertheimer, M. R., and Hébert, M.-J. (2007) Nitrogen-rich

coatings for promoting healing around stent-grafts after endovascular aneurysm repair, *Biomaterials 28*, 1209-1217.

77. Friedrich, J., Kühn, G., Mix, R., Fritz, A., and Schönhals, A. (2003) Polymer surface modification with monofunctional groups of variable types and densities, *Journal of Adhesion Science and Technology 17*, 1591-1617.

78. Girard-Lauriault, P. L., Mwale, F., Iordanova, M., Demers, C., Desjardins, P., and Wertheimer, M. R. (2005) Atmospheric Pressure Deposition of Micropatterned Nitrogen-Rich Plasma-Polymer Films for Tissue Engineering, *Plasma Processes and Polymers 2*, 263-270.

79. Girard-Lauriault, P.-L., Truica-Marasescu, F., Petit, A., Wang, H. T., Desjardins, P., Antoniou, J., Mwale, F., and Wertheimer, M. R. (2009) Adhesion of Human U937 Monocytes to Nitrogen-Rich Organic Thin Films: Novel Insights into the Mechanism of Cellular Adhesion, *Macromolecular Bioscience 9*, 911-921.

80. Miwa, J., Suzuki, Y., and Kasagi, N. (2008) Adhesion-Based Cell Sorter With Antibody-Coated Amino-Functionalized-Parylene Surface, *Microelectromechanical Systems, Journal of 17*, 611-622.

81. Truica-Marasescu, F., and Wertheimer, M. R. (2008) Nitrogen-Rich Plasma-Polymer Films for Biomedical Applications, *Plasma Processes and Polymers 5*, 44-57.

82. Truica-Marasescu, F., Girard-Lauriault, P.-L., Lippitz, A., Unger, W. E. S., and Wertheimer, M. R. (2008) Nitrogen-rich plasma polymers: Comparison of films deposited in atmospheric- and low-pressure plasmas, *Thin Solid Films 516*, 7406-7417.

83. Haupt, M., Barz, J., and Oehr, C. (2008) Creation and Recombination of Free Radicals in Fluorocarbon Plasma Polymers: An Electron Spin Resonance Study, *Plasma Processes and Polymers 5*, 33-43.

84. Finke, B., Rebl, H., Hempel, F., Schäfer, J., Liefeith, K., Weltmann, K.-D., and Nebe, J. B. (2014) Aging of Plasma-Polymerized Allylamine Nanofilms and the Maintenance of Their Cell Adhesion Capacity, *Langmuir 30*, 13914-13924.

85. Pruden, K. G., Sinclair, K., and Beaudoin, S. (2003) Characterization of parylene-N and parylene-C photooxidation, *Journal of Polymer Science Part A: Polymer Chemistry 41*, 1486-1496.

86. Gołda, M., Brzychczy-Włoch, M., Faryna, M., Engvall, K., and Kotarba, A. (2013) Oxygen plasma functionalization of parylene C coating for implants surface: Nanotopography and active sites for drug anchoring, *Materials Science and Engineering: C 33*, 4221-4227.

87. Santucci, V., Maury, F., and Senocq, F. (2010) Vapor phase surface functionalization under ultra violet activation of parylene thin films grown by chemical vapor deposition, *Thin Solid Films 518*, 1675-1681.

88. Yang, Z., Tu, Q., Wang, J., Lei, X., He, T., Sun, H., and Huang, N. (2011) Bioactive Plasma-Polymerized Bipolar Films for Enhanced Endothelial Cell Mobility, *Macromolecular Bioscience 11*, 797-805.

89. Yang, Z., Yang, Y., Yan, W., Tu, Q., Wang, J., and Huang, N. (2013) Construction of Polyfunctional Coatings Assisted by Gallic Acid to Facilitate Co-Immobilization of Diverse Biomolecules, *ACS Applied Materials & Interfaces 5*, 10495-10501.

90. Zhou, J., Khodakov, D. A., Ellis, A. V., and Voelcker, N. H. (2012) Surface modification for PDMS-based microfluidic devices, *ELECTROPHORESIS 33*, 89-104.

91. Chen, H.-Y., McClelland, A. A., Chen, Z., and Lahann, J. (2008) Solventless Adhesive Bonding Using Reactive Polymer Coatings, *Analytical Chemistry 80*, 4119-4124.

92. Xu, J., and Gleason, K. K. (2010) Conformal, Amine-Functionalized Thin Films by Initiated Chemical Vapor Deposition (iCVD) for Hydrolytically Stable Microfluidic Devices, *Chemistry of Materials 22*, 1732-1738.

93. Zorlutuna, P., Annabi, N., Camci-Unal, G., Nikkhah, M., Cha, J. M., Nichol, J. W., Manbachi, A., Bae, H., Chen, S., and Khademhosseini, A. (2012) Microfabricated Biomaterials for Engineering 3D Tissues, *Advanced Materials 24*, 1782-1804.

94. Wright, D., Rajalingam, B., Karp, J. M., Selvarasah, S., Ling, Y., Yeh, J., Langer, R., Dokmeci, M. R., and Khademhosseini, A. (2008) Reusable, reversibly sealable parylene membranes for cell and protein patterning, *Journal of Biomedical Materials Research Part A 85A*, 530-538.

95. Wright, D., Rajalingam, B., Selvarasah, S., Dokmeci, M. R., and Khademhosseini, A. (2007) Generation of static and dynamic patterned co-cultures using microfabricated parylene-C stencils, *Lab on a Chip 7*, 1272-1279.

96. Li, C., Wu, P.-M., Jung, W., Ahn, C. H., Shutter, L. A., and Narayan, R. K. (2009) A novel lab-on-a-tube for multimodality neuromonitoring of patients with traumatic brain injury (TBI), *Lab on a Chip 9*, 1988-1990.

97. Kuo, J. T. W., Kim, B. J., Hara, S. A., Lee, C. D., Gutierrez, C. A., Hoang, T. Q., and Meng, E. (2013) Novel flexible Parylene neural probe with 3D sheath structure for enhancing tissue integration, *Lab on a Chip 13*, 554-561.

98. Tai, Y.-C., and Wang, X.-Q. (2004) Parylene micro check valve and fabrication method thereof, In *U.S. Patent*, U.S. Patents.

99. Xie, J., Miao, Y., Shih, J., Tai, Y.-C., and Lee, T. D. (2005) Microfluidic Platform for Liquid Chromatography−Tandem Mass Spectrometry Analyses of Complex Peptide Mixtures, *Analytical Chemistry 77*, 6947-6953.

100. Sikanen, T., Franssila, S., Kauppila, T. J., Kostiainen, R., Kotiaho, T., and Ketola, R. A. (2010) Microchip technology in mass spectrometry, *Mass Spectrometry Reviews 29*, 351-391.

101. Hong-seok, N., Hesketh, P. J., and Frye-Mason, G. C. (2002) Parylene gas chromatographic column for rapid thermal cycling, *Journal of Microelectromechanical Systems 11*, 718-725.

102. Hong-seok, N., Kyoung-sik, M., Andrew, C., Peter, J. H., and Wong, C. P. (2004) Wafer bonding using microwave heating of parylene intermediate layers, *Journal of Micromechanics and Microengineering 14*, 625.

103. Noha, H.-S., Huangb, Y., and Hesketha, P. J. (2004) Parylene micromolding, a rapid and low-cost fabrication method for parylene microchannel, *Sensors and Actuators B: Chemical 102*, 78-85.

104. Rajaraman, S., Noh, H.-s., Hesketh, P. J., and Gottfried, D. S. (2006) Rapid, low cost microfabrication technologies toward realization of devices for dielectrophoretic manipulation of particles and nanowires, *Sensors and Actuators B: Chemical 114*, 392-401.

105. Kim, H. S., and Najafi, K. (2003) Wafer bonding using parylene and wafer-level transfer of free-standing parylene membranes, In *TRANSDUCERS, Solid-State Sensors, Actuators and Microsystems, 12th International Conference on, 2003*, pp 790-793, IEEE.

106. Ziegler, D., Suzuki, T., and Takeuchi, S. (2006) Fabrication of Flexible Neural Probes With Built-In Microfluidic Channels by Thermal Bonding of Parylene, *Journal of Microelectromechanical Systems 15*, 1477-1482.